University of Massachusetts Medical School
eScholarship@UMMS

GSBS Dissertations and Theses | Graduate School of Biomedical Sciences

1992-07-01

Structure and Function of Cytoplasmic Dynein: a Thesis

Bryce M. Paschal
University of Massachusetts Medical School

Let us know how access to this document benefits you.

Follow this and additional works at: https://escholarship.umassmed.edu/gsbs_diss

 Part of the Amino Acids, Peptides, and Proteins Commons, Cells Commons, Enzymes and Coenzymes Commons, Genetic Phenomena Commons, and the Nucleic Acids, Nucleotides, and Nucleosides Commons

Repository Citation

Paschal BM. (1992). Structure and Function of Cytoplasmic Dynein: a Thesis. GSBS Dissertations and Theses. https://doi.org/10.13028/zk8v-xy13. Retrieved from https://escholarship.umassmed.edu/gsbs_diss/82

This material is brought to you by eScholarship@UMMS. It has been accepted for inclusion in GSBS Dissertations and Theses by an authorized administrator of eScholarship@UMMS. For more information, please contact Lisa.Palmer@umassmed.edu.

STRUCTURE AND FUNCTION OF CYTOPLASMIC DYNEIN

A Thesis Presented

By

Bryce Mark Paschal

Submitted to the Faculty of the
University of Massachusetts Graduate School of Biomedical Sciences, Worcester
in partial fulfillment of the requirements for the degree of:

DOCTOR OF PHILOSOPHY IN MEDICAL SCIENCES

Cell Biology
July, 1992

COPYRIGHTS

1. Chapter II of this thesis was copyrighted in 1989 by Macmillan Magazines Ltd.

Title: Interaction of brain cytoplasmic dynein and MAP2 with a common sequence at the C-terminus of tubulin.

Authors: Bryce M. Paschal, Robert A. Obar, and Richard B. Vallee.

Journal: Nature 342:569-572.

2. Chapter III of this thesis was copyrighted in 1992 by the Rockefeller University Press.

Title: Molecular cloning of a cytoplasmic dynein subunit: homology with a flagellar dynein polypeptide.

Authors: Bryce M. Paschal, Atsushi Mikami, K. Kevin Pfister, and Richard B. Vallee.

Journal: J. Cell Biology (In press)

STRUCTURE AND FUNCTION
OF CYTOPLASMIC DYNEIN

A thesis
By
Bryce Mark Paschal

Approved as to style and content by:

Dr. Robert H. Singer, Chairman of Committee

Dr. Louis J. DeGennaro, Member

Dr. Reid J. Gilmore, Member

Dr. Kenneth S. Kosik, Member

Dr. Jeanne B. Lawrence, Member

Dr. Richard B. Vallee,
Thesis Advisor

Dr. Thomas B.Miller, Dean of
Graduate School of Biomedical
Sciences

Department of Cell Biology
July 1992

This work is dedicated to my wife, Angie. Your patience, encouragement, and sacrifice have helped to make this possible.

ACKNOWLEDGEMENTS

I thank my colleagues at the Worcester Foundation for Experimental Biology for their technical and intellectual contributions. I thank Richard Vallee for providing a stimulating research environment, and for his financial support from 1985 to 1992.

ABSTRACT

In previous work I described the purification and properties of the microtubule-based mechanochemical ATPase cytoplasmic dynein. Cytoplasmic dynein was found to produce force along microtubules in the direction corresponding to retrograde axonal transport. Cytoplasmic dynein has been identified in a variety of eukaryotes including yeast and human, and there is a growing body of evidence suggesting that this "molecular motor" is responsible for the transport of membranous organelles and mitotic chromosomes.

The first part of this thesis investigates the molecular basis of microtubule-activation of the cytoplasmic dynein ATPase. By analogy with other mechanoenzymes, this appears to accelerate the rate-limiting step of the cross-bridge cycle, ADP release. Using limited proteolysis, site-directed antibodies, and N-terminal microsequencing, I identified the acidic C-termini of α and β-tubulin as the domains responsible for activation of the dynein ATPase.

The second part of this thesis investigates the structure of the 74 kDa subunit of cytoplasmic dynein. The amino acid sequence deduced from cDNA clones predicts a 72,753 dalton polypeptide which includes the amino acid sequences of nine peptides determined by microsequencing. Northern analysis of rat brain poly(A) revealed an abundant 2.9 kb mRNA. However, PCR performed on first strand cDNA, together with the sequence of a partially matching tryptic peptide, indicate the existence of three

isoforms. The C-terminal half is 26.4% identical and 47.7% similar to the product of the *Chlamydomonas ODA6* gene, a 70 kDa subunit of flagellar outer arm dynein. Based on what is known about the *Chlamydomonas* 70 kDa subunit, I suggest that the 74 kDa subunit is responsible for targeting cytoplasmic dynein to membranous organelles and kinetochores of mitotic chromosomes.

The third part of this thesis investigates a 50 kDa polypeptide which co-purifies with cytoplasmic dynein on sucrose density gradients. Monoclonal antibodies were produced against the 50 kDa subunit and used to show that it is a component of a distinct 20S complex which contains additional subunits of 45 and 150 kDa. Moreover, like cytoplasmic dynein, the 50 kDa polypeptide localizes to kinetochores of metaphase chromosomes by light and electron microscopy. The 50 kDa-associated complex is reported to stimulate cytoplasmic dynein-mediated organelle motility *in vitro*. The complex is, therefore, a candidate for modulating cytoplasmic dynein activity during mitosis.

TABLE OF CONTENTS

LIST OF FIGURES AND TABLES

CHAPTER I

INTRODUCTION

Microtubule-based motility is a feature common to most types of eukaryotic cells. Processes as diverse as the beating of cilia and flagella, transport of membranous organelles, and chromosome segregation during mitosis are accomplished by microtubules and their associated proteins. The microtubule-associated proteins (MAPs) are of two general types, structural and mechanochemical. The structural MAPs such as MAP1A, 1B, 2A, 2B and tau promote the assembly and stabilization of microtubule polymer by binding with high affinity to the surface of the microtubule lattice. The mechanochemical MAPs cytoplasmic dynein and kinesin are force-producing molecules which couple the energy of ATP hydrolysis with microtubule-based movement.

The discovery of microtubule-based motors was facilitated by advances in light microscopy in the early 1980's (Allen et al. 1981). The combination of differential interference contrast microscopy and video image processing made it possible to view individual microtubules and associated organelle transport in squid axoplasm (Allen et al., 1983). Using this technology, Vale and coworkers purified a soluble factor which when adsorbed to glass coverslips promoted the gliding of microtubules (Vale et al., 1985a). The factor, which was named kinesin, also powered the transport of polystyrene beads and membranous organelles along microtubules.

Kinesin was found to be an anterograde motor, as defined by the inherent polarity of the microtubule. However, when unfractionated squid cytosol was used in the motility assays, microtubule-based transport was observed in both the anterograde and retrograde directions (Vale et al., 1985b). The pharmacological profile of the retrograde activity differed from that of kinesin, and its activity persisted in cytosol after immunodepletion using anti-kinesin antibodies. These data seemed to indicate that a distinct protein was responsible for retrograde transport, though its identification remained elusive.

The discovery of cytoplasmic dynein in our laboratory came as a result of our interest in microtubule-associated ATPases. Collins and Vallee (1986) showed that sea urchin egg cytosol contained a novel ATPase activity which was potently stimulated by the presence of microtubules, suggesting a role in mechanochemistry. Furthermore, it established a biochemical assay for cytosolic microtubule-activated enzymes.

Curiously, the ATP hydrolysis rate initially reported for kinesin was 10 nmol/min/mg (Vale et al., 1985a). This activity, which is at the level of detectability, seemed low in comparison with the ATPase activity of other microtubule-based mechanoenzymes such as flagellar dynein (>1000 nmol/min/mg; Johnson, 1985). I reasoned that the kinesin ATPase, like that of the sea urchin factor described by Collins and Vallee (1986), might be stimulated by microtubules. This proved to be correct. Our lab and others found that the kinesin

ATPase was activated several-fold by microtubules (B.P., unpublished data; Kuznetsov et al., 1986). More important was my observation that ATPase activity profiles of gel filtration columns (used to purify kinesin) revealed the presence of a second microtubule-activated ATPase which eluted just before kinesin. We purified this activity to homogeneity (Paschal et al., 1987), and as discussed below, demonstrated that it was a microtubule-based retrograde motor (Paschal and Vallee, 1987). In addition, the properties of this enzyme were consistent with its identification as a cytoplasmic form of what had previously been known as a ciliary and flagellar enzyme (Paschal and Vallee, 1987; Vallee et al., 1988).

Properties of cytoplasmic dynein.

Cytoplasmic dynein was found to be a multi-subunit complex containing polypeptides with molecular weights of 53, 55, 57, 59, 74, and 440 kDa in a stoichiometry of 1:1:1:1:3:2 (Paschal et al., 1987; Vallee et al., 1988). In accordance with axonemal (ciliary and flagellar) dynein nomenclature, the >400 kDa polypeptides are referred to as heavy chains and the 53-74 kDa accessory subunits are referred to as intermediate chains. Cytoplasmic dynein does not contain low molecular weight (14-20 kDa) light chains which are typically found associated with axonemal dynein. Scanning transmission electron microscopy (STEM) revealed that the holoenzyme has a mass of 1.2 mDa and contains two large globular "heads" (diameter=13.7 nm) connected to a basal domain the

morphology of which is less well defined. The heads, which probably correspond to the high molecular weight catalytic heavy chains, are thought to represent the structures which interact with the microtubules in a mechanochemical cross-bridge cycle. The composition of the basal domain of cytoplasmic dynein is unknown, though it seems reasonable to predict that it contains one or more of the accessory subunits.

One of the hallmarks of a mechanochemical enzyme is an associated nucleotidase activity which is stimulated upon binding to the appropriate cytoskeletal polymer (reviewed by Johnson, 1985). Thus, the ATPases of myosin and axonemal dynein are stimulated by actin filaments and microtubules, respectively. The ATPase of cytoplasmic dynein is activated up to seven-fold by polymeric tubulin (Paschal et al., 1987). The K_m for microtubules is 0.16 mg/ml and the V_{max} at saturating tubulin concentrations is 186 nmol/min/mg (Shpetner et al., 1988). The microtubule-activated ATPase exhibits a steep dependence on ionic strength, being inhibited by ~70% at 100 mM KCl. Increasing the ionic strength appears to decrease the apparent affinity of cytoplasmic dynein for microtubules, since the the K_m for microtubules is dramatically increased while the V_{max} is relatively unaffected (Shpetner et al., 1988). The actin-activated ATPase of myosin is similarly affected by elevated ionic strength (Eisenberg and Moos, 1968).

The biochemical analysis of a variety of ATPases has been aided by the use of pharmacological reagents. Cytoplasmic dynein,

like axonemal dynein (Gibbons et al., 1978), is potently inhibited by sodium metavanadate with half-maximal inhibition observed at 5-10 μM (Shpetner et al., 1988). The adenosine analogue EHNA is also an effective inhibitor of both forms of dynein, inhibiting the cytoplasmic enzyme by 85% (at 1 mM) when assayed in high ionic strength buffer (Shpetner at al., 1988; Penningroth et al., 1985). Cytoplasmic dynein is also sensitive to NEM (67% inhibition at 1 mM), though this sulfhydryl alkylating reagent inhibits the activity of many other cytosolic proteins. Inhibitors of membrane-bound ATPases (ouabain, sodium azide, oligomycin) did not inhibit the cytoplasmic dynein ATPase (Shpetner et al., 1988).

The force producing properties of cytoplasmic dynein have been studied with several *in vitro* motility assays. Cytoplasmic dynein supported gliding of microtubules on glass coverslips at 1.25 ± 0.11 μm/sec (mean ± SD; Paschal et al., 1987). Chlamydomonas flagellar axonemes were used to determine that cytoplasmic dynein generates force towards the "minus ends" of microtubules (Paschal and Vallee, 1987), a direction opposite to that observed for kinesin (Vale et al., 1985). Cytoplasmic dynein is also referred to as a retrograde motor since its direction of force production along axonal microtubules would be from the synaptic terminal towards the cell body (Paschal and Vallee, 1987; Vallee et al., 1989).

Evidence for cytoplasmic dynein-mediated organelle transport using reconstituted motility systems.

A role for cytoplasmic dynein in retrograde organelle transport is supported by experiments using pharmacological reagents and *in vitro* motility systems. Retrograde axonal transport in detergent-permeabilized lobster axons was inhibited by sodium metavanadate (Forman et al., 1983a) and EHNA (Forman et al., 1983b), both of which inhibit the cytoplasmic dynein ATPase (Paschal and Vallee, 1987; Shpetner et al., 1988). Microtubule-dependent pigment granule aggregation in permeabilized melanophores was also blocked by these reagents (Clark and Rosenbaum, 1982).

While these pharmacological data are consistent with a dynein-like motor activity, more compelling evidence has come from the use a photocleavage reaction which inactivates cytoplasmic dynein. Exposure of purified cytoplasmic dynein to UV light in the presence sodium vanadate and MgATP resulted in cleavage of the high molecular weight (>400 kDa) catalytic subunit into enzymatically-inactive fragments of 185 and 225 kDa (Paschal et al., 1987). Application of the photocleavage reaction to a cell-free system containing organelles, cytosol, and taxol-polymerized microtubules resulted in >90% inactivation of the retrograde vesicle transport activity (Schroer et al., 1989; Schnapp and Reese, 1989). Subsequent addition of cytoplasmic dynein to the UV light-inactivated system partially restored retrograde organelle motility. Purified cytoplasmic dynein is not sufficient to support vesicle motility, suggesting that

additional soluble factors are necessary to drive organelle motility (Schroer et al.,1989).

The role of microtubule-based motors has also been examined in an assay which reproduces some of the fusion events in the endocytic pathway. In vivo, endocytic vesicles derived from apical and basolateral domains of MDCK epithelial cells converge at the level of late endosomes (Bomsel et al., 1989). In a cell-free assay, this fusion event was stimulated 25-fold by the presence of microtubules (Bomsel et al., 1990). UV light irradiation in the presence of sodium vanadate and MgATP reduced the fusion event by 60%, suggesting cytoplasmic dynein may act as a motor for endosome transport (op. cit.).

Immunolocalization studies suggest a role for cytoplasmic dynein in organelle and chromosome transport.

The normally observed organization and distribution of endosomes and lysosomes (Herman and Albertini, 1984; Matteoni and Kreis, 1987), the Golgi apparatus (Wehland et al., 1983a; Rogalski and Singer, 1984), and the endoplasmic recticulum (Terasaki et al., 1986) is disrupted by treating cells with drugs such as nocadazole which depolymerize the microtubule network. After microtubules are allowed to reassemble, endosomes, lysosomes and Golgi elements translocate along linear tracts towards the microtubule-organizing center (MTOC) and resume their normal perinuclear location (Matteoni and Kreis, 1987; Ho et al., 1989). The microtubules of

interphase cells are oriented with their minus ends at the MTOC, suggesting the transport of these organelles was probably driven by the minus end-directed motor cytoplasmic dynein.

The results obtained by immunocytochemistry with antibodies to cytoplasmic dynein support a specific role for this enzyme in organelle and chromosome motility. Lin and Collins (1992) found that an anti-serum generated against native cytoplasmic dynein reacted with vesicular structures which concentrate near the MTOC. The vesicles were found to accumulate rhodamine-labeled dextran, indicating they are probably late endosomes and lysosomes. The authors also noted weak staining which was coincident with structures labeled with fluorescein-conjugated wheat germ agglutinin, suggesting that Golgi elements may be transported by cytoplasmic dynein (Lin and Collins, 1992). Since wheat germ agglutinin labels structures in addition to the Golgi apparatus, this issue will require analysis using Golgi-specific markers.

The immunolocalization of cytoplasmic dynein in experimentally-modified axons of the peripheral nervous system has also suggested an association with membranous organelles. When the saphenous nerves of mice were ligated to block axonal transport, immunofluorescence microscopy revealed an accumulation of cytoplasmic dynein immunoreactivity on both the proximal and distal sides of the ligation (Hirokawa et al., 1990) while kinesin immunoreactivity became concentrated primarily on the proximal side (Hirokawa et al., 1991). Analysis by electron microscopy

revealed the accumulation of mitochondria and tubulovesicular elements proximal to the ligation, and lysosomes, multi-vesicular bodies, and mitochondria on the distal side (Hirokawa et al., 1990). Using cryoultrathin sections and gold labeled secondary antibodies, the authors showed that some of the membranous organelles were decorated by anti-dynein antibodies. The appearence of cytoplasmic dynein on both sides of the site of ligation presumably reflects its ongoing delivery to the axon terminus (anterograde direction) prior to its utilization as the motor for the transport of organelles back to the cell body (retrograde direction).

Evidence for a role for cytoplasmic dynein in chromosome movement during cell division has also been obtained. During anaphase A, chromosomes attached to the mitotic spindle are transported along microtubules towards the spindle poles (minus end-directed). It was suspected that cytoplasmic dynein might be the motor activity responsible since the poleward direction of chromosome movement corresponds to that of organelles undergoing retrograde transport in axons. Polyclonal and monoclonal antibodies have been used to show that cytoplasmic dynein is indeed a component of the kinetochore of chromosomes isolated from Hela, CHO, and chicken cells (Pfarr et al., 1990; Steuer et al., 1990; Wordeman et al., 1991). Staining was also demonstrated in whole mitotic cells, although the kinetochore labeling was obvious only during prometaphase (Pfarr et al., 1990). Immunoelectron microscopy has further shown that cytoplasmic dynein is localized to

the fibrous corona, the outermost structure of the kinetochore (Wordeman et al., 1991). These immunocytochemical observations have been complemented by results from an in vitro assay which showed that a microtubule motor activity in the kinetochores of isolated chromosomes has cytoplasmic dynein-like properties (Hyman and Mitchison, 1991; see also Vallee, 1991).

Based on my earlier work on the *in vitro* properties of cytoplasmic dynein (Paschal et al., 1987; Paschal and Vallee, 1987; Vallee et al., 1988; Shpetner et al., 1988) as well as the existing physiology, pharmacology, and cytology, this enzyme appears to be the motor responsible for membranous organelle transport and some aspects of chromosome movement during mitosis. The experiments described in this thesis were designed to provide insight into the molecular basis of the interaction of cytoplasmic dynein with microtubules and its subcellular targets.

CHAPTER II

INTERACTION OF BRAIN CYTOPLASMIC DYNEIN AND MAP2 WITH A COMMON SEQUENCE AT THE C-TERMINUS OF TUBULIN

Two types of microtubule-associated proteins (MAPs) have been identified in neuronal cells. The fibrous MAPs, including MAP1A and1B, MAP 2A, 2B and 2C, MAP 4, and the tau MAPs represent fibrous molecules that project from the microtubule surface (Voter and Erickson, 1982; Hirokawa et al., 1985; Hirokawa et al., 1988). These proteins are thought to be structural components of the cytoskeleton which organize and space microtubules and other cytoskeletal fibers. They also promote the assembly of tubulin polymer in vitro, and probably determine the stability of microtubules in vivo as well. A second, distinct class of MAPs has been identified which is involved in microtubule-associated movement. These proteins are mechanochemical ATPases which are thought to provide the forces necessary for bidirectional organelle transport and perhaps other motile phenomena such as chromosome movement. These proteins include kinesin (Vale et al., 1985a) and cytoplasmic dynein (Paschal et al., 1987, Paschal and Vallee, 1987).

Nothing is known about the site of interaction of the mechanochemical proteins with the microtubule. However, evidence has accumulated that the prime site of interaction of MAP2 and tau is with the C- (carboxyl) terminus of both the α (alpha) and β (beta) subunits of the tubulin dimer (Serrano et al., 1984; Littauer et al.,

1986). This conclusion was based on analysis of MAP binding to proteolytically modified tubulin and to tubulin fragments and synthetic peptides (Serrano et al., 1984; Littauer et al., 1986; Maccioni et al., 1988). Removal of the C-terminus of α and β-tubulin with the protease subtilisin was reported to decrease the binding of MAP 2 to microtubules (Serrano et al., 1984). The site of cleavage was proposed to reside ~40 amino acids in from the C-terminus based on the apparent 4 kD reduction in the size of the subunits after the protease treatment.

The present study describes the effect of MAP2 on the interaction of cytoplasmic dynein with microtubules. It was motivated by observations made during our initial characterization of brain cytoplasmic dynein. We observed that in the presence of ATP, microtubules glided over the surface of coverslips which had been coated with cytoplasmic dynein (Paschal et al., 1987). This provided direct evidence for its force-producing activity, and subsequently allowed us to show that it generated force in the direction corresponding to retrograde axonal transport (Paschal and Vallee, 1987). In the course of this work we noted that microtubule gliding activity was inconsistent in crude dynein preparations, but improved dramatically during purification. This suggested that some other component of brain microtubules, possibly some of the previously described MAPs, were capable of inhibiting dynein activity.

We report here that purified MAP2 and other MAP preparations are, indeed, potent inhibitors of cytoplasmic dynein-mediated motility as well as the microtubule activated ATPase of dynein, suggesting that MAP2 and other proteins in this class may be important modulators of motility in vivo. By proteolytic modification of tubulin, we found that the site of interaction of dynein with microtubules is at the C-terminus of α and β-tubulin, the region previously reported to be the site for the interaction of MAP2. Finally, by monitoring the modification of tubulin with sequence-specific antibodies, we made the surprising finding that the key interaction site for both MAP2 and dynein may consist of only a tetrapeptide sequence at the extreme C-terminus of α-tubulin, and a similar sequence near the C-terminus of the β-subunit.

Materials and Methods

Protein purification.

Cytoplasmic dynein was purified as previously described (Paschal et al., 1987; Paschal et al., 1991; see also Materials and Methods, Chapter IV). Microtubule protein was prepared from bovine brain by cycles of temperature-dependent assembly and disassembly (Vallee, 1986). Tubulin was purified from microtubule protein by ion exchange chromatography on DEAE Sephadex (Vallee, 1986). MAP2 and tau were purified from a heat-stable MAPs

fraction by Bio-gel A5m chromatography. Protein concentrations were determined with the BCA reagent (Smith et al., 1985).

Assay of cytoplasmic dynein activity.

Microtubule gliding motility was assayed by video enhanced differential interference contrast microscopy as described (Paschal et al., 1987) in 20 mM Tris, pH 7.6, containing 50 mM KCl, 5 mM $MgSO_4$, and 0.5 mM EDTA (Tris-KCl buffer). The final assay volume (10 µl) contained 0.1 mg/ml microtubules, 0.08 mg/ml cytoplasmic dynein, and 2 mM MgATP.

The microtubule-activated ATPase of cytoplasmic dynein was measured as described in the presence of taxol-stabilized microtubules (Paschal et al., 1987). To examine the effect of MAP2 on the ATPase, purified MAP2 was added to the taxol-stabilized microtubules 15 minutes prior to the assay. Protease-modified microtubules (see below) were sedimented at 40,000 g for 30 minutes, washed successively with Tris-KCl buffer containing 0.5 M NaCl and Tris-KCl buffer alone.

Proteolytic digestions.

Pure tubulin subunits (5 mg/ml) were equilibrated into Tris-KCl buffer by chromatography on Sephadex G-25, assembled into microtubules using excess taxol, and digested with protease at 37°C. The concentrations of subtilisin and thermolysin (Boehringer Mannheim, Indianapolis, IN) are specified in the legends. Subtilisin

was inactivated by the addition of PMSF to 5 mM, and thermolysin digestion was terminated by the addition of EGTA to 5 mM.

Gel electrophoresis and immunoblotting.

For optimal resolution of α and β-tubulin, samples were analyzed on 7% polyacrylamide gels containing 0.1% sodium lauryl sulfate (Sigma, St. Louis, MO) at pH 9.2 ((Sackett et al., 1985). Electroblotting onto nitrocellulose was performed in a methanol-containing buffer (Towbin et al., 1979). Samples for microsequence analysis were blotted onto Immobilon (Millipore, Medford, MA) and visualized by Coomassie blue staining. The bands were excised and subjected to N-terminal microsequencing (Matsudaira, 1987).

The anti-tyr and anti-Glu antibodies, provided by Dr. J. Bulinski, were used as unfractionated serum diluted 1:500. The monoclonal antibodies DM1A and DM1B (Amersham, Arlington Heights, IL) were used as ascites fluid diluted 1:1000. Immunoblots were reacted with peroxidase-labeled secondary antibodies (Cappel, Durham, NC) and developed with 4-chloro-1-napthol and hydrogen peroxide.

Results

MAP2 inhibits the interaction of dynein with microtubules.

Purification of cytoplasmic dynein involves assembly of microtubules in brain cytosolic extracts, followed by ATP extraction

of the dynein and further fractionation on sucrose density gradients. When the crude ATP extracts were evaluated for their ability to support microtubule gliding, only a small fraction of the microtubules displayed any motility. Movement was intermittent and the microtubules appeared to be impeded in their forward progress as though adhered to the coverslip at sites along their length. In contrast, sucrose gradient-purified dynein supported smooth and uninterrupted gliding of >90% of the microtubules in the preparation. Other than tubulin, the major polypeptides separated from dynein during this latter step of purification are the high M_r MAPs (Paschal et al., 1987), suggesting that these proteins might be responsible for the poor motility at earlier stages of purification.

To test this possibility directly, we assayed for gliding activity using taxol-stabilized microtubules with or without MAPs. Microtubules containing MAPs (Figure 1, lane 1) displayed no motility, while those from which the MAPs had been extracted with 0.5 M NaCl (lane 2) showed excellent gliding motility. MAPs prepared from calf brain by a variety of procedures were combined with microtubules composed of purified tubulin and assayed for gliding activity. The samples used for these experiments included unfractionated DEAE-purified MAPs, purified MAP2 and tau, and microtubule binding fragments of heat stable MAPs prepared by chymotrypsin digestion (Vallee, 1986). All of these preparations were found to inhibit microtubule gliding.

In the case of the high molecular weight MAPs, inhibition of motility could be envisaged to result from steric hindrance of the interaction of the microtubule with dynein on the coverslip by the extremely long (~90-100 nm) MAP arms (Voter and Erickson, 1982). Alternatively, it might reflect competition between dynein and the other MAPs for a common microtubule-binding site. To distinguish between these possibilities we examined the effect of purified MAP2 on the brain cytoplasmic dynein ATPase activity (Figure 2). MAP2 was found to inhibit the microtubule activated component of the ATPase activity by 80%, with 50% inhibition occurring at a MAP 2:tubulin dimer ratio of 1:15 mol:mol (Figure 2). Microtubule-binding fragments of MAP2 produced by chymotryptic digestion of calf brain microtubules followed by exposure to elevated temperature (Vallee, 1986) also inhibited the dynein ATPase by 80-97% (not shown). Together, these results indicated that cytoplasmic dynein and MAP2 competed for common or overlapping binding sites on the microtubule surface.

Interaction of dynein with the tubulin carboxyl terminus.

In view of evidence that MAP2 interacts with the C-terminus of α and β-tubulin (Serrano et al., 1984; Littauer et al., 1986), we exposed microtubules to subtilisin and examined the effect of this treatment on the interaction with cytoplasmic dynein. Since the assembly of subtilisin-treated tubulin subunits leads to the formation of morphologically abberant polymers (Serrano et al.,

1986) we used taxol-stabilized microtubules as the substrate for the protease. Thin section electron microscopy revealed that subtilisin had no detectable effect on the morphology of the taxol-stabilized microtubules (Figure 3). Nonetheless, the fragmentation pattern was identical to that obtained by digestion of tubulin dimers (Bhattacharyya et al., 1985). Proteolysis proceeded sequentially, first with the cleavage of β and subsequently with the cleavage of α-tubulin (Figure 4A; Sackett et al., 1985). We confirmed the removal of the carboxyl region of α-tubulin by probing with an antibody which recognizes the C-terminus in its tyrosinated form (anti-tyr, Gunderson et al., 1984). The shift of α-tubulin to a faster migrating species (120') was coincident with the loss of antibody immunoreactivity. Similarly, the shift in β-tubulin resulted in the loss of immunoreactivity with an antibody directed to the extreme C-terminus (residues 439-445; see Banerjee et al., 1988) of this subunit (not shown). Subtilisin treatment of microtubules greatly reduced the binding of the high molecular weight MAPs to microtubules as previously reported (Serrano et al., 1984). We note that the binding of the MAP1 polypeptides as well as MAP2 was reduced.

Figure 4B shows the effect of microtubules on the cytoplasmic dynein ATPase during the time-course of subtilisin digestion. The microtubule-activated ATPase activity was reduced by 80% after digestion of both α and β-tubulin. About 50% of the reduction could be accounted for by the digestion of β alone, while the remainder

was accounted for by the digestion of α-tubulin. We also measured ATPase activity as a function of microtubule concentration. In the presence of undigested microtubules, the ATPase activity saturated at ~1 mg/ml (Figure 4C, upper curve), consistent with previous data from our laboratory (Shpetner et al., 1988). Subtilisin digestion of the microtubules greatly reduced the extent of activation (Figure 4C, lower curve). In a separate experiment, the removal of the C-terminus of β-tubulin (with α-tubulin left intact) increased the Km from 0.53 mg/ml (control) to 2.22 mg/ml (not shown). We conclude that the C-terminus of both α and β-tubulin are directly involved in activation of the cytoplasmic dynein ATPase.

The residual microtubule activation after subtilisin treatment suggested that there could be an additional site of interaction with dynein. We treated taxol-stabilized microtubules with thermolysin, a protease which had been reported to cleave the α subunit of tubulin at a single site (Brown and Erickson, 1983). The α-tubulin shifted to a position near that of β-tubulin (Figure 5A) corresponding to an apparent loss of ~5 kD (op. cit.). The retention of C-terminal immunoreactivity (anti-tyr) indicated that , in contrast to subtilisin, the site of cleavage was near the N- (amino) terminus. To establish the exact site of cleavage, we subjected the thermolysin-digested tubulin to N-terminal microsequence analysis. The resulting sequence, IGGGDDSF, identified the site of cleavage on α-tubulin as the N-side of isoleucine 42 (cf. Ponstingl et al., 1981). Exposure of dynein to thermolysin-treated microtubules revealed no detectable

effect on the microtubule-activated ATPase activity (Figure 5B). We also found that unfractionated MAPs rebound to thermolysin-cleaved tubulin (not shown), indicating that the N-terminus of α-tubulin is required neither for activation of the dynein ATPase or for binding to the structural MAPs.

Site of subtilisin cleavage.

As noted above, we monitored the removal of the C-terminus of α-tubulin with a site-directed antibody prepared against the terminal octapeptide of the tyrosinated form of α-tubulin, referred to as anti-tyr tubulin (Gunderson et al., 1984). In the course of these experiments, we also used an antibody prepared against the same sequence but lacking the C-terminal tyrosine (op. cit.). This antibody is referred to as anti-Glu since glutamic acid is the C-terminal amino acid. The immunoreactivity of each of the two antibodies is monospecific for the sequence against which it was generated.

To our surprise, the anti-Glu antibody was immunoreactive with the subtilisin-treated tubulin (Figure 6A). This was in contrast to the result obtained with the anti-tyr antibody and suggested that the site of cleavage was much closer to the C-terminus (Figure 6B) than previously reported (Serrano et al., 1984; Maccioni et al., 1986). This conclusion was corroborated by the immunoreactivity with antibody DM 1A (Figure 6A), a probe reported to show its strongest reactivity with amino acids 426-430 of alpha tubulin (Breitling and Little, 1986). Thus, the epitopes for the DM 1A monoclonal antibody

and the site directed detyrosinated tubulin (anti-Glu) antibody both reside in the region previously thought to be removed by subtilisin treatment. In addition, the modified tubulin was reactive with antibody DM 1B (Figure 6A), a monoclonal reported to react with amino acids 416-430 of β-tubulin (Breitling and Little, 1986).

Together, these data indicated that subtilisin removed a very limited number of amino acids from the C-terminus of α and β-tubulin. To determine whether the apparent molecular weight shift on gels might have been due to similtaneous cleavage of the N-terminus, the subtilisin-treated tubulin was subjected to N-terminal microsequence analysis. The resulting sequences were MRECIS and MREIVH for α and β-tubulin, respectively, which correspond to the N-termini of the intact subunits. Direct C-terminal sequencing of the subtilisin-treated tubulin failed to provide useful information despite repeated attempts (D. Lane, Harvard Microchemistry Facility, personal communication).

Discussion

Our earlier observation that microtubule gliding motility improved during the purification of brain cytoplasmic dynein indicated that brain microtubules contained a motility inhibitory factor (Paschal et al., 1987). Here we have shown that the high molecular weight MAPs inhibit microtubule gliding, suggesting that they were responsible for the earlier observation. Inhibition of motility could in part be due to interference by the long MAP arms

with the accessibility of microtubules to the dynein-coated coverslip. However, inhibition of the dynein ATPase (Figure 2) indicates that the MAPs compete with cytoplasmic dynein for binding sites on the microtubule surface. This was independently confirmed by the observation that the chymotryptic binding fragments of the MAPs were sufficient to inhibit motility and ATPase activities. We found that both purified MAP2 (Figure 2) and tau (B. P., preliminary observations) inhibited the cytoplasmic dynein ATPase activity. This result is consistent with recent evidence indicating homology within the microtubule binding domains of MAP2 and tau (Lee et al., 1988; Lewis et al., 1988).

Both MAP2 and tau have been reported to interact with the C-terminus of α and β-tubulin (Serrano et al., 1984; Littauer et al., 1986; Maccioni et al., 1988), and our MAP inhibition data suggest that the C-termini are likely sites for the interaction of cytoplasmic dynein as well. The earlier localization of the MAP2 and tau binding sites was in part based on the loss of MAP binding after modification of tubulin with subtilisin (Serrano et al., 1984). This protease was reported to remove the C-termini of both α and β-tubulin, though our work has now raised serious questions as to the precise sites of subtilisin cleavage (Figure 6, and see below). Thermolysin was used to modify microtubules in the present study, and found to specifically remove the N-terminus of α-tubulin.

Unlike earlier workers, we used taxol-stabilized microtubules as the substrate for proteolytic modification. This was to minimize

the likelihood that proteolytic modification would alter the structure of the microtubule, and perhaps indirectly affect the interaction with cytoplasmic dynein. In fact, we found that both rates and patterns of fragmentation for taxol-stabilized microtubules were the same as had been reported using tubulin dimers as substrate, and that the microtubules were of normal morphology after enzymatic modification. Our data indicate that at least three of the polypeptide termini of α and β-tubulin are exposed on the microtubule surface. This is consistent with the accessibility of the termini in the polymer to enzymes (Kumar et al., 1981) and to antibodies (Wehland et al., 1983b). The accessibility of amino acids 41-42 to thermolysin suggests that the acetylation site at lysine 40 of α-tubulin is also exposed on the microtubule surface.

We found that subtilisin treatment dramatically reduced the ability of microtubules to stimulate the brain cytoplasmic dynein ATPase. Lineweaver-Burke plots of experiments such as shown in Figure 4C indicated that this effect was principally due to a decreased affinity of microtubules for dynein, reflected by the large increase in K_m. The time course of digestion indicated that both α and β-tubulin were involved in the interaction. Subtilisin-treated microtubules also showed a reduced ability to glide on dynein coated coverslips. We note, however, that even after extensive digestion of the microtubules (to the point where C-terminal tyrosine was undetectable by immunoblotting) some activation of the dynein ATPase (Figure 4) and some microtubule gliding were observed.

These data suggest that tubulin residues other than those liberated by subtilisin probably contribute to the dynein interaction site.

Digestion with thermolysin had no effect on the ability of microtubules to activate the dynein ATPase. This indicated that the N-terminus of α-tubulin is probably not involved in the interaction of the microtubule with cytoplasmic dynein. This result has particular significance because sequence analysis of the thermolysin-digested tubulin revealed the removal of ~5 kD from the N-terminus, including the site of tubulin acetylation. Thus, our data suggest that this post-translational modification, the function of which is unknown, is not involved in regulating dynein activity.

The site of subtilisin cleavage was initially assigned to the C-terminus based on the loss of ^{14}C-labeled tyrosine that had been introduced at this end of the polypeptide by tubulin tyrosine ligase (Serrano et al., 1984). The site of cleavage of β-tubulin could not be similarly monitored due to the lack of an appropriate labelling mechanism. Subtilisin cleavage was estimated to release ~4 kD from each subunit based on the change in electrophoretic mobility (Serrano et al., 1984). In a subsequent study, however, native gel electrophoresis indicated that the charge reduction in the tubulin dimer following subtilisin digestion corresponded to the net loss of about 9 negatively charged amino acids (Sackett et al., 1985). This is substantially fewer than would be predicted from the removal of 4 kDa from the C-termini of the two subunits.

We confirmed that the C-terminus of α-tubulin was removed by subtilisin by using the anti-tyr antibody. We have also established that the sequence removed from β-tubulin is at the C-terminus, since a mAb directed against the terminal nonapeptide failed to react with the subtilisin-treated tubulin. However, two different antibodies which recognize sequences near the C-terminus of α-tubulin, and one antibody which recognizes a sequence near the C-terminus of β-tubulin, all reacted with the subtilisin-treated tubulin. We considered the possibilty that the large electrophoretic shift could result from the loss of ~4 kD from the N-termini. However, direct N-terminal sequence analysis of the subtilisin modified α and β-tubulin revealed that the N-termini remained intact. Thus, we conclude that removal of only a small portion of the tubulin C-terminus results in an anomalously large electrophoretic shift of each subunit.

How close to the C-terminus is the site of subtilisin cleavage? Remarkably, the persistence of reactivity with the anti-Glu antibody suggests that the site must reside within the final eight amino acids of α-tubulin. We note that the antibody shows no reactivity with the tyrosinated form of tubulin (Gunderson et al., 1984). This suggests that the epitope must include the carboxyl end of the immunogenic heptapeptide GEEEGEE. We find only one way in which a similar epitope can be generated by proteolysis, and that is by removal of the four C-terminal amino acids of α-tubulin. This, interestingly, exposes exactly the same tetrapeptide sequence found in the native

detyrosinated tubulin molecule. Thus, the epitope likely consists of the sequence EGEE, with antibody recognition requiring the C-terminal glutamic acid to be unmodified. Cleavage at this site disrupts the cytoplasmic dynein and MAP interaction with the microtubule. This seems to imply that the sequence EGEE represents not only the anti-Glu epitope, but the site of interaction of MAP 2 and dynein as well. However, subtilisin cleavage would then generate a new MAP interaction site, much as its generates a new epitope for the anti-Glu antibody. Thus, the interaction site may be somewhat larger than EGEE, for example EEGEE, or it may span the subtilisin cleavage site. This could explain why subtilisin cleavage inhibits the dynein interaction with the microtubule but does not completely abolish it (Figure 4B,C).

We note that, despite the relative variable nature of the α and β-tubulin C-termini, EGEE and EEGEE are both well conserved phylogenetically (reviewed by Cleveland and Sullivan, 1985; Little and Seehaus, 1988). EGEE is found at the C-termini of 15 of 21 metazoan α-tubulins, and EDEE in one Drosophila α-tubulin. EEGEE or related sequences (such as DEGEE) are found in the same tubulins. Twelve of 24 β-tubulins contain EEGEE or EEAEE close to their C-termini. This suggests that this may be the site of dynein and MAP interaction in the β as well as the α-subunit. It is conceivable that some variant forms of tubulin bind MAPs and cytoplasmic dynein via only the α or β-subunit, or have a decreased affinity for the associated proteins.

It has been estimated by Wolff and coworkers that a total of nine acidic residues are lost from the αβ dimer upon subtilisin treatment (Sackett et al., 1985). Our model predicts the removal of three regative charges from the α-subunit, suggesting that six acidic residues are removed from the β-subunit. The loss of six negatively charged amino acids from the C-terminus of β-tubulin is consistent with cleavage site lying between the DM 1B epitope, which is preserved during subtilisin treatment, and the sequence EGEE, which is presumably lost. Our findings are also consistent with an earlier study which examined the binding of MAPs to protease-derived and synthetic tubulin peptides imobilized on nitrocellulose (Littauer et al., 1986). Based on the binding to overlapping peptides, it was concluded that the sequence GEFEEEG in rat β-tubulin was involved in the interaction with MAP2 and tau. The sequence EFEE within this region could be functionally equivalent to EGEE, though we suggest that the sequence EEGED, which represents the C-terminal continuation of this sequence, is also a candidate for the MAP binding site. In a separate study, peptides derived from the C-terminal region of α-tubulin showed a weak interaction with MAP2 and tau (Maccioni et al., 1988), and no attempt was made to precisely define the binding site. Our data, and those of Bhattacharyya et al. (1985) and Littauer et al. (1986) all indicate that the MAP and cytoplasmic dynein interaction site is much smaller than previously proposed (Serrano et al., 1984; Maccioni et al., 1986). On the basis of the shift in electrophoretic mobility and amino acid analysis of the subtilisin

digestion products, Maccioni and coworkers (Serrano et al., 1984; Maccioni et al., 1986) placed the site of subtilisin cleavage at Phe^{408} and Phe^{418} in α and β-tubulin, respectively.

Our results with the anti-Glu antibody indicate that a limited sequence within the pentultimate eight amino acids of α-tubulin is involved in cytoplasmic dynein and MAP interaction. However, they do not address the role of the C-terminal tyrosine in α-tubulin. Extensive evidence indicates a correlation between the removal of this tyrosine by a specific tubulin carboxypeptidase with increased stability of the microtubule (Gunderson et al., 1987). However, dramatic differences in MAP binding of tyrosinated and detyrosinated tubulin have not been observed (J. C. Bulinski, personal communication).

Recently, Rodionov and coworkers (Rodionov et al., 1990) have reported than kinesin interacts with a domain of tubulin which is outside of the C-terminal region characterized in this study. The authors also suggested that cytoplasmic dynein binds outside the C-terminal region based on a sedimentation experiment with subtilisin-modified tubulin (op. cit.). In preliminary experiments, we also have observed limited rebinding of cytoplasmic dynein to subtilisin-tubulin. These data indicate that the site of interaction of cytoplasmic dynein with tubulin is complex. Thus, the acidic C-terminal region identified in the present study is necessary for activation of the dynein ATPase, while sequences outside the C-

terminus may be sufficient for rebinding of cytoplasmic dynein to tubulin.

The existence of a common site for the interaction of the structural MAPs and cytoplasmic dynein with microtubules would seem to be problematic for the cell. Perhaps there are distinct populations of MAP-containing and MAP-free microtubules in cells, the latter serving as the tracks for organelle transport. Trains of organelles have, in fact, been observed in lobster axons following release from a cold block, suggesting that transport may occur along a subset of microtubules (Miller et al., 1987).

It is also possible that the MAPs serve as regulators of motility in the cell. Since MAP2 is restricted in its distribution to neuronal dendrites (DeCamilli et al. 1984), it could potentially serve to prevent certain classes of organelles from entering the dendrite. Alternatively, if the cellular levels of MAPs are below saturation for tubulin binding sites, the MAPs could serve to regulate the rate or frequency of organelle movement. This role would be analogous to that of tropomyosin regulation of myosin. Since phosphorylation of the microtubule binding domain of MAP2 has been found to weaken its affinity for microtubules (Burns et al., 1984), this modification could, in turn, serve to regulate dynein function.

Clearly, further work will be needed to explore the implications of this novel role for the MAPs, and to determine the effect of the C-terminal tyrosine on the interaction of microtubules with MAPs and with the motor molecules.

Figure Legends

Figure 1. Microtubules with and without MAPs differ in gliding activity. Taxol-stabilized microtubules were assayed for dynein-mediated gliding activity in the presence and absence of MAPs. The samples were analyzed on an 8% polyacrylamide gel. The MAP-containing microtubules (lane 1) displayed no motility (-), while removal of the MAPs with Tris-KCl containing 0.5 M NaCl (lane 2) restored gliding activity (+).

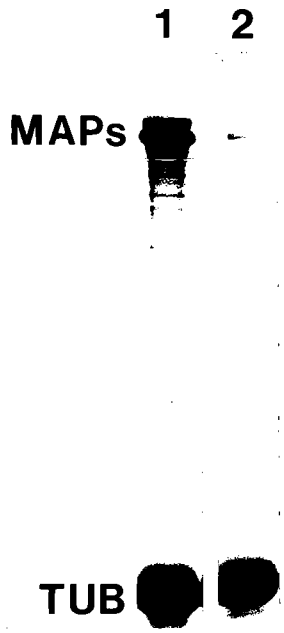
1 2
MAPs
TUB
— —
− +

Figure 2. The microtubule activated ATPase activity of cytoplasmic dynein is inhibited by MAP2. The data shown represents the microtubule activated ATPase activity after subtraction of the basal activity.

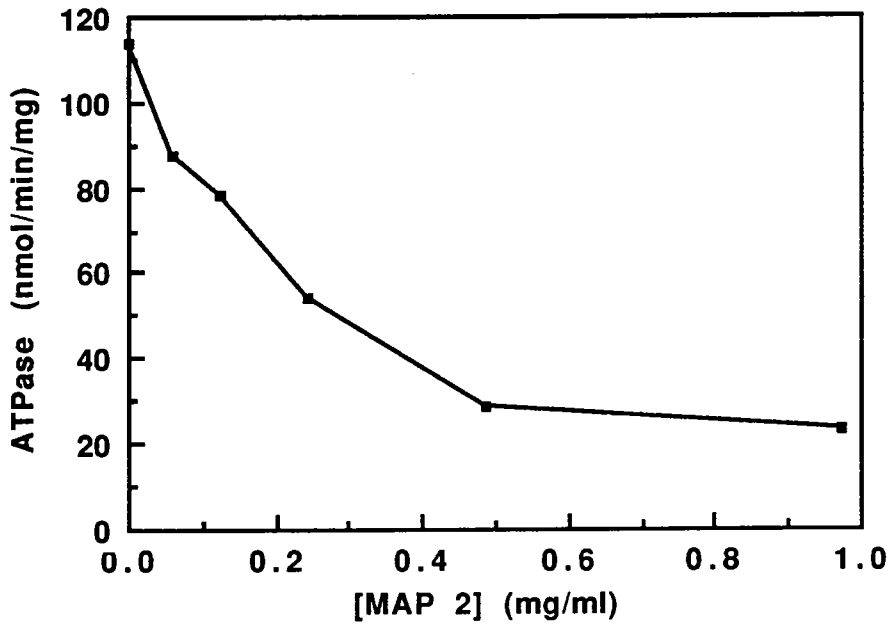
120
100
80
60
40
20
0
ATPase (nmol/min/mg)
0.0
0.2
0.4
0.6
0.8
1.0
[MAP 2] (mg/ml)

Figure 3. Thin section electron microscopy of unmodified and subtilisin-treated taxol-stabilized microtubules. Microtubules were digested for 0 (A,B), 15 (C), and 140 minutes (D,E) and processed for electron microscopy as previously described (Vallee, 1982). Protease-treated microtubules maintain a normal morphology when stabilized with taxol prior to digestion. In contrast, digestion of tubulin dimers with subtilisin results in the formation of hook-like structures (cf. Serrano et al., 1986). Bar, 50 nm.

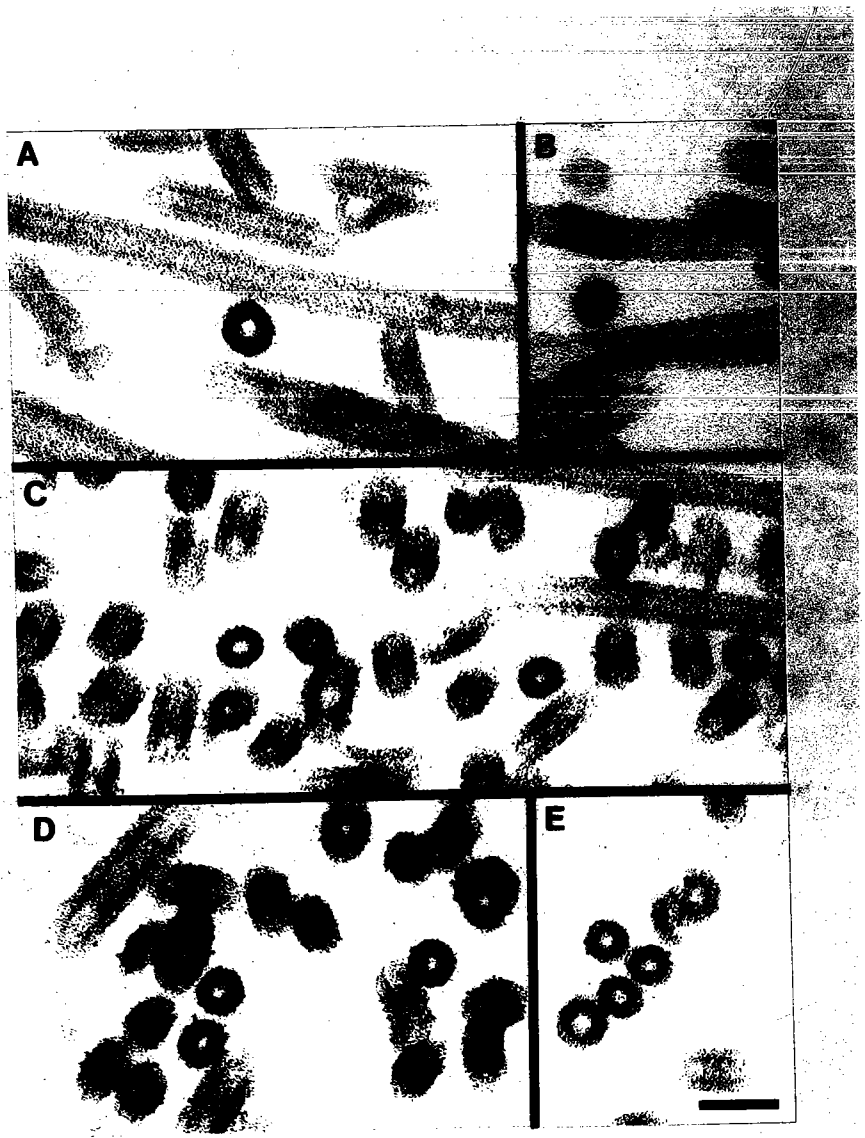
A
B
C
D
E

Figure 4. The effect of subtilisin digestion of α and β-tubulin on cytoplasmic dynein ATPase activity. (A) Electrophoretic analysis of digested tubulin. Taxol-stabilized microtubules were exposed to subtilisin for 0, 60, and 120 minutes and examined by Coomassie Blue staining (CB) and immunoblotting with an antibody to the tyrosinated form of α-tubulin (anti-tyr). β-tubulin was observed to shift to a lower molecular weight by 60 minutes, while α-tubulin shifted to a lower molecular weight by 120 minutes. The shift of α-tubulin coincided with the loss of immunoreactivity, indicating that the C-terminus of α-tubulin was removed during subtilisin digestion. (B) Effect of subtilisin digestion on microtubule activation of the dynein ATPase. Taxol-stabilized microtubules were exposed to subtilisin for the times indicated, and assayed for activation of the dynein ATPase. The reduction in activity appears biphasic, with a relatively rapid decline corresponding to the digestion of β-tubulin, and a slower decline corresponding to the digestion of α-tubulin. (C) The ATPase activity of cytoplasmic dynein as a function of microtubule concentration. ATPase activity in the presence of untreated microtubules (■) and microtubules previously exposed to subtilisin for 140 minutes (○). The data in B and C are expressed after subtraction of the basal (unstimulated) ATPase.

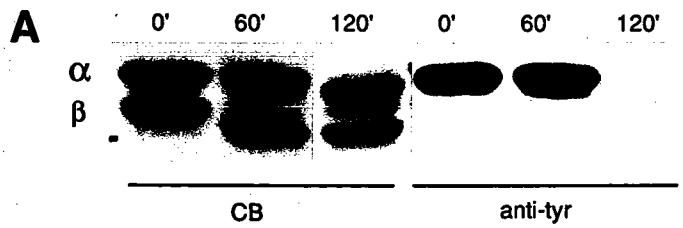
A
0'
60'
120'
0'
60'
120'
α
β
CB
anti-tyr

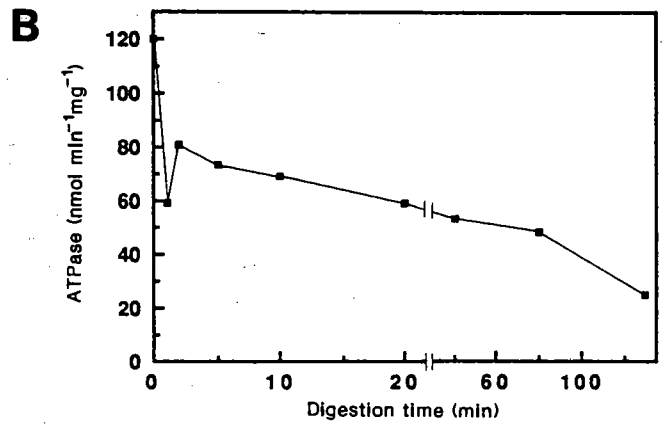
B
ATPase (nmol min⁻¹mg⁻¹)
120
100
80
60
40
20
0
0
10
20
60
100
Digestion time (min)

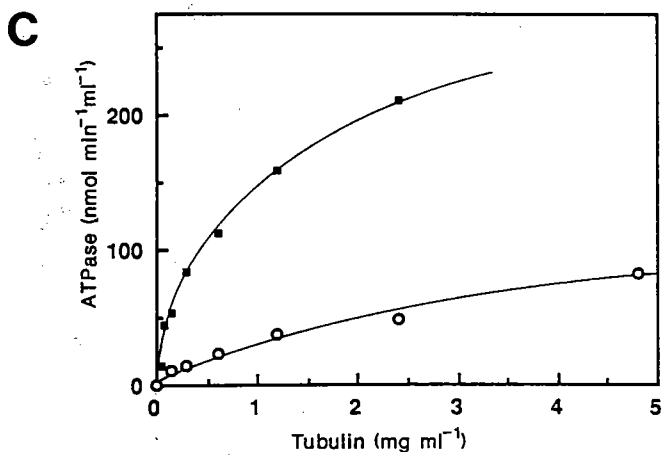
C
ATPase (nmol min⁻¹ml⁻¹)
200
100
0
0
1
2
3
4
5
Tubulin (mg ml⁻¹)

Figure 5. The effect of thermolysin digestion of α-tubulin on cytoplasmic dynein ATPase activity. (A) Electrophoretic analysis of digested tubulin. Taxol-stabilized microtubules were exposed to 0, 0.1%, and 1.0% thermolysin and examined by Coomassie blue staining (CB) or immunoblotting with the anti-tyr antibody used in figure 4A. The shift of α-tubulin to a faster migrating species did not result in a loss of reactivity, indicating that the N-terminus was removed during digestion. (B) The microtubule-activated ATPase activity of cytoplasmic dynein as a function of microtubule concentration. ATPase activity in the presence of untreated microtubules (■) and microtubules previously exposed to 1.0% thermolysin for 15 minutes (○). The data shown represents the microtubule-activated ATPase activity after subtraction of the basal activity.

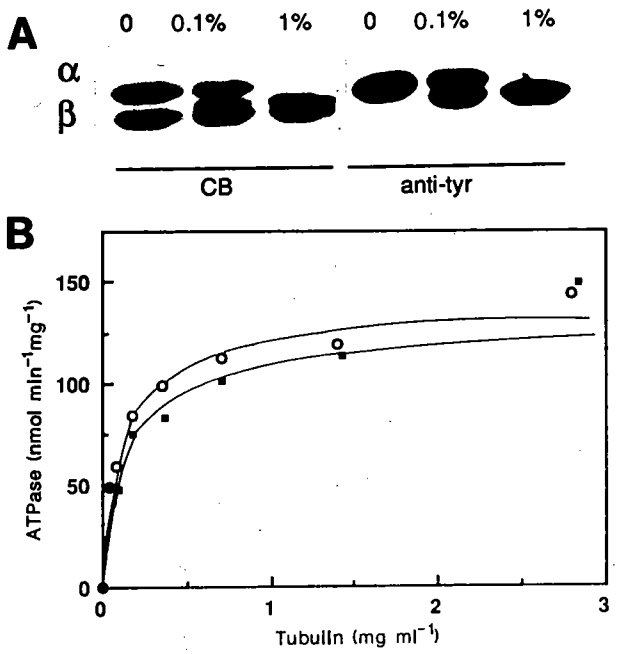
A
0
0.1%
1%
0
0.1%
1%
α
β
CB
anti-tyr
B
150
100
50
0
0
1
2
3
ATPase (nmol min^{-1}mg^{-1})
Tubulin (mg ml^{-1})

Figure 6. Analysis of the sites of subtilisin cleavage. (A) Immunoblot analysis of subtilisin-treated tubulin. Taxol-stabilized microtubules were digested with 1.2% subtilisin for 60 and 120 minutes and analyzed by gel electrophoresis and immunoblotting. CB, Coomassie blue; TYR, immunoblot using a site directed antibody generated against the C-terminal sequence GEEEGEEY of tyrosinated α-tubulin (Gunderson et al., 1984); GLU, site-directed antibody generated against GEEEGEE of detyrosinated α-tubulin (op. cit.); DM1A, mAb reported to react most strongly with amino acids 426-430 of α-tubulin (Breitling and Little, 1986); DM1B, mAb whose epitope lies within amino acids 416-430 of β-tubulin (op. cit.). The anti-Glu reactivity was weaker with the subtilisin fragment, but was clearly positive. (B) Schematic representation of protease cleavage sites and epitope locations within the C-terminal regions of α and β-tubulin. The positions of the subtilisin (Sub) and thermolysin (Therm) cleavage sites deduced from the present study are indicated, along with the previously proposed sites of subtilisin cleavage (open arrows). On the basis of the shift in electrophoretic mobility and amino acid analysis of the subtilisin digestion products, the sites of subtilisin cleavage were previously assigned to Glu^{417}-Phe^{418} and Glu^{407}-Phe^{408} in α and β-tubulin, respectively (Serrano et al., 1984; Maccioni et al., 1986). Our results are consistent with the removal of a total of nine acidic residues from the tubulin dimer as judged by native gel electrophoresis (Sackett et al., 1985). The antibody JDR.3B8 was generated against the sequence EGEEDEA, which

corresponds to the C-terminus of β-tubulin (Banerjee et al., 1988). The subtilisin cleavage site in β-tubulin (dashed line) is predicted to fall between the DM1B and JDR.3B8 epitopes, the latter of which is lost by subtilisin treatment. (C) C-terminal sequence of porcine α and β-tubulin beginning at the previous proposed subtilisin cleavage sites (single letter code). The sequence of the peptide used to generate the anti-Glu antibody is bracketed. The sequence EGEE (bold) comprises a significant portion of the anti-Glu epitope, and of the MAP2 and cytoplasmic dynein interaction site as well.

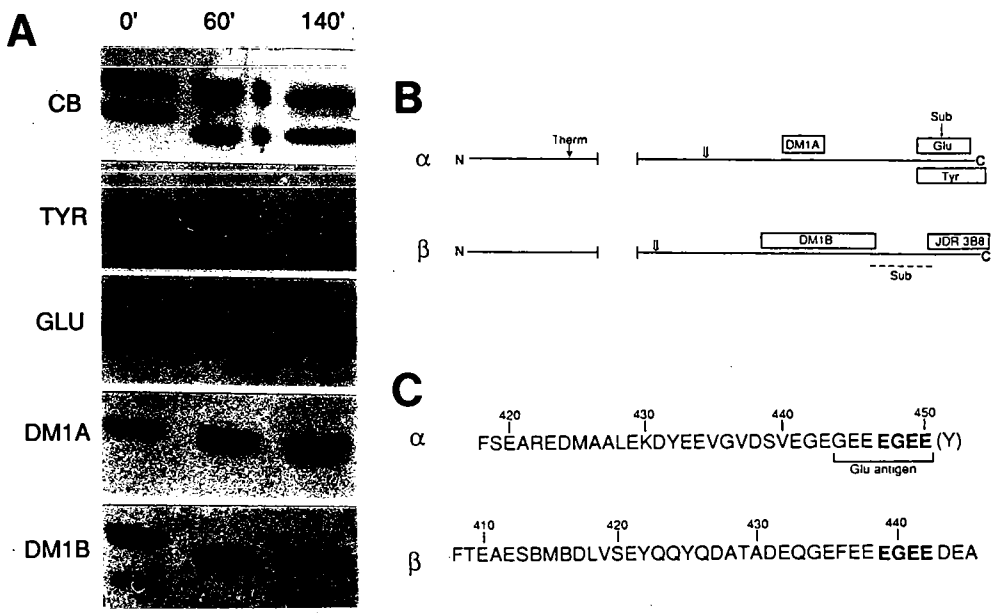
A
0'
60'
140'
CB
TYR
GLU
DM1A
DM1B
B
α
N
Therm
DM1A
Sub
Glu
Tyr
C
β
N
DM1B
JDR 388
Sub
C
C
α
420
430
440
450
FSEAREDMAALEKDYEEVGVDSVEGEGEE EGEE (Y)
Glu antigen
β
410
420
430
440
FTEAESBMBDLVSEYQQYQDATADEQGEFEE EGEE DEA

CHAPTER III

MOLECULAR CLONING OF THE 74 kDa SUBUNIT OF MAMMALIAN CYTOPLASMIC DYNEIN REVEALS HOMOLOGY WITH THE 70 kDa SUBUNIT OF *CHLAMYDOMONAS* FLAGELLAR OUTER ARM DYNEIN

Cytoplasmic dynein is a multisubunit enzyme complex which couples ATP hydrolysis with force production towards the microtubule minus end (Paschal et al., 1987; Paschal and Vallee, 1987). It is thought to be responsible for retrogrograde axonal transport (Paschal and Vallee, 1987; Schnapp and Reese, 1989; Schroer et al., 1989; Hirokawa et al., 1990; Lacy and Haimo, 1992) as well as minus end-directed movements of organelles such as lysosomes (Lin and Collins, 1992) and chromosomes (Reider and Alexander, 1990; Pfarr et al., 1990; Steuer et al., 1990; Hyman and Mitchison, 1991).

Biochemical and structural studies of cytoplasmic dynein have revealed several common properties with its axonemal counterparts, but significant differences as well (Paschal et al., 1987; Shpetner et al., 1988; Vallee et al., 1988). Among the conserved features are the high molecular weight heavy chains, responsible for ATP hydrolysis and force production. Both cytoplasmic and axonemal dyneins also contain a collection of accessory subunits, known in the case of axonemal dyneins as intermediate and light chains. However, the composition of accessory subunits is strikingly different between axonemal and cytoplasmic forms of the enzyme, suggesting that

these polypeptides may specify distinct functions. Cytoplasmic dynein from mammalian brain, testis, and liver all contain copurifying polypeptides of 150, 74, 59, 57, 55, 53 and 40-50 kDa (Paschal et al., 1987; Neely and Boekelheide, 1988; Collins and Vallee, 1989). The intermediate and light chains of axonemal dyneins range in size from 69-120 kDa and 14-20 kDa depending on the species examined (Pfister et al., 1982; Piperno and Luck, 1979; Tang et al., 1982; reviewed by Johnson, 1985).

Relatively little is known about the function of the accessory subunits, but recent work has suggested that several of these polypeptides could be involved in subcellular targeting. The most extensively studied axonemal dynein accessory subunits are those of *Chlamydomonas* flagellar outer arm dynein. Direct evidence for a role for these proteins in targeting has come from cross-linking studies in detergent permeabilized axonemes, which revealed direct binding between the 80 kDa intermediate chain and alpha tubulin (King et al., 1991). The 80 kDa subunit can also be dissociated from the dynein holoenzyme in a complex with the 70 kDa intermediate chain (Mitchell and Rosenbaum, 1986), the latter of which has been localized to the base of the holoenzyme by immunoelectron microscopy (King and Witman, 1990). The 70 kDa subunit has been identified as the product of the *ODA6* gene in *Chlamydomonas* (Mitchell and Kang, 1991) and mutations in this locus result in defective flagellar motility (Kamiya, 1988). Whether the accessory subunits of cytoplasmic dynein are similarly localized and play

comparable roles in organelle or kinetochore targeting remain unanswered questions of considerable importance.

To address the role of the cytoplasmic dynein accessory subunits, we have set out to determine their primary structures by cDNA cloning. In an earlier study we described the molecular cloning and sequencing of a 150 kDa cytoplasmic dynein-associated polypeptide. We found this polypeptide to be the apparent mammalian homologue of a similar-sized *Drosophila* protein, the product of the *Glued* locus (Holzbaur et al., 1991). The $p150^{Glued}$ polypeptide is present in most (Collins and Vallee, 1989; Gill et al., 1991), but not all cytoplasmic dynein preparations (Paschal et al., 1987). It also is a component of a biochemical fraction reported to stimulate in vitro vesicle motility (Schroer and Sheetz, 1991), though a specific role for the 150 kDa polypeptide in the active fraction has not been resolved.

The present study regards the molecular cloning of the 74 kDa subunit of cytoplasmic dynein. This polypeptide has been found to copurify with the brain cytoplasmic dynein complex at a constant stochiometry of 3.1 $\pm$ .2 :1 (mean $\pm$ SD) by sucrose gradient centrifugation, gel filtration, ion exchange, and hydroxylapatite chromotography (Paschal et al., 1987). It has also been found at comparable levels in cytoplasmic dynein purified from rat liver and testis (Collins and Vallee, 1989; Neely and Boekelheide, 1988), and what appears to be the same polypeptide has been described in Hela cells (Pfarr et al., 1990) and chick brain (Steuer et al., 1990).

We report here the primary structure of the 74 kDa subunit along with evidence for the existence of at least three isoforms. We find that the 74 kDa species contains significant sequence identity with the product of the *ODA6* locus in *Chlamydomonas* (Mitchell and Kang, 1991), the 70 kDa intermediate chain of outer arm dynein (Mitchell and Kang, 1991). This suggests that the cytoplasmic and axonemal intermediate chains may carry out related functions within their respective holoenzymes.

Materials and Methods

Protein chemistry.

Cytoplasmic dynein was purified from calf brain white matter cytosol as previously described (Paschal et al., 1991). For peptide sequencing, the 20S sucrose gradient fractions were pooled and centrifuged at 45,000 rpm for 16 hours in a 50Ti rotor (Beckman Instruments, Palo Alto, CA) to concentrate the cytoplasmic dynein. The resulting small, clear pellet was resuspended in 0.5 ml of SDS PAGE sample buffer (Laemmli, 1970) modified to contain 10% SDS, and boiled for 10 minutes. The sample, containing approximately 250 μg of total protein, was applied to a 9% polyacrylamide minigel (Biorad, Richmond, CA) and electrophoresed at 25 milliamps constant current. The gel was transferred to nitrocellulose (0.45 μm pore size, Schleicher and Schuell, Keene, NH) in a methanol-containing buffer (Towbin et al.,1979) at 100 volts constant voltage for one hour. The nitrocellulose filter was stained with 0.1% Ponceau S in 1% acetic acid for 1 minute to visualize protein. The filter was destained for 1-2 minutes in 1% acetic acid. The 74 kDa band was excised and further destained in 0.2 mM NaOH for 1-2 minutes, washed in distilled water, and stored wet at -20°C until use. Trypsin digestion of the nitrocellulose-immobilized protein (in situ digestion), elution of the peptides, and HPLC using a C_{18} reverse phase column were carried out essentially as described (Aebersold, 1989). The amino acid sequences of seven HPLC-purified peptides were determined on an

Applied Biosystems Model 470A sequenator at the Worcester Foundation for Experimental Biology Protein Chemistry Facility.

The sequence of peptide 8 was derived from an SDS PAGE-purified 40 kDa tryptic fragment of 20S dynein, the details of which will be described elsewhere. Peptide 9 was generated by Staphylococcus aureus V8 protease digestion of SDS PAGE-purified 74kDa protein (Gooderham, 1984). The fragments resulting from the V8 digest were separated on a 9% polyacrylamide gel, transferred to Immobilon (Millipore, Medford, MA), visualized by Coomassie blue staining, and excised for N-terminal microsequence analysis (Matsudaira, 1987).

cDNA cloning.

The 57 base sense strand oligonucleotide, 5'-AAGCCTGTGGCTGTGACAGGCATGGCCTTCCCCACAGGGGATGTGAACAACT TTGTG-3', was a "guessmer" whose design was based on the sequence of peptide 6 (Lathe, 1985). Subsequent cDNA sequence analysis revealed this oligonucleotide to be 87.7% identical with the actual 74 kDa cDNA. An oligo$(dT)_{12-18}$ primed λgt10 library (provided by Dr. Atsushi Mikami, Worcester Foundation) prepared from adult rat brain poly(A) RNA was plated and screened using standard methods (Sambrooke et al., 1989). Hybridization of the ^{32}P end-labeled 57mer (8 x 10^6 cpm/pmol oligonucleotide) was carried out in 6X SSC, 5X Denhardt's solution, 0.5% SDS, 100 μg/ml sheared salmon sperm DNA, and 0.05 M sodium phosphate, pH 6.8, at 52°C overnight. The

final wash condition, determined empirically, was 1X SSC/0.1% SDS at 56°C for 25 minutes. The positive clones were plaque purified by two additional rounds of screening. The inserts of four clones ranging in size from 1.4 to 2.6 kbp were amplified by polymerase chain reaction (PCR) using λgt10 forward and reverse primers, restriction digested with the enzymes AluI, HaeIII, and HinfI (New England Biolabs, Beverly, MA), repaired with Klenow, and electrophoresed on a 2% agarose gel. The gel was photographed and processed for Southern blotting according to standard methods (Sambrooke et al., 1989) using the membrane Duralon-UV (Stratagene, La Jolla, CA). The blot was probed with the 57mer as described above, and the final wash condition was .2X SSC/.1%SDS at 60°C for 30 minutes. An AluI fragment of ~100 bp was found to hybridize to the 57mer under these conditions.

The ~100 bp AluI fragment was purified by adsorption to glass beads (GeneClean, Bio 101, La Jolla, CA) and subcloned into EcoRV and alkaline phosphatase-treated pBluescript SK(-) vector. Double stranded DNA sequencing with Sequenase (US Biochemical, Cleveland, OH) was performed according to the supplier's recommendations, except that primer annealing was at 60°C for 30 minutes.

The λ DNA was prepared from polyethylene glycol precipitated phage (Sambrooke et al., 1989) and subcloned into EcoRI and alkaline phosphatase-treated pBluescript SK(-). The 2.6 kbp insert of p74 contains an internal EcoRI site, and was, therefore, subcloned as two

fragments. The orientation of the two fragments was unambiguously established by comparison with the sequence of peptide 9 which spans the internal EcoRI restriction site. Subclones of the p74 cDNA were sequenced on both strands as described above.

All sequence manipulations, with the exception of the coiled-coil prediction (see legend to Figure 9), were performed with Genetics Computer Group Software (University of Winsconsin). The statistical significance of alignment scores was evaluated using the RDF2 Program (Lipman and Pearson, 1985) according to the equation z = (similarity score - mean of random scores)/ (SD of random scores). A value of $z > 10$ is considered significant (op. cit.).

Analysis of transcripts encoding 74kDa isoforms.

Northern blotting was carried out by standard methods (Sambrooke et al., 1989) using the Duralon-UV membrane. The blot was probed with the 839 bp 5' EcoRI fragment of p74 labeled with ^{32}P by nick translation. The probe for β-actin message, designed from the highly conserved second exon, was the antisense oligonucleotide 5'-CCAAATCTTCTCCATATCGTCCCAGTTGGT-3' (Nudel et al., 1983).

Transcript analysis by PCR was performed on first strand cDNA prepared using rat brain poly(A) RNA, AMV reverse transcriptase (BRL, Bethesda, MD), and oligo$(dT)_{12-18}$ primers. Twenty-eight cycles of PCR were carried out using Taq polymerase (Perkin Elmer, Norwalk, CT) and standard nucleotide, primer, and buffer

concentrations (Innis et al., 1990). The initial denaturation was at 95°C for 2 minutes. Denaturation during cycling was at 94°C for 30 seconds, primer annealing was at 52°C for 30 seconds, and extension was at 72°C for 30 seconds. The PCR products were repaired with Klenow, analyzed on a 4% NuSieve GTG agarose gel (FMC BioProducts, Rockland, ME), and subcloned into pBluescript for sequencing. The primer pairs are given below, with the corresponding region amplified in parentheses. a: 5'-GCAAATATGTCTGACAAGAGCG-3' and 5'-GGAGTGCTCACTGATTTCGAAG-3' (153-475). b: 5'-TCTTCGAAATCAGTGAGCACTC-3' and 5'-CCAGCTCTCGGCCGCTGTAGTC-3' (453-933). c: 5'-CCTCCAAGAGAGCTGACGGAAG-3' and 5'-TGTTCCAAACCAAGGCCACTCC-3' (786-1128). d: 5'-GCTGATGGTTGCTTCTTATAGC-3' and 5'-CCATTCCTGTAACAGCCACAGG-3' (1055-1488). e: 5'-TCAACAACTTCGTGGTCGGCAG-3' and 5'-TATTGGCGCGGATCTCCACCAG-3' (1507-2046). f: 5'-GACCTCTGGAACCTCAACAGTG-3' and 5'-GACACCGATACGGAAAGGACA-3' (1824-2195).

Gel electrophoresis and immunoblotting.

SDS PAGE was performed according to the method of Laemmli (1970), with the acrylamide concentrations noted in the legends. The gel in Fig.6 was a 5-10% polyacrylamide gradient with dimensions 160 x 140 x 1.5 mm, and was electrophoresed at 30 milliamps constant current. The method of Oakley et al. (1980) was used for silver staining. For western blots, post-transfer nitrocellulose filters

were blocked overnight in a solution containing 5% nonfat dry milk, 0.1% Tween-20, and 1 mM sodium azide in TBS. The anti-74kDa monoclonal antibody was used as ascites fluid in TBS containing .1% Tween-20 and 2% BSA. The dilutions were 1:1000 or 1:10,000 for 1 or 16 h incubations, respectively. Washes (3 x 20 minutes each) were in TBS containing 0.1% Tween-20. The secondary antibody was an affinity-purified peroxidase-conjugated sheep anti-mouse diluted 1:10,000 in TBS containing 0.1% Tween-20 and 2% BSA. Detection was achieved with Enhanced Chemiluminescence (Amersham, Arlington Heights, IL), using exposure times of 2-5 seconds.

Preparation of samples for expression analysis.

Tissue samples were taken from adult male Sprague-Dawley rats (Charles River Laboratories, Wilmington, MA). Tissues were homogenized with a motor-driven teflon pestle unit at 2000 rpm in 2 vol of buffer containing 100 mM Pipes, 1 mM $MgSO_4$, 0.25 M sucrose, and 1 mM PMSF. The homogenate was centrifuged for 30 seconds at half speed in a tabletop centrifuge to sediment debris and unbroken cells. Brain samples at different stages of development were prepared in a similar manner, except that sucrose was omitted and homogenization was performed using a Dounce tissue grinder. Aliquots for SDS PAGE and protein determination (Bicinchoninic acid method, Pierce, Rockford, IL) were frozen in liquid nitrogen and stored at -80°C until use.

Ram testes, prepared from tissue which had been stored at

-80°C, was homogenized with a teflon pestle and processed as described above. Pig tracheal cilia, a kind gift of Dr. Annette Hastie, Thomas Jefferson University School of Medicine, were prepared according to published methods (Hastie, 1991). Ram sperm tails were generously provided by Drs. Jovi San Agustin and George Witman (Worcester Foundation), and were isolated essentially as described by Calvin (1976).

Results

Isolation of cDNA's encoding the 74 kDa polypeptide.

Tryptic peptides prepared from the nitrocellulose-immobilized 74 kDa electrophoretic species by in situ digestion were purified by HPLC on a C_{18} column (Figure 7). The sequences of seven peptides as determined by pulse liquid phase microsequencing are shown in Figure 7. Two additional peptide sequences were obtained from tryptic digestion of dynein in solution (peptide 8) and from Staphylococcus aureus protease digestion of SDS PAGE-purified 74 kDa (peptide 9).

Using the amino acid sequence of peptide 6, a 57 nucleotide "guessmer" was designed taking into account codon bias and the selective deficiency of the intercodon dinucleotide pair 5' C-G 3' in higher eukaryotes (Lathe, 1985). An adult rat brain λgt10 cDNA library was screened and four clones containing inserts of 1.5 to 2.6 kb were isolated. The inserts were amplified by polymerase chain reaction (PCR) using λgt10 library primers, and examined by restriction enzyme analysis and Southern blotting with the 57mer probe. The fragment patterns generated with AluI, HaeIII, and HinfI revealed extensive overlap between the four clones. A short (~100 bp) AluI fragment which hybridized to the 57mer probe was sequenced, and the deduced amino acid sequence was found to match exactly with that of tryptic peptide 6. The longest cDNA,

designated p74, was amplified in *E. coli* and subcloned into pBluescript for DNA sequencing.

The first 158 bp of the p74 cDNA was found to be closed in all reading frames (Figure 8). Translation initiation is predicted to begin with the first in-frame AUG at base 159, which is preceded by a purine (A) in the -3 position (Kozak, 1991). The open reading frame encodes a 643 amino acid polypeptide with an isoelectric point of 4.9 and a molecular weight of 72,753 daltons, in good agreement with our estimate of 74,000 daltons by SDS PAGE. The open reading frame terminates with the stop codon UAA, and is followed by 568 bp of 3' untranslated sequence including the polyadenylation signal AAUAAA and a terminal poly A tract. The amino acid sequences of all nine peptides were identified within the single open reading frame. Single amino acid substitutions were observed in peptide 5 (valine for isoleucine) peptide 7 (serine for asparagine), and peptide 9 (threonine for valine and arginine for aspartic acid). Surprisingly, despite an exact match over the first twelve residues, peptide 4 diverged completely from the deduced amino acid sequence after the first aspartic acid. This issue will be addressed further below.

Inspection of the deduced amino acid sequence reveals a striking density of charged residues in the first 220 amino acids including two predicted alpha helical regions, the amino (N-) terminal 60 amino acids and another 90 amino acids centered about residue 240 (Figure 9A). The highly charged N-terminal region, which shows a significant degree of surface probability (Figure 9A),

includes the sequences $^{13}RK(X)_{10}KKRK$ and $^{42}KK(X)_{10}RKRR$ (one letter code, $(X)_{10}$ denotes a ten residue spacer). These sequences are similar to the bipartite nuclear targeting signal of *Xenopus* nucleoplasmin, $KR(X)_{10}KKKK$ (Robbins et al., 1991).

We analyzed the 74 kDa sequence for the presence of heptad repeats with the potential to form coiled-coil structures using the algorithm developed by Lupas et al. (1991). Residues 2-44 show a high probability (>0.99) of forming a coiled-coil structure which contains six heptad repeats (Figure 9B). Since this number of repeats is close to the minimum number (four to five) required to form a stable coiled-coil structure, it may be involved in interchain rather than intrachain interactions.

Relationships to other dynein polypeptides.

We searched the GenBank, EMBL, and SwissProt data bases with the complete 74 kDa coding sequence and found no significant relatedness to other proteins. However, a direct comparison of 74 kDa with a 70 kDa subunit of *Chlamydomonas reinhardtii* flagellar dynein (Mitchell and Yang, 1991) revealed that the two polypeptides are 23.9% identical and 47.5% similar. A dotplot comparison of the aligned sequences is shown in Figure 10A. The C-terminal halves of the cytoplasmic and flagellar polypeptides are 26.4% identical and 47.7% similar. The optimal alignment of this region (Figure 10B) obtained with the GCG Program BESTFIT required only four minor gaps in the cytoplasmic sequence and five minor gaps in the flagellar

sequence. The region of highest identity (28.5%) spans amino acids 330-598 and 208-473 of the cytoplasmic and flagellar polypeptides, respectively.

To evaluate the statistical significance of the extent of sequence identity between the cytoplasmic and flagellar polypeptides, we compared the authentic alignment score with the mean of the alignment scores of the 74 kDa sequence and 1000 randomized 70 kDa sequences using the RDF2 Program (Lipman and Pearson, 1985). The mean score of the authentic alignment of the full-length comparisons was 34.74 SD (z value) above the mean score of the randomized sets, indicating that the match between the cytoplasmic and flagellar polypeptides is indeed significant. This analysis applied to the C-terminal comparison (26.4% identity) gave a z value of 34.88. In contrast, a comparison of the N-terminal halves of the two polypeptides (20.1% identity) revealed a z value of -0.33, indicating that a statistically significant relationship is restricted to the C-terminal region.

Our earliest attempts to isolate cDNA's encoding the 74 kDa polypeptide using a monoclonal antibody had led to the selection of nine clones encoding the 150 kDa dynein-associated polypeptide (Holzbaur et al., 1991). This result, and our demonstration of cross-reactivity by immunoblotting (op. cit.) and immunoprecipitation (Paschal et al., in preparation) suggested a potential structural relationship between the two species. Comparison of their primary sequences revealed that the two polypeptides are 21.7% identical.

However, analysis using the RDF2 Program indicates the authentic alignment score is only 1.49 SD above the mean score of the randomized sets, suggesting that this degree of relatedness is probably not significant. Alignments generated by the GCG programs BESTFIT and GAP did not reveal any common domains in the 74 and 150 kDa species, though the sequence LKAE is found in the N-terminal region of both polypeptides. Since the monoclonal antibody recognizes bacterially-expressed 150 kDa, the epitope is probably not defined by a posttranslational modification. It is more likely that the epitope resides in secondary structure conserved between the two polypeptides.

Analysis of transcripts encoding 74 kDa isoforms.

The mass analysis of cytoplasmic dynein by scanning transmission electron microscopy and the stoichiometry of the copurifying subunits indicated that there are approximately three copies of the 74 kDa subunit per complex (Paschal et al., 1987; Vallee et al., 1988). On well-resolving SDS PAGE gels, two to three bands can be identified, each of which is recognized by an anti-74 kDa monoclonal antibody (Figure 11A, and unpublished data). To determine the basis for 74 kDa heterogeneity, we probed northern blots of adult rat brain poly(A) RNA and observed a single, albeit broad, species at 2.9 kb (Figure 11B).

As a further means of testing for mRNA heterogeneity, overlapping regions of first strand rat brain cDNA were amplified by

PCR (Figure 11C). Each of the primer pairs generated a product of the expected size. In addition, PCR amplification of the region corresponding to bases 453-933 of the cDNA generated a second, smaller product which migrated at about 430 bp. The larger PCR product yielded a sequence identical to that of p74. However, the sequence of the smaller PCR product revealed that it contained a 63 base deletion (Figure 11D). The corresponding polypeptide is predicted to have a 21 amino acid deletion and a total molecular weight of 70,383 daltons.

Analysis of expression 74 kDa.

Given the significant relatedness of the rat 74 kDa cytoplasmic and *Chlamydomonas* 70 kDa flagellar dynein polypeptides (Figure 10A,B), we tested whether mammalian cilia and flagella contain proteins which are immunologically related to the brain cytoplasmic dynein 74 kDa species. Western blotting using our anti-74 kDa monoclonal antibody identified a major immunoreactive species of 74 kDa in sheep testes, consistent with the M_r of the subunit in rat, mouse, calf, and human (Figure 12A, and unpublished data). In contrast to this result, no reactivity was seen with a 74 kDa species in isolated ram sperm flagella and pig tracheal cilia; however, strong immunoreactivity was observed with a 67 kDa polypeptide (Figure 12A). Since purified mammalian ciliary dynein contains a 67 kDa intermediate chain (Hastie, 1991), our results suggest immunological relatedness between the axonemal and cytoplasmic dynein subunits

Examination of other rat tissues revealed that expression of the 74 kDa polypeptide was highest in brain and testes (Figure 12B), consistent with the yield of cytoplasmic dynein from these sources (Paschal et al., 1987; Neely and Boekelheide, 1988; Collins and Vallee, 1989). The expression of 74 kDa as a function of brain development was relatively constant from day 1 through day 29 (Figure 12C).

Discussion

We have determined the nucleotide and deduced polypeptide sequences of the 74 kDa cytoplasmic dynein intermediate chain from mammalian brain. Significant relatedness was found with only one other polypeptide, the 70 kDa intermediate chain of flagellar outer arm dynein from *Chlamydomonas reinhardtii* (Mitchell and Kang, 1991). This suggests that the genes for the intermediate chains for cytoplasmic and axonemal dyneins evolved from a common ancestral gene, and raises the possibility of related functions for these polypeptides within the respective holoenzymes, as discussed below.

Functional implications of 74kDa/70kDa homology.

Molecular genetic analysis of the *Chlamydomonas* 70 kDa intermediate chain has revealed an essential role in flagellar dynein function (Kamiya, 1988; Mitchell and Kang, 1991). *oda*6 mutants fail to assemble flagellar outer arms, resulting in a reduced beat frequency (Kamiya, 1988). It is unknown whether the dynein complex fails to assemble in these mutants, or whether it assembles but fails to attach to the A subfiber microtubule. Recently identified intragenic revertents of *oda*6 have an apparently normal complement of outer arms, but are still abnormal with regard to beat frequency (D.R. Mitchell, personal communication). This indicates

that the force-tranducing activity of the holoenzyme is closely linked with the function of the 70 kDa intermediate chain.

Electron microscopy with anti-70 kDa monoclonal antibodies has show this polypeptide to be located at the base of the flagellar dynein complex (King and Witman, 1990), which is closely associated with the A subfiber microtubule in the axoneme (Goodenough and Heuser, 1984). The 70 kDa polypeptide can be isolated as a heterodimer with a second intermediate chain of 80 kDa (Mitchell and Rosenbaum, 1986), which can be chemically crosslinked to alpha tubulin in detergent permeabilized axonemes (King et al., 1991). Together, these data suggest a model whereby the 70-80 kDa heterodimer constitutes a subcomplex which is responsible for structural binding of the flagellar outer arm dynein to the A subfiber microtubule (King and Witman, 1990).

The relationship reported here between the primary structure of the flagellar 70 kDa and cytoplasmic 74 kDa accessory subunits suggest that the latter is also likely to be located at the base of the cytoplasmic dynein complex. This is consistent with analysis by scanning transmission electron microscopy which revealed the base of the axonemal (Johnson and Wall, 1983; Witman et al., 1983) and cytoplasmic (Vallee et al., 1988) dynein complexes to have a similar mass, which could be accounted for by the combined masses of most of the non-catalytic subunits.

By analogy with the 70 kDa flagellar subunit, the 74 kDa cytoplasmic dynein subunit may also play a role in substrate

attachment. In the case of cytoplasmic dynein there is little evidence for the nucleotide-insensitive, microtubule-binding site found in axonemal dynein (Paschal et al., 1987; Shpetner et al., 1988). Instead a growing body of evidence points to a specific interaction of cytoplasmic dynein with minus end directed organelles (Paschal and Vallee, 1987) such as lysosomes (Lin and Collins, 1992; Matteoni and Kreis, 1987), neuronal vesicles (Schnapp and Reese, 1989; Schroer et al., 1989; Hirokawa et al., 1990; Lacy and Haimo, 1992), chromosomes (Reider and Alexander, 1990; Pfarr et al., 1990; Steuer et al., 1990; Hyman and Mitchison, 1991), and possibly the Golgi apparatus (Rogalski and Singer, 1984). Thus, our finding of a structural relationship between the flagellar and cytoplasmic dynein subunits suggests a role for the 74 kDa species in attachment to the organelle surface and to the kinetochore. Whether the 74 kDa subunit links the cytoplasmic dynein holoenzyme to these structures directly or indirectly will be an important issue to be resolved by further work.

Comparison of the primary structures of cytoplasmic 74 kDa and flagellar 70 kDa.

Several features of the primary structures of the cytoplasmic 74kDa and flagellar 70kDa polypeptides are conserved. The two polypeptides are similar in total mass and have very acidic isoelectric points, 4.9 (this study) and 5.2 (Mitchell and Kang, 1991) for the cytoplasmic and flagellar subunits, respectively. The

cytoplasmic and flagellar subunits contain a total of nine and eight cysteines, respectively. Seven of these are located in the homologous C-terminal region of each polypeptide, indicating that the number and relative distributions of cysteines has been conserved. Most conspicuous is the amino acid sequence homology within the C-terminal halves, which are 26.4% identical and 47.7% similar. It seems reasonable to assume that the C-terminal halves of the two polypeptides are involved in a conserved function such as binding to the dynein heavy chains. In the case of the axonemal polypeptide, extraction of the *Chlamydomonas* outer arm dynein complex with increasing levels of SDS revealed the 70 kDa subunit to be the last polypeptide released from the β heavy chain, consistent with a direct interaction between these two species (Mitchell and Rosenbaum, 1986).

The N-terminal regions of the 70 kDa and 74 kDa subunits appear to be unrelated, suggesting that this domain is specialized for functions unique to the flagellar and cytoplasmic enzymes, respectively. The amino acid composition of this region of the 74kDa cytoplasmic subunit is unusual, with lysine, arginine, glutamic and aspartic acid comprising 65% of the N-terminal 60 amino acids. Within this highly-charged region are two nucleoplasmin-type bipartite nuclear targeting signals. There is, as yet, no evidence for localization of cytoplasmic dynein to the kinetochore prior to nuclear envelope breakdown. However, a search of the SwissProt data base revealed that the nucleoplasmin-type motif is conserved in nearly

half of all nuclear proteins, and it occurs in less than 5% of non-nuclear proteins (Robbins et al., 1991). Thus, a potential role for this motif in nuclear targeting of cytoplasmic dynein warrants further investigation.

The charge clusters in the N-terminus of the 74 kDa polypeptide are also reminiscent of sequences which have been postulated to mediate dimerization in some eukaryotic transcription factors (reviewed by Brendel and Karlin, 1989). For example, the essential region of Fos which is necessary for Fos-Jun dimerization contains a mixed charge cluster (Turner and Tjian, 1989). In this regard, we note that the N-terminal 44 amino acids are strongly predicted to participate in coiled-coil formation. We predict a role for this domain in subunit-subunit interactions or in the binding of hypothetical receptors on the surface of cytoplasmic organelles or kinetochores.

Multiplicity of isoforms.

In earlier work, approximately three copies 74 kDa polypeptide were deduced to copurify with each cytoplasmic dynein holoenzyme. This conclusion was based on the relative content of the 74 kDa species as determined by gel densitometry (Paschal et al., 1987) and the mass of the holoenzyme as determined by scanning transmission electron microscopy (Vallee et al., 1988). SDS gels show some evidence of 74 kDa heterogeneity, revealing from one to three bands depending on the gel system. In the present study, northern blotting

and PCR were used to test for possible transcript heterogeneity. This analysis and the peptide sequence data are consistent with the existence of three isoforms which differ near their N-termini. The molecular weight of the polypeptide calculated from the predicted amino acid sequence of the full-length cDNA is 72,753 daltons, and the PCR analysis predicts a second isoform of 70,383 daltons assuming there are no additional deletions or insertions. This is about the difference we estimate between the largest and smallest electrophoretic species from well-resolving gels. The sequence of peptide 4 indicates there is a third, distinct isoform which contains an insertion after residue 113. Together, the multiple isoforms suggested by the sequence data seem likely to account for the three similarly-sized polypeptides which migrate at approximately 74 kDa on SDS gels (Figure 11A,D).

The importance of multiple forms of 74 kDa in cytoplasmic dynein function is unknown. They may account for the 3:1 stochiometry of 74 kDa:holoenzyme complex (Paschal et al., 1987; Vallee et al., 1988). However, it appears that the 74 kDa isoforms are expressed unequally, both from examination of protein gels (Figure 11A) and from the relative intensity of PCR products generated across the region of transcript heterogeneity (Figure 11C). Such unequal expression could be better explained by differences in isoform composition between individual cytoplasmic dynein molecules with some forms predominating. In this case a role for isoform diversity in specifying function would seem a reasonable

speculation, for example in targeting cytoplasmic dynein to the surface of different organelles or to the kinetochore

While the multiple sequences may be generated by an alternative splicing mechanism, we note that preliminary genomic Southerns are more complex than expected for a single copy gene. Further work will be needed to resolve this issue.

Evolutionary considerations.

One of the noteworthy differences between cytoplasmic, flagellar, and ciliary dyneins is in the composition of their accessory subunits. Nonetheless, some evidence for immunological relatedness of evolutionarily distant flagellar dynein intermediate chains has been obtained. King and coworkers (King et al., 1990) showed that a monoclonal antibody directed against the 70 kDa flagellar dynein subunit in *Chlamydomonas* recognized subunits of M_r 73 kDa and 76 kDa in trout and sea urchin, respectively. A second monoclonal antibody directed against the 80 kDa subunit in Chlamydomonas, also recognizes the 73 kDa subunit in trout. These data suggest some degree of conservation within the primary structure of metazoan and protozoan flagellar dynein subunits. Our observation of cross-reactive mammalian brain, flagellar, and ciliary polypeptides suggests that the cytoplasmic and axonemal intermediate chains in the same taxonomic class are related as well.

Our discovery of a relationship between mammalian cytoplasmic and algal axonemal dynein accessory subunits points to a

common origin for the two genes. Assuming that cytoplasmic microtubules predate axonemal microtubules (though for a counterargument see Margulis, 1981), it seems reasonable to speculate that the ancestral gene would have encoded a cytoplasmic dynein component. Molecular cloning of the mammalian axonemal subunit and comparison with the 74 kDa polypeptide sequence should provide additional insight into their structural, functional, and evolutionary relationships.

Figure Legends

Figure 7. *In situ* tryptic digestion of the 74kDa intermediate chain of brain cytoplasmic dynein. (A) HPLC elution profile of tryptic peptides chromatographed on a C_{18} reverse phase column. Sequence was obtained from the seven peptides indicated. (B) N-terminal amino acid sequences of peptides generated by in situ tryptic digestion (1-7), by tryptic digestion in solution (8), and by Staphlococcus aureus V8 protease digestion (9). The *in situ* digestion, HPLC, and microsequencing were performed by Dr. John Leszyk at the Worcester Foundation.

A

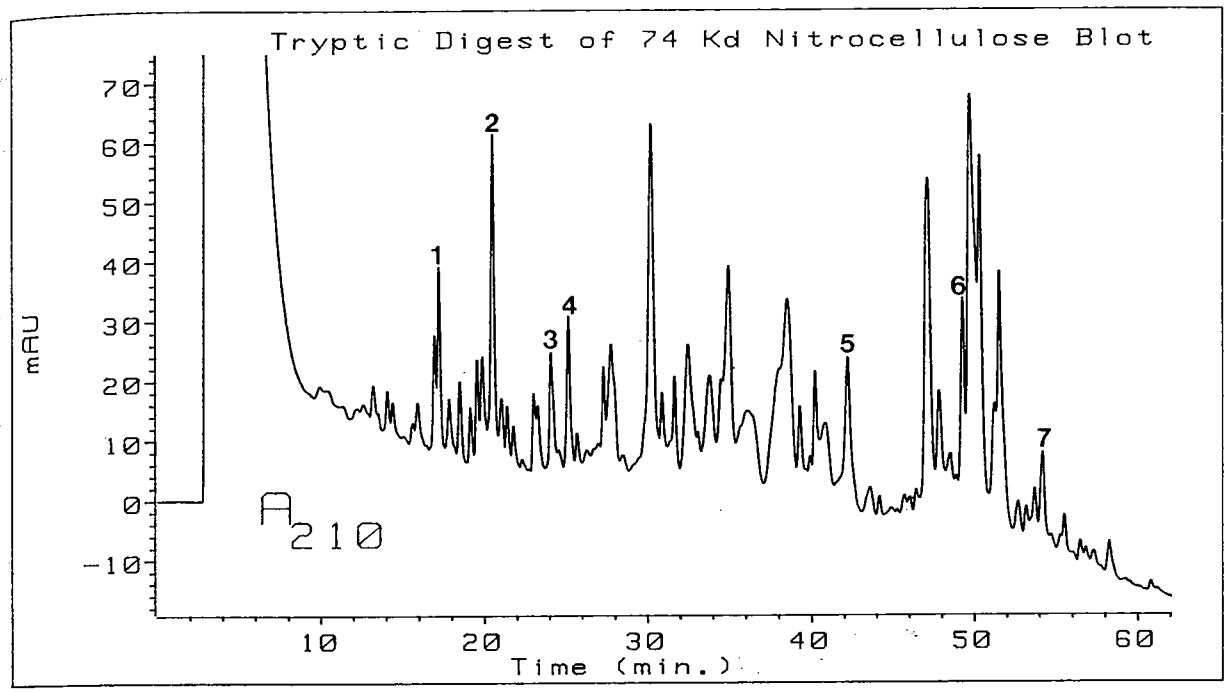

B

1 TPVQR
2 WAQGGK
3 EVVSYSK
4 SVSTPSEAGSQDSGDGAVG
5 ITQV
6 SKPVAVTGMAFPTGDVNNFV
7 LDLWNLNNDT

8 KTTPEYVFHXQ
9 VKEAPPRELTEEEKQQILHSEEFLIFFXRTIDVI

Figure 8. Nucleotide and predicted amino acid sequences of the full-length rat brain cDNA (p74) encoding the 74kDa intermediate chain of brain cytoplasmic dynein. The sequences of nine peptides derived from the bovine 74kDa subunit are underlined. Translation from the predicted translation initiation site AUG (159) to the termination codon UAA (2088) would produce a polypeptide of molecular weight 72,753, in good agreement with our estimate of 74 kDa from SDS gels (Paschal et al., 1987). The 3' untranslated sequence includes the polyadenylation signal AAUAAA (2623) and a terminal poly A tract. The GCG program MOTIFS revealed a total of 27 potential phosphorylation sites, two for cAMP dependent kinase (R/KXXS/T), seven for protein kinase C (S/TXR/K), and 18 for casein kinase II (S/TXXD/E). These sequence data are available from EMBL/GenBank/DDBJ under accession number X66845.

```
1    CCAAGCTCAGGAGAGAGGAAGTGATCGCTCCGGGAGGAGCTAGCCTAGCCGCGCAGTGAGACAGCACATCCTGCTGGCGCGGGCCCGCTG   90
91   CTCCCCGTCCTCCCGCGCCTCCTCCACCACCTCAGTGAGCCTCCGCAGACAGCATCCAGGAAGCAAATATGTCTGACAAGAGCGACCTAA  180
                                                                    M  S  D  K  S  D  L  K    8

181  AAGCTGAGCTGGAGCGCAAAAAGCAGCGCTTAGCGCAGATAAGAGAGGAGAAGAAACGGAAGGAAGAGGAGAGGAAAAAGAAAGAGGCAG  270
9      A  E  L  E  R  K  K  Q  R  L  A  Q  I  R  E  E  K  K  R  K  E  E  E  R  K  K  K  E  A  D   38

271  ATATGCAGCAGAAGAAAGAGCCCGTTCCAGATGACTCCGATCTGGACCGCAAACGACGAGAGACAGAAGCTTTGCTTCAGAGCATCGGCA  360
39     M  Q  Q  K  K  E  P  V  P  D  D  S  D  L  D  R  K  R  R  E  T  E  A  L  L  Q  S  I  G  I   68

361  TATCGCCGGAGCCCCCTCTAGTGCAGCCGCTGCATTTTTTAACATGGGATACCTGTTATTTTCATTATTTAGTCCCAACCCCTATGTCTC  450
69     S  P  E  P  P  L  V  Q  P  L  H  F  L  T  W  D  T  C  Y  F  H  Y  L  V  P  T  P  M  S  P   98

451  CCTCTTCGAAATCAGTGAGCACTCCCAGTGAAGCTGGAAGCCAAGACGATCTGGGGCCATTAACAAGGACCCTGCAGTGGGACACAGACC  540
99     S  S  K  S  V  S  T  P  S  E  A  G  S  Q  D  D  L  G  P  L  T  R  T  L  Q  W  D  T  D  P  128

541  CCTCAGTGCTCCAGCTGCAGTCAGACTCAGAACTTGGGAGAAGACTGAACAAGCTGGGCGTGTCAAAGGTTACCCAGGTGGATTTCCTGC  630
129    S  V  L  Q  L  Q  S  D  S  E  L  G  R  R  L  N  K  L  G  V  S  K  V  T  Q  V  D  F  L  P  158

631  CTAGGGAGGTGGTATCCTACTCCAAGGAGACACAGACTCCTCTTGCAACTCATCAGTCAGAAGAGGATGAGGAAGATGAGGAGATGGTTG  720
159    R  E  V  V  S  Y  S  K  E  T  Q  T  P  L  A  T  H  Q  S  E  E  D  E  E  D  E  E  M  V  E  188

721  AGCCCAAAGTTGGTCATGATTCTGAACTGGAAAATCAAGACAAAAAGCAGGAGACAAAGGAAGCCCCTCCAAGAGAGCTGACGGAAGAAG  810
189    P  K  V  G  H  D  S  E  L  E  N  Q  D  K  K  Q  E  T  K  E  A  P  P  R  E  L  T  E  E  E  218

811  AAAAACAGCAGATCCTGCACTCAGAGGAATTCCTCATCTTCTTTGACCGAACGATCCGAGTGATTGAACGAGCTCTGGCTGAGGACTCTG  900
219    K  Q  Q  I  L  H  S  E  E  F  L  I  F  F  D  R  T  I  R  V  I  E  R  A  L  A  E  D  S  D  248

901  ACATCTTTTTTGACTACAGCGGCCGAGAGCTGGAGGAGAAAGATGGGGATGTACAGGCTGGAGCCAACCTTTCTTTCAACCGTCAGTTCT  990
249    I  F  F  D  Y  S  G  R  E  L  E  E  K  D  G  D  V  Q  A  G  A  N  L  S  F  N  R  Q  F  Y  278

991  ATGATGAGCATTGGTCTAAGCACCGGGTGGTCACATGTATGGACTGGTCTCTCCAGTACCCTGAGCTGATGGTTGCTTCTTATAGCAACA 1080
279    D  E  H  W  S  K  H  R  V  V  T  C  M  D  W  S  L  Q  Y  P  E  L  M  V  A  S  Y  S  N  N  308

1081 ATGAAGATGCTCCCCATGAACCAGATGGAGTGGCCTTGGTTTGGAACATGAAGTTCAAGAAAACCACACCAGAATATGTCTTCCACTGTC 1170
309    E  D  A  P  H  E  P  D  G  V  A  L  V  W  N  M  K  F  K  K  T  T  P  E  Y  V  F  H  C  Q  338

1171 AGTCCTCTGTGATGTCAGTCTGCTTTGCCCGTTTCCATCCTAATTTGGTGGTTGGTGGCACCTATTCAGGCCAGATTGTCCTCTGGGACA 1260
339    S  S  V  M  S  V  C  F  A  R  F  H  P  N  L  V  V  G  G  T  Y  S  G  Q  I  V  L  W  D  N  368

1261 ATCGCAGTCATCGAAGAACCCCTGTCCAGAGGACCCCCTTGTCAGCCGCTGCACACACACATCCTGTGTACTGTGTCAATGTTGTTGGGA 1350
369    R  S  H  R  R  T  P  V  Q  R  T  P  L  S  A  A  A  H  T  H  P  V  Y  C  V  N  V  V  G  T  398

1351 CCCAGAATGCTCACAACCTGATCACTGTCTCTACCGATGGCAAAATGTGTTCCTGGAGCCTGGACATGCTCTCAACCCCACAGGAGAGCA 1440
399    Q  N  A  H  N  L  I  T  V  S  T  D  G  K  M  C  S  W  S  L  D  M  L  S  T  P  Q  E  S  M  428

1441 TGGAGCTGGTGTACAACAAGTCCAAGCCTGTGGCTGTTACAGGAATGGCCTTCCCGACGGGAGATGTCAACAACTTCGTGGTCGGCAGTG 1530
429    E  L  V  Y  N  K  S  K  P  V  A  V  T  G  M  A  F  P  T  G  D  V  N  N  F  V  V  G  S  E  458

1531 AGGAAGGTACCGTCTACACAGCTTGTCGTCATGGAAGCAAAGCAGGCATTGGTGAGGTCTTTGAAGGTCACCAAGGGCCAGTGACAGGCA 1620
459    E  G  T  V  Y  T  A  C  R  H  G  S  K  A  G  I  G  E  V  F  E  G  H  Q  G  P  V  T  G  I  488

1621 TTAACTGCCACATGGCAGTGGGTCCCATCGACTTTTCTCATCTGTTTGTCACATCATCATTTGACTGGACTGTCAAACTGTGGACCACAA 1710
489    N  C  H  M  A  V  G  P  I  D  F  S  H  L  F  V  T  S  S  F  D  W  T  V  K  L  W  T  T  K  518

1711 AGCACAACAAGCCGCTCTACTCCTTTGAAGACAATGCAGACTATGTGTACGATGTCATGTGGTCCCCCGTGCATCCCGCGCTCTTTGCCT 1800
519    H  N  K  P  L  Y  S  F  E  D  N  A  D  Y  V  Y  D  V  M  W  S  P  V  H  P  A  L  F  A  C  548

1801 GCGTGGACGGGATGGGGCGCTTGGACCTCTGGAACCTCAACAGTGACACCGAGGTGCCAACAGCAAGTGTGGCTATTGAGGGGGCTTATG 1890
549    V  D  G  M  G  R  L  D  L  W  N  L  N  S  D  T  E  V  P  T  A  S  V  A  I  E  G  A  Y  A  578

1891 CCCTAAACCGGGTTCGTTGGGCACAAGGTGGTAAGGAAGTTGCAGTAGGTGACTCAGAAGGCCGCATCTGGATCTACGATGTTGGAGAGC 1980
579    L  N  R  V  R  W  A  Q  G  G  K  E  V  A  V  G  D  S  E  G  R  I  W  I  Y  D  V  G  E  L  608

1981 TTGCGGTTCCCCACAATGATGAATGGACGCGATTTGCCCGGACCCTGGTGGAGATCCGCGCCAATAGGGCTGACAGCGAGGAGGAAGGTG 2070
609    A  V  P  H  N  D  E  W  T  R  F  A  R  T  L  V  E  I  R  A  N  R  A  D  S  E  E  E  G  A  638

2071 CGGTTGAGTTAGCTGCCTAAATGTGAGCCCAGTCTGCACGCTGTGGCTCCCATCCTTCCATTCTAGAACTCAGTCTGCAGCCAAGGCCCC 2160
639    V  E  L  A  A  *

2161 TGTGCAGTGTTTGGTGTCCTTTCCGTATCGGTGTCCCCGTGGCAACTTGGGTGCCATATTGTGCAGTGTTTCCCCATATCCTCCCCATGT 2250
2251 ACCCTACTCACCCGAAATCCACCACAGCATTTCTACCTTTGTGTCCCTGTCTCAAGAAACAAAATGGGGGAGGGAACCCTTAGGGGTTTA 2340
2341 GTTGTTGCCTTTTAACTACTTGGTAGCTGTATTTAATAGCTGGAAACCTCTGGTTGAATTTGTGCTTACATGTACTTCTGGCGTAGTCCT 2430
2431 ATTAAATCCATATGAAGCCAGATATGATTGGGTGCAGATGTGGCGTGCCTCGTGATACGGTGCAGGGCCAAAGACTTGAGATGTGGTGTT 2520
2521 TTACATGGTGATTCACATTATGAATGGATTTACTACAAGAACATTGCTGCTCCTTATTTATTGTAACGTGCTGCATGGAACATATTTATT 2610
2611 TGAAAGCATTAAAATAAACGATCTTAGAGCAAAAAAAAAAAAAAAAA
```

Figure 9. Structural features of the 74kDa polypeptide. (A) The surface probability was predicted using the method of Emini et al. (1985). Secondary structure predictions are based on the method of Garnier et al. (1978). The graphic representation was generated with the GCG Programs PEPTIDESTRUCTURE and PLOTSTRUCTURE on a Vax 11/750 computer. In the uppermost plot, regions predicted to reside on the surface of the polypeptide are indicated by positive values. In the secondary structure analysis, regions which are predicted to be β-turn, α-helix, and β-sheet are indicated when the line in the respective graph is in the up position. Amino acid coordinates are shown along the bottom. (B) Probability of forming a coiled-coil structure. The coiled-coil prediction algorithm analyzes the relative occurence of amino acids at the seven positions of the heptad repeat using the sequences of the coiled-coil domains of myosins, tropomyosins, and keratins as a database (Lupas et al., 1991).

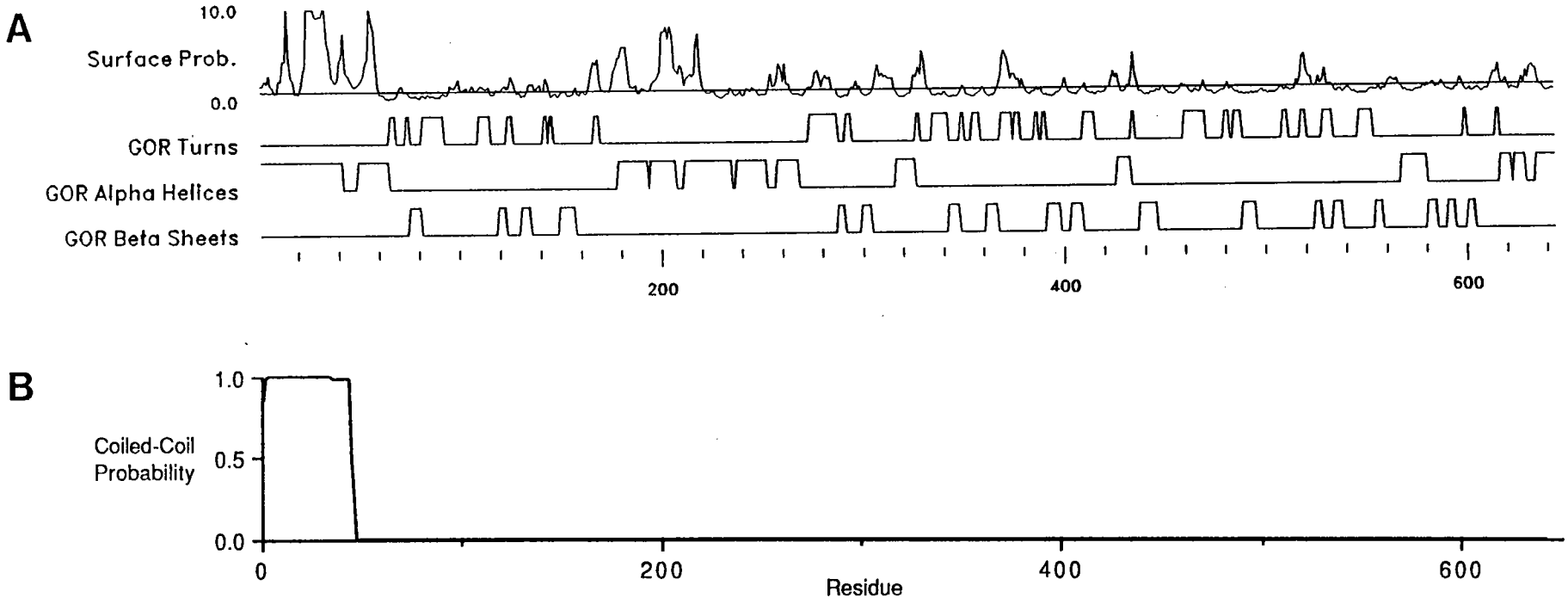
A
10.0
Surface Prob.
0.0
GOR Turns
GOR Alpha Helices
GOR Beta Sheets
200
400
600
B
1.0
Coiled-Coil
Probability
0.5
0.0
0
200
400
600
Residue

Figure 10. Alignment of the deduced polypeptide sequences of rat cytoplasmic 74 kD and *Chlamydomonas* flagellar 70 kDa intermediate chains. (A) Comparison of the full-length polypeptides generated using the GCG Programs COMPARE and DOTPLOT with a stringency of 15 in a window size of 30. Overall the two polypeptides show 23.9% identity and 47.5% similarity. (B) Comparison of the C-terminal regions of the cytoplasmic (cyto) and flagellar (flag) subunits using the GCG Program BESTFIT with the default settings. Beginning at amino acids 330 and 208 of the cytoplasmic 74 kDa and flagellar 70 kDa sequences, respectively, the polypeptides are 26.4% identical and and 47.7% similar. Comparisons $\geq$ similarity threshold of 1.5 are indicated by vertical bars, and represent identities. Comparisons $\geq$ the similarity threshold of 0.5 are indicated by colons, and those $\geq$ 0.1 are indicated by single dots.

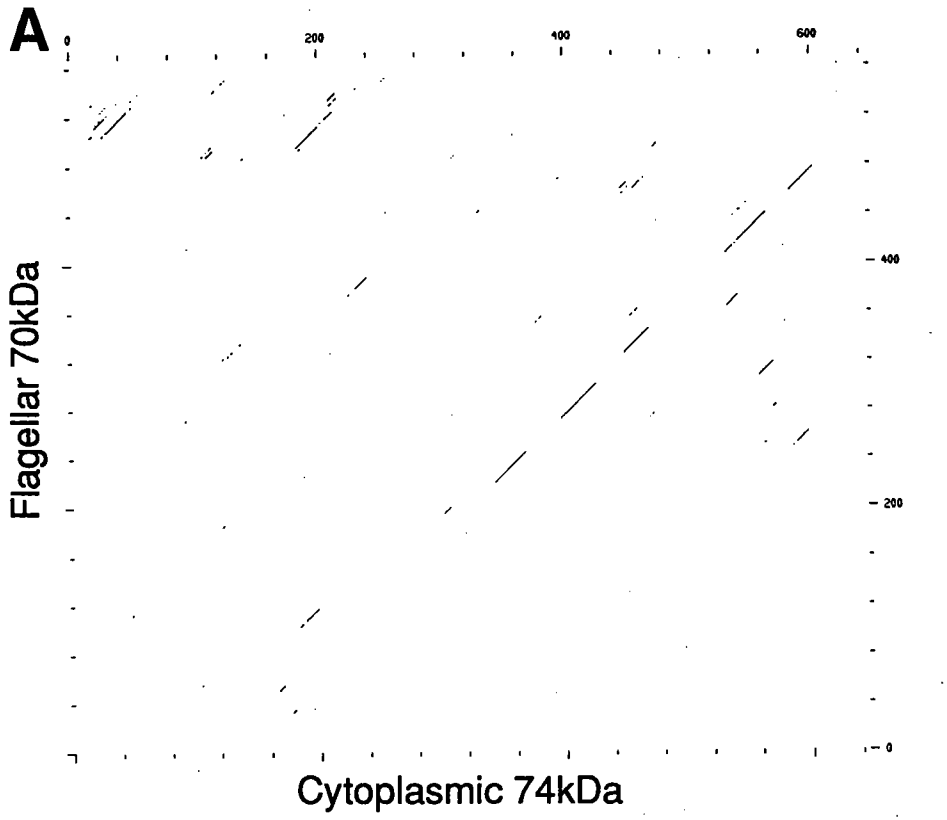

B

```
cyto   TPEYVFHCQSSVMSVCFARFHPNLVVGGTYSGQIVLWDNR  369
       |||| : . | : :. |.  . |||.:| |.||:..:| |
flag   TPEYEMVPTSQICCAKFNLKDNNLVGAGQYNGQLAYFDVR  247

cyto   SHRRTPVQRTPLSAAAHTHPVYCVNVVGTQNAHNLITVST  409
       .  ..||: ||: .  | .|:| .. :....: : :||||
flag   KG.NGPVEATPI.DISHRDPIYDFAWLQSKTGTECMTVST  285

cyto   DGKMCSWSLDMLSTPQESMELVYNKSK.PVAVTGMAFPT.  448
       ||.: .|.| .:... |.|.|  ..|. .|:...:.:.|
flag   DGNVLWWDLRKMNECVENMPLKEKNSETTVGGVCLEYDTN  325

cyto   GDVNNFVVGSEEGTVYTACRHGSKAG..IGEVFEGHQGPV  486
       ::..||:||.|:| ::.. |.:..:.  :  |:.||:||:
flag   AGPTNFMVGTEQGQIFSCNRKAKNPVDRVKYVLSGHHGPI  365

cyto   TGINCHMAVGPIDFSHLFVTSSFDWTVKLWTTKHNKPLYS  526
       |    :  .|:: ..:: .:.:.  |.: .|  ..|:..
flag   YG....LRRNPFNSKYFLSIGDWTARVWVEDTAVKTPILT  401

cyto   FEDNADYVYDVMWSPVHPALFACVDGMGRLDLWNLNSDTE  566
       . ::.|: :. ||| :|::| .:.  | :|:|:|  . :
flag   TKYHPTYLTGGTWSPSRPGVFFTIKMDGAMDVWDLYYKHN  441

cyto   VPTASVAIEGAYALNRVRWAQGGKEVAVGDSEGRIWIYDV  606
       || .|.: :..||. .  .::| .||||.|:| ..:.::
flag   EPTLTVQV.SDLALTAFAVQESGGTVAVGTSDGCTSVLQL  480

cyto   G.ELAVPHNDEWTRFARTLVEIRANRADSEEEGAVELAA*  644
       : :|. :  .|...:. .:.|  ..|... |.:  |
flag   STGLSEASPAEKANIN.AMFERETTREKNLEKAIKEAKVK  519

flag   ARKEQGRRDEVKDNVTEEQLKALEDEFFKTTDPAVGGGYG  559

flag   AGEGAAAE*                                 567
```

Figure 11. Identification of multiple 74 kDa isoforms and mRNA's. (A) SDS PAGE showing heterogeneity of the 74kDa polypeptides. A linear gradient of 5-10% acrylamide was used, and the gel was stained with silver by the method of Oakley et al. (1980). (B) Northern blot of adult rat brain poly(A) RNA (10 μg) probed with an 839 bp EcoRI fragment of p74. An abundant 2.9 kb message was detected in brain, and in testes as well (not shown). (C) PCR analysis of transcripts encoding portions of the 74 kDa subunit. Diagram illustrates the full-length cDNA and the six overlapping regions (a-f) of the open reading frame (ORF) amplified by PCR. Also shown is an ethidium bromide-stained agarose gel (4% NuSieve) of the PCR products resulting from amplification of first strand brain cDNA. Two products were generated using primers corresponding to region b, which were subcloned into pBluescript for dideoxy sequencing. (D) Comparison of the amino acid sequence predicted from a subclone of the smaller PCR product amplified from region b with the full-length cDNA (p74) and tryptic peptide 4. The 21 amino acid deletion, deduced from the 63 bp deletion in the smaller PCR product, is indicated by the horizontal bar. Amino acid identities in the three isoforms are shown in boldface type. Peptide 4 was identical to the sequence encoded by the cDNA at 12 contiguous residues, but then diverged completely after the first aspartic acid (regular type). This suggests that it represents a third isoform, though it is possible that the divergent residues in the peptide are due to species-specific sequence differences.

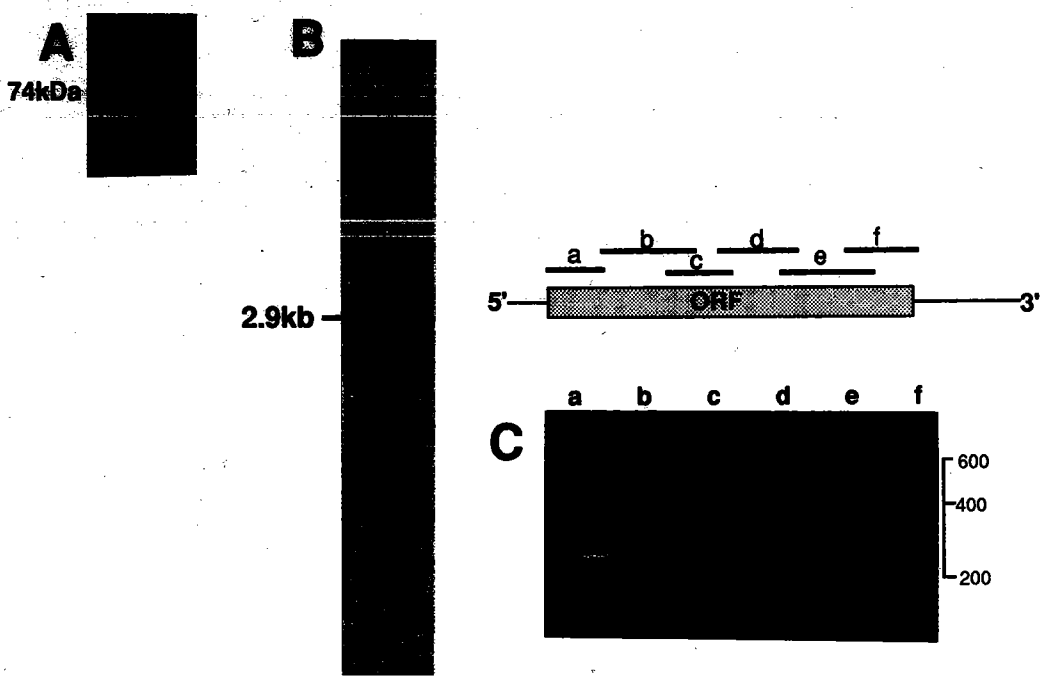

D

	102	
PCR	SVSTPSEAGSQDDLGPLTR	RLNKLGVSPEPT...
p74	...SVSTPSEAGSQDDLGPLTRTLQWDTDPSVLQLQSDSELGRRLNKLGVSPEPT...	
peptide 4	SVSTPSEAGSQDSGDGAVG	

Figure 12. Tissue distribution and developmental expression of the 74 kDa cytoplasmic dynein subunit, and identification of cross-reactive axonemal species. (A) Nitrocellulose blot of a 7% polyacrylamide gel of ram testes and flagella and pig cilia reacted with a monoclonal antibody against the 74 kDa cytoplasmic dynein subunit. A major immunoreactive product of M_r 74 kDa was observed in sheep testes, while flagella and cilia showed only a M_r 67 kDa species. (B) Nitrocellulose blot of an 8% polyacrylamide gel of adult rat tissues. 50 μg of total protein was applied to each lane. Expression was highest in brain and testes and lowest in cardiac and skeletal muscle. The weak immunoreactivity with a M_r 67 kDa species in rat and sheep testes may reflect the presence of spermatozoa. (C) Nitrocellulose blot of an 8% polyacrylamide gel of whole rat brain samples (50 μg total protein per lane) prepared on day 1 through day 29 of development.

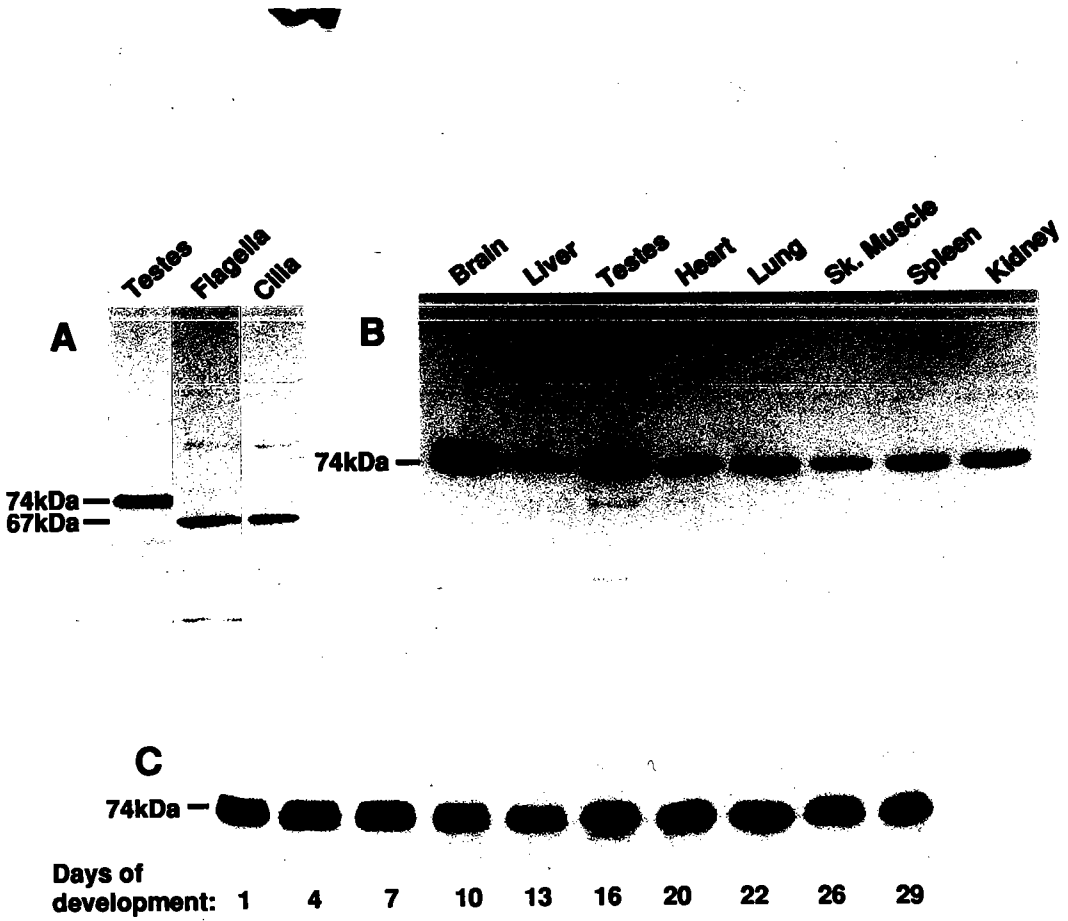
A
Testes
Flagella
Cilia
74kDa
67kDa
B
Brain
Liver
Testes
Heart
Lung
Sk. Muscle
Spleen
Kidney
74kDa
C
74kDa
Days of development:
1
4
7
10
13
16
20
22
26
29

CHAPTER IV

IDENTIFICATION OF A 50 kDa SUBUNIT OF A 20S CYTOSOLIC COMPLEX AND ITS LOCALIZATION TO THE KINETOCHORE OF MITOTIC CHROMOSOMES

There is a growing body of evidence which suggests that the motor proteins cytoplasmic dynein and kinesin account for most, if not all, of the microtubule-based transport in eukaryotic cells (reviewed by Vallee and Shpetner, 1991). The mechanism by which these microtubule-based motors interact with cytoplasmic targets remains obscure. However, recent progress in the analysis of the non-catalytic polypeptides of *Chlamydomonas* dynein indicates that subcellular targeting is mediated by the co-purifying 70 and 80 kDa accessory subunits. As discussed in the previous chapter, immunoelectron microscopy (King and Witman, 1990), chemical cross-linking (King et al., 1991), and microtubule binding data (S. King, personel communication) suggest that a 70/80 kDa heterodimer provides the structural link between the holoenzyme and the A-subfiber microtubule in the axoneme. This data, together with the sequence relationship between the cytoplasmic dynein 74 kDa subunit and the flagellar 70 kDa subunit, led us to propose that 74 kDa is responsible for targeting the cytoplasmic enzyme to structures such as membranous organelles and kinetochores (Paschal et al., in press).

In addition to the 74 kDa subunit, cytoplasmic dynein also contains four accessory polypeptides with molecular weights of 53, 55, 57, and 59 kDa. The function of the 53-59 kDa species is unknown. However, they are components of cytoplasmic dynein purified from brain, liver, and testes (Paschal et al., 1987; Collins and Vallee, 1989), suggesting a role in both neuronal and non-neuronal cytoplasmic dynein function.

We set out to develop monoclonal antibodies (mAb) specific for the 53-59 and 74 kDa accessory polypeptides of cytoplasmic dynein as reagents for probing their function. The two hybridoma lines which were subsequently isolated secrete mAb's which react with a 50 kDa polypeptide which is present in purifed cytoplasmic dynein at only trace levels. There was no evidence suggesting that 50 kDa is a proteolytic product of the previously described 53-59 kDa subunits of 20S cytoplasmic dynein. The 50 kDa polypeptide was detected in brain, fibroblast, and epithelial cells from several species, indicating that its function is probably conserved in most cell types.

The polypeptide composition of native immunoprecipitations indicates that the 50 kDa polypeptide is a component of a multi-subunit 20S complex reported to stimulate cytoplasmic dynein-mediated vesicle transport *in vitro* ("dynactin", Gill et al., 1991). Furthermore, we have used immunoelectron microscopy to show that, like cytoplasmic dynein (Wordeman et al., 1991), the 50 kDa polypeptide localizes to the fibrous corona of the kinetochore. This

raises the intriguing possibility that the dynactin complex may play a role in modulating the activity of cytoplasmic dynein during mitosis.

Materials and Methods

Protein purification.

Cytoplasmic dynein was purified from bovine brain cytosol as previously described (Paschal et al., 1987; 1991). Briefly, white matter was dissected from five calf brains and homogenized in 1.0 vol of ice-cold extraction buffer by two passes (2000 rpm) in a motor-driven Teflon pestle homogenizer (Kontes, Vineland, NJ). The extraction buffer consisted of 10 mM sodium phosphate, 100 mM sodium glutamate, pH 7.0, containing 1 mM $MgSO_4$, 1 mM EGTA, protease inhibitors (1 mM PMSF, 10 μg/ml leupeptin, 10 μg/ml tosyl argine methyl ester, 1 μg/ml pepstatin A) and 1 mM dithiothreitol. The homogenate was centrifuged at 24,000 g for 30 min at 2°C. The supernate was recovered and centrifuged at 150,000 g for 60 minutes at 2°C. The high speed supernate, referred to as brain cytosol, was recovered and stored on ice.

To assemble the microtubules, taxol (10 mM stock in dimethylsulfoxide) was added to a final concentration of 20 μM and the cytosol was incubated at 37°C for 12 minutes with occasional mixing. The microtubules were collected by centrifugation at 40,000 g for 30 min at 35°C through a 7.5% sucrose cushion made in extraction buffer. Buffer washes and nucleotide extractions were

performed by thorough resuspension of the microtubule pellet in extraction buffer alone, or buffer supplemented with 3 mM GTP and 3 mM AMP-PNP, or 5 mM ATP. The resuspended pellets were subsequently recentrifuged to yield a supernate and pellet.

The ATP extract was fractionated on a 5-20% sucrose gradient prepared in 20 mM Tris, pH 7.6, containing 50 KCl, 5 mM $MgSO_4$, and 0.5 mM EDTA. The gradients were centrifuged at 125,000 g for 16 hr at 4°C. Under these conditions, cytoplasmic dynein sediments in a symmetrical peak at 20S.

Monoclonal antibody production.

Monoclonal antibodies were produced by the method of Brodsky (1985) as modified by Pfister et al. (1989). Briefly, approximately 5 μg of 20S cytoplasmic dynein in Ribi adjuvant (Chem Research, Hamilton, MT) was injected into the footpads of 6-week old female Balb/c mice at 3 day intervals for a total of seven injections. An intraperitoneal injection of 20S cytoplasmic dynein (100 μg) without adjuvant was given 3 days prior to the fusion. The popliteal lymph node lymphocytes were fused with NS-1 myeloma cells at a ratio of two lymphocytes per myeloma cell in the presence of 37% polyethylene glycol and 5% dimethylsulfoxide. The fusion was plated into 24-well dishes in spleenocyte-conditioned RPMI 1640 medium containing 20% fetal calf serum and 1X Hybrimax hybridoma enhancing supplement (Sigma, St. Louis, MO). HAT (hypoxanthine-aminopterin-thymidine)-resistant colonies were

screened by immunoblotting and immunofluorescence against 20S cytoplasmic dynein and 3T3 cells, respectively. The antibody isotypes (IgG_1, 50-1; IgM, 50-2) were determined with a kit from Sigma (St. Louis, MO).

Gel electrophoresis and immunoblotting.

Gel electrophoresis was carried out according to the method of Laemmli (1970) using polyacrylamide mini-gels (BioRad, Richmond, CA). Immunoblotting using nitrocellulose (0.45 μm pore size, Schleicher and Schuell, Keene, NH) or PVDF membrane (0.45 μm pore size, Millipore, Medford, MA) was performed in a methanol-containing buffer (Towbin et al., 1979). Culture fluid from the 50-1 and 50-2 hybridomas was used undiluted when using 4-chloro-napthol as the substrate for detection of peroxidase-labeled secondary antibody, and 1:10 when using Enhanced Chemiluminescence (ECL) development. The anti-74 kDa mAb (ascites fluid) was used at 1:1000 or 1:20,000 with 4-chloro-napthol or ECL development, respectively.

Immunoprecipitation.

Immunoprecipitations were performed on extracts prepared from ^{35}S-methionine-labeled 3T3 cells. Approximately 10^5 cells were labeled for 24-48 hr with 100 μCi ^{35}S-methionine. The labeled 3T3 cells were harvested by trypsinization, washed with DMEM containing 20% FCS, and lysed in 1 ml of TBS containing 1% NP-40

and protease inhibitors. The cell extract was then clarified by centrifugation at 10,000 g for 20 minutes at 4°C. Alternatively, the washed cells were resuspended in TBS with protease inhibitors, mechanically disrupted with a Teflon homogenizer, and clarified as above.

The antibody affinity beads were pre-loaded by mixing goat anti-mouse agarose beads (Hyclone, Logan, UT) with 50 vol of hybridoma culture fluid for at least 24 hours at 4°C. The beads were recovered by a brief centrifugation and washed five times with TBS containing 0.5% NP-40 or Tween-20. 100 µl of a 50% bead suspension was combined with 0.5 ml of labeled extract, and the sample was mixed with gentle agitation overnight at 4°C. The beads were then washed five times with TBS containing 0.5% NP-40, and the immunoselected polypeptides were eluted with 1X Laemmli sample buffer lacking reducing agent. β-mercaptoethanol was added to the bead eluate to a final concentration of 5%, and the samples were analyzed by gel electrophoresis and autoradiography.

Native immunoprecipitations were performed using rat brain cytosol. Whole rat brains (adult Sprague Dawley) were homogenized (see above) in 2 vol of Pipes-Hepes buffer (50 mM Pipes, 50 mM Hepes, pH 7.0, containing 2 mM $MgSO_4$, 1 mM EDTA, and protease inhibitors). The homogenate was centrifuged successively at 40,000 g for 30 minutes and 150,000 g for 60 minutes, both at 2°C. NP-40 was added to the cytosol to a final concentration of 0.1%, and the cytosol was pre-cleared with goat anti-mouse agarose beads for 1

hour at 4°C. 100 µl of pre-loaded affinity beads (see above) was combined with 1 ml of rat brain cytosol, and the samples were gently agitated for 6 hours at 4°C. The beads were washed twice with TBS containing 0.1% NP-40, eluted as described above, and analyzed by gel electrophoresis and immunoblotting.

Immunofluorescence microscopy.

Cell lines were maintained and processed for immunofluorescence microscopy by standard methods. Cells were grown on glass coverslips for 24-48 hours, rinsed in 37°C PBS, and fixed in methanol at -20°C for 5 minutes. The coverslips were rehydrated, blocked in Tris-buffered saline (TBS) containing 10% bovine serum albumin, and incubated with primary antibody for 1 hour at 37°C in a humid chamber. The 50-1 and 50-2 hybridoma culture fluids were used undiluted, and the CREST serum (provided by Dr. Bill Brinkley, Baylor University) was used at a dilution of 1:200. Following at least three rinses in TBS, fluorescently-labeled secondary antibodies were diluted in 10% BSA and incubated as above. After washing in TBS, the coverslips were mounted in gelvatol and viewed on a Zeiss Axioskop microscope equipped with a 100X Plan-Neofluar objective and a Zeiss MC100 camera (transfer factor, 0.25X). All photomicrographs were recorded using the automatic exposure mode with T-Max film (ASA 400).

The CREST and 50-2 staining patterns were compared by double label immunofluorescence microscopy on NIH 3T3 cells. The

images were enlarged photographically (final magnification, 3250x) and traced onto acetate sheets. The number of CREST-positive structures aligning with foci recognized by the 50-2 mAb was determined for the two nuclei shown in Figure 30.

Chinese Hamster Ovary (CHO) chromosomes, isolated from vinblastine sulfate-treated cells, were provided by Dr. Linda Wordeman, University of California, San Francisco. CHO chromosomes were pre-fixed for 10 minutes in 0.5% formaldehyde, sedimented onto glass coverslips through a 30% glycerol cushion, and post-fixed for 5 minutes in methanol at -20°C. Alternatively, the chromosomes were fixed in either formaldehyde or -20°C acetone. The coverslips were then processed for immunofluorescence microscopy exactly as described above for whole cells.

Immunoelectron microscopy.

The isolated CHO chromosomes were processed for immunoelectron microscopy by Dr. Linda Wordeman as described by Wordeman et al. (1991). Briefly, the chromosomes were fixed in 0.5% paraformaldehyde for 10 minutes at 20°C, centrifuged onto glass coverslips through a glycerol cushion, and labeled with the 50-1 mAb. After rinsing, the samples were fixed in 6% glutaraldehyde and 1% OsO_4 in 62 mM S-collidine buffer (Ted Pella, Inc.), rinsed in double distilled water, dehydrated in ethanol, and embedded in LR White resin (Polysciences, Inc., Warrington, PA). The samples were

sectioned, mounted on grids, and labeled with goat anti-mouse antibody conjugated to 5 nm gold particles.

Results

Biochemical analysis of a 50 kDa component of 20S cytoplasmic dynein.

We used cytoplasmic dynein purified by microtubule affinity and sucrose gradient centrifugation (Paschal et al., 1987) as the immunogen for monoclonal antibody (mAb) production. Two mAb's were isolated and characterized in detail. mAb 50-1 (IgG_1) reacts with a 50 kDa electrophoretic species in 20S cytoplasmic dynein (Figure 13A) which is distinct from the 53, 55, 57 and 59 kDa intermediate chains (Paschal et al., 1987). The 50 kDa polypeptide was detected in calf and rat brain, NIH 3T3, and PtK cells (Figure 13B). No reaction was observed with chicken, however, suggesting that the mAb's crossreactivity may be restricted to mammals.

The second mAb (50-2) is an IgM which recognizes 20S cytoplasmic dynein immobilized on nitrocellulose. The epitope is denatured by treatment with Laemmli sample buffer and boiling (Figure 13C) and, therefore, the antibody does not react with protein on immunoblots. Both the 50-1 and 50-2 mAb's immunoprecipitate a single electrophoretic species of 50 kDa from ^{35}S-methionine-labeled 3T3 cell extracts prepared by lysis with 1% NP-40 (Figure 13D).

To evaluate whether the 50 kDa species is a component of cytoplasmic dynein, we tested for co-purification with the 74 kDa subunit of the cytoplasmic dynein complex (Paschal et al., 1987). In the initial steps of taxol-dependent microtubule assembly and sedimentation, 78% of the 74 kDa subunit and 29% of the 50 kDa polypeptide co-sedimented with microtubules (Figure 14, lane 2). The level of the 50 kDa polypeptide in the microtubule pellet fraction may have been underestimated because the heavy tubulin band causes distortion of the 50-60 kDa region of the gel. Only trace amounts of the 50 and 74 kDa polypeptides were released from microtubules by the initial buffer wash (lane 3) and virtually none was released by the second buffer wash (lane 5). Extraction with GTP and AMP-PNP, a nucleotide combination which releases dynamin from microtubules (Shpetner and Vallee, 1989), also failed to dissociate detectable 50 or 74 kDa polypeptides (lane 7). However, treatment of the microtubules with ATP resulted in release of 47% and 54% of the 50 and 74 kDa polypeptides, respectively. Thus, while much of the 50 kDa species remained in the post-microtubule supernate in the first step of the purification, the fraction which did co-sediment with microtubules appeared to behave in a manner similar to that of the 74 kDa subunit of cytoplasmic dynein.

The ATP extract (Figure 14, lane 9) was subsequently fractionated by sucrose gradient centrifugation, and the samples were analyzed by gel electrophoresis, immunoblotting, and gel densitometry. The 50 kDa polypeptide was only faintly visible by

Coomassie blue staining (arrowhead, Figure 15A), but its presence in the 20S fraction was clearly seen using the 50-1 mAb (Figure 15B). A densitometric comparison of the cytoplasmic dynein heavy chain (gel) with the 50 kDa polypeptide (blot) indicated that the two species co-sedimented at a constant ratio throughout the 20S peak (Figure 15C), consistent with a direct physical interaction. To test this possibility further, we performed the sucrose gradient fractionation of the ATP extract in the presence of 0.6 M NaCl. We reasoned that, as with axonemal dyneins (Foltz and Asai, 1988), the elevated ionic strength would reduce the sedimentation coefficient of cytoplasmic dynein. The cytoplasmic dynein complex displayed a shift in S-value from 20S to 16S (Figure 16). The 50 kDa polypeptide exhibited the same shift in sedimentation coefficient, suggesting an ionic strength independent interaction with the cytoplasmic dynein complex.

The fact that much of the 50 kDa species remained in the post-microtubule supernate at the initial stage of the cytoplasmic dynein purification (Figure14, lane 1) raised the possibility that 50 kDa might exist in two states, in association with cytoplasmic dynein or free in solution. Furthermore, if 50 kDa sedimented at 20S because of its interaction with cytoplasmic dynein, then it might be possible to identify a pool of 50 kDa (which is not cytoplasmic dynein-associated) at a lower S-value. To test this hypothesis, we fractionated brain cytosol by sucrose gradient centrifugation and determined the sedimentation profile of cytoplasmic dynein by

measurement of CTPase activity (Shpetner et al., 1988) and of 50 kDa by immunoblotting with the 50-1 mAb. All of the the 50 kDa polypeptide appeared to sediment in a single peak at 20S, coincident with a peak of CTPase activity (Figure 17). In addition, we considered the possibility that 50 kDa is quantitatively bound to cytoplasmic dynein in brain cytosol, but that binding of the holoenzyme to microtubules results in dissociation of most of the 50 kDa polypeptide. This was tested by parallel sucrose gradient fractionation of brain cytosol and a post-microtubule supernate (Figure 18A) followed by immunoblotting with the 50-1 mAb. In both cases the 50 kDa polypeptide sedimented quantitatively at 20S (Figure 18B). The results of Figures 17 and 18 imply that the 50 kDa polypeptide is part of an independent 20S complex. However, we cannot exclude the possibility that 50 kDa sediments at 20S by virtue of its association with the residual cytoplasmic dynein in the post-microtubule supernate.

Native immunoprecipitation using mAb's against the 50 kDa polypeptide and cytoplasmic dynein.

As an alternative approach to determining whether the 50 kDa polypeptide is associated with cytoplasmic dynein, we performed native immunoprecipitations using brain cytosol. The immunoprecipitates were generated using antibodies against the 50 kDa polypeptide (50-1 mAb) and the 74 kDa intermediate chain of

cytoplasmic dynein and analyzed by Coomassie blue staining and immunoblotting.

The anti-50 kDa immunoprecipitate contained polypeptides of M_r 45 kDa as well as a doublet at ~150 kDa (Figure 19A). The 50 kDa polypeptide in this sample was obscured by the antibody heavy chain, but its presence was readily revealed by immunoblotting (Figure 19B). In contrast, the anti-74 kDa immunoprecipitate contained, in addition to the 74 kDa subunit, the high molecular weight cytoplasmic dynein heavy chain (DHC, Figure 19A). Immunoblotting of this sample did not reveal any 50 kDa polypeptide (Figure 19B).

We have shown previously that cytoplasmic dynein prepared by ATP extraction of brain microtubules contains nine polypeptides with molecular weights of 440, 74, 59, 57, 55, and 53 kDa (Paschal et al., 1987). Cytoplasmic dynein released from brain microtubules by a high salt treatment appears to be more complex in its composition. In addition to the subunits found in ATP-extracted preparations (see above), salt-extracted cytoplasmic dynein fractionated by sucrose gradient centrifugation contains the150 kDa mammalian homologue of the *Drosophila Glued* protein ($p150^{Glued}$, Holzbaur et al., 1991). To determine if the 150 kDa polypeptide doublet present in the anti-50 immunoprecipitate is related to the 150 kDa component of salt-extracted cytoplasmic dynein, the blot was re-probed with affinity-purified anti-serum to $p150^{Glued}$. The antibody reacted with both molecular weight forms of the 150 kDa doublet in the 50 kDa

immunoprecipitate (Figure 19C). The anti-p150^{Glued} antibody did not react with components of the anti-74 kDa immunoprecipitate or with the sample prepared with beads alone.

Together, these data suggest that the 50 kDa polypeptide in brain cytosol exists in a complex with the 45 and 150 kDa species. The 45, 50, and 150 kDa polypeptides can be detected as trace components of 20S cytoplasmic dynein (arrowheads, Figure 19D). Moreover, the M_r and relative ratios of these polypeptides suggests that the complex is the likely mammalian equivalent of the 20S "dynactin" particle purified from chick brain cytosol (Gill et al., 1991).

Native immunoprecipitations were also performed on ^{35}S-methionine-labeled 3T3 cell extracts. Both anti-50 kDa mAb's immunoprecipitated 45 and 50 kDa species (Figure 20). In addition, the 50-2 mAb immunoprecipitated a 60 kDa species. The apparent absence of the 150 kDa polypeptide in these immunoprecipitates could be a result of proteolysis, thought it is formally possible that it dissociated from the complex because of the ~100-fold dilution of the cytosol.

Immunolocalization of the 50 kDa polypeptide to the kinetochore of isolated chromosomes.

The above experiments identified the 50 kDa polypeptide as a component of a complex which has been reported to stimulate cytoplasmic dynein-based vesicle motility *in vitro* (Schroer and

Sheetz, 1991; Gill et al., 1991). We therefore examined its subcellular location to determine if its distribution was consistent with a such a role in vivo as well. Since several antibodies prepared against cytoplasmic dynein have been reported to label the the kinetochore, (Pfarr et al., 1990; Steur et al., 1990, Zinkowski et al., 1991; Wordeman et al., 1991), we performed immunofluorescence microscopy on isolated CHO chromosomes. The 50-1 mAb revealed labeling in the form of pairs of spots at the primary constriction, a pattern which is suggestive of reactivity with centromere or kinetochore antigens (Figure 21).

To resolve the localization of the 50 kDa polypeptide more precisely, we performed immunoelectron microscopy on isolated CHO chromosomes using 5 nm gold-labeled secondary antibodies. Labeling at the kinetochore was restricted to the fibrous corona (Figure 22B,C,D), a pattern observed for cytoplasmic dynein using a mAb against the 74 kDa intermediate chain (Wordemen et al., 1991). Immunostaining with secondary antibodies alone resulted in minimal labeling of the chromosomes (Figure 22A). The presence of the 50 kDa polypeptide in the isolated chromosome fraction was confirmed by immunoblotting (Figure 23).

Immunolocalization of the 50 kDa polypeptide in mitotic cells.

To further test for whether the 50 kDa polypeptide is a kinetochore component, we examined its distribution in mitotic cells. Indian muntjac cells were chosen for this analysis because of their

low chromosome number (2n=6, females) and their relatively large kinetochores. Immunofluorescence microscopy using the 50-1 mAb did not, however, reveal an obvious kinetochore staining pattern (Figure 24). Rather, we observed labeling of spindle poles along with diffuse cytoplasmic staining (Figure 24A,C,E). We also noted some limited labeling of the mitotic spindle in the region adjacent to the poles (Figure 24A). Incubation with the secondary antibody alone did not result in labeling of these structures (Figure 24G). Comparable results were obtained using the 50-2 mAb on mitotic 3T3 cells as well (Figure 25).

The apparent discrepancy in labeling of isolated chromosomes and dividing cells could be explained by (1) the inaccessibility of the the antibody to antigens situated between the chromosome and the spindle fibers, or (2) an inability to resolve the kinetochore staining because of the diffuse cytoplasmic fluorescence. In an attempt to address the first possibility, we isolated 3T3 cells by mitotic shakeoff, sedimented them onto polylysine-coated glass coverslips to flatten the cells, and examined them by double label immunofluorescence microscopy with the 50-2 mAb and CREST antisera. The CREST antigens, which are mostly centromeric proteins, were clearly labeled at metaphase, anaphase, and telophase (Figure 26B,D,F). The 50-2 mAb did not reveal any kinetochore staining, though it did show a diffuse, granular cytoplasmic pattern (Figure 26A,C,E) similar to that obtained with the 50-1 mAb using Indian muntjac cells.

To address the possibility that kinetochore reactivity might have been obscured by cytoplasmic labeling of the 50 kDa polypeptide, we extracted mitotic Hela cells with 0.2% NP-40 prior to fixation in -20°C methanol. This treatment releases many cytosolic proteins but leaves cytoplasmic dynein bound at the kinetochore (Pfarr et al., 1990). The staining was essentially identical to that shown in Figure 26, that is, the diffuse cytoplasmic staining persisted and there was no evidence of kinetochore labeling (data not shown).

Immunolocalization of the 50 kDa polypeptide in interphase cells.

Immunofluorescence microscopy was performed on several cell lines to determine the interphase distribution of the 50 kDa polypeptide. The 50-1 mAb showed faint, diffuse cytoplasmic staining in interphase Indian muntjac cells (Figure 27A), similar to that obtained in mitotic cells. Some cells showed staining of a single spot in the region of the nucleus, raising the possibility that the 50 kDa may associate with the microtubule-organizing center.

The 50-2 mAb also revealed a diffuse and sometimes granular cytoplasmic staining pattern in 3T3 cells, but it also labeled discrete foci in the nucleus, distinct from nucleoli (Figure 28A,C). Interestingly, the nuclear reactivity is manifest in only a subset of cells, suggesting that it may be cell-cycle dependent. For example, the phase contrast image in Figure 28 shows seven nuclei, only two of which revealed obvious nuclear labeling with the 50-2 mAb. The

nuclear staining was also observed in 3T3 cells fixed with formaldehyde (Figure 29).

Some of the foci labeled with the 50-2 mAb appeared as pairs of dots, suggesting that the reactivity was with centromeres. Double label immunofluorescence microscopy was performed, using the CREST antiserum as a marker for centromeric antigens (Figure 30). The coincidence of staining with the 50-2 mAb and CREST antiserum was low. For example, only about 3% of the CREST-positive structures co-align with the foci detected with the 50-2 mAb in the two nuclei shown in Figure 30A-F. This indicated that the nuclear antigen recognized by the 50-2 mAb is probably not a centromere antigen. Double label immunofluorescence also revealed the nuclear staining was different from that obtained with human autoimmune sera to the recently described "novel nuclear domains" (Maul et al., 1991).

Discussion

In previous work we identified cytoplasmic dynein as a multi-subunit complex composed of at least nine polypeptides (Paschal et al., 1987). These include a pair of high molecular weight (>400 kDa) catalytic heavy chains and seven accessory polypeptides, the molecular weights of which range from 53 to 74 kDa (Paschal et al., 1987). These polypeptides are thought to represent integral subunits of the complex because they co-purify with the heavy chain

at constant stoichiometry by sucrose gradient centrifugation and ion exchange, gel filtration, and hydroxylapatite chromatography (Paschal et al., 1987). The function of the intermediate chains is unknown, though recent sequence analysis of the 74 kDa polypeptide has suggested a role subcellular targeting (Paschal et al., in press).

In the present study, we set out to develop mAb's specific for the accessory subunits of cytoplasmic dynein. Immunoblotting with sera from mouse tail bleeds indicated that an immune response was elicited against the 53-74 kDa subunits as well as several additional polypeptides which co-sediment with cytoplasmic dynein at 20S. Two hybridoma cell lines were subsequently cloned and characterized. The mAb's secreted by these cell lines react with a 50 kDa polypeptide which is present as a minor component of 20S cytoplasmic dynein.

We interpreted the high S-value of this species as an indication of a probable interaction with cytoplasmic dynein, because the predicted sedimentation coefficient for a monomeric, 50 kDa globular protein is only ~3-4S (Cantor and Schimmel, 1980). A series of experiments were carried out to test whether the 50 kDa polypeptide is indeed a subunit of cytoplasmic dynein. Although only a relatively small fraction of the 50 kDa polypeptide was found to co-purify with cytoplasmic dynein in the initial microtubule assembly step, the portion which did co-sediment with microtubules subsequently behaved in a manner similar to the 74 kDa subunit. Furthermore, the 50 kDa polypeptide and cytoplasmic dynein co-

sedimented on sucrose gradients in both low and high salt, despite the decrease in S-value for the complex in high salt.

Surprisingly, native immunoprecipitations using brain cytosol indicated that the 50 kDa polypeptide can be recovered in a complex along with electrophoretic species of 45 and 150-160 kDa. The anti-50 kDa immunoprecipitate contained only trace levels of the cytoplasmic dynein 74 kDa subunit, suggesting that the 20S sedimentation value observed for the 50 kDa polypeptide is a consequence of its interaction with the 45 and 150 kDa polypeptides rather than dynein.

Relationship to other 20S complexes.

A comparison of the molecular weight of the components immunoprecipitated with the 50-1 mAb (45, 50, 150-160 kDa) with those found in previously characterized complexes of comparable S-value in mammalian cytosol (Table I) indicates that we have probably isolated the mammalian equivalent of the chicken dynactin complex (Gill et al., 1991), so named because of its reported ability to activate cytoplasmic dynein in a vesicle motility assay (see below). The dynactin complex purified from 20S cytoplasmic dynein by MonoQ chromatography was reported to contain polypeptides of 32, 37, 45, 50, 62, 150, and 160 kDa at an apparent molar stoichiometry of 1:1:8:3:1:1:1, respectively (Gill et al., 1991). Components of 32, 37, and 62 kDa detected in chicken dynactin were not obviously present in the anti-50 kDa immunoprecipitate, though the relatively high

background and may have precluded their detection by Coomassie blue staining (Figure 19).

There are two additional pieces of evidence which support our identification of the 50 kDa-associated complex as dynactin. First, the 150 kDa doublet in the anti-50 kDa immunoprecipitate is recognized by an affinity-purified antibody to p150^{Glued} (Holzbaur et al., 1991). Molecular cloning has shown that the 150 kDa component of dynactin purified from chick brain cytosol is the avian homologue of p150^{Glued} (Gill et al., 1991; see below). Second, the 45 and 50 kDa polypeptides both appear as supra-stochiometric components relative to the 150 kDa doublet in both the purified chicken dynactin (op. cit.) and in the immunoprecipitate isolated with the anti-50 kDa mAb (Figure 19A).

The dynactin complex has been reported to play a role in cytoplasmic dynein-mediated vesicle motility *in vitro*. A reconstituted system containing KI-extracted membranes, microtubules, and purified cytoplasmic dynein did not show measurable vesicle motility. Supplementing the system with MonoQ-purified dynactin complex resulted in microtubule-based vesicle movements at a frequency of 3.7 $\pm$ 0.3 (mean $\pm$ SD) movements per minute (Gill et al., 1991). We note, however, that the frequency of dynactin-stimulated movement in this assay was ~10-fold less than that which was observed with crude extracts of chick embryo fibroblasts (Dabora and Sheetz, 1988).

Although the molecular basis for the stimulation of cytoplasmic dynein activity is unknown, the structure of the 150 kDa component of the dynactin complex has been deduced by cDNA cloning in both rat (Holzbaur et al., 1991) and chicken (Gill et al., 1991). The rat and chicken 150 kDa polypeptides are the apparent homologues of the 148 kDa product of the *Glued* locus in *Drosophila*. The rat and *Drosophila* polypeptides are 31% identical (Holzbaur et al., 1991) and the chicken and *Drosophila* polypeptides are 50% identical (Gill et al., 1991). The function of this polypeptide in *Drosophila* is unknown, though genetic analysis indicates that *Glued* encodes a product which is essential for the survival of many cell types; defects are most dramatically manifested in neurons (Harte and Kankel, 1982).

Subcellular distribution of the 50 kDa polypeptide.

The subcellular distribution revealed by immunofluorescence microscopy with the anti-50 kDa mAb's seems consistent with a potential role in modulating cytoplasmic dynein activity. The 50 kDa polypeptide was observed associated with the primary constriction of isolated chromosomes (Figure 21), indicating that it might reside at the centomere or kinetochore. We were able to demonstrate by immunoelectron microscopy that, like cytoplasmic dynein (Wordeman et al., 1991), it is restricted to the fibrous corona of the kinetochore (Figure 22). We note that the anti-50 kDa reactivity is eliminated by extraction of the chromosomes with 150 mM KI (L. Wordeman, personal communication). This treatment releases

cytoplasmic dynein but not centromeric antigens from chromosomes (Wordeman et al., 1991).

Immunofluorescence microscopy using mitotic cells revealed spindle pole staining, similar to that obtained with several antibodies to cytoplasmic dynein (see below). However, obvious kinetochore labeling was not observed. This result seems to be in conflict with our immunofluorescence and immunoelectron microscopy data, and with the fact that blots of isolated chromosomes contain a 50 kDa immunoreactive species. There are several possible explanations to account for this apparent discrepancy. For example, the 50 kDa antigen may not be accessible to antibody because of epitope-masking in the mitotic spindle. In this regard, it is noteworthy that the detection of cytoplasmic dynein at the kinetochore in whole cells using other antibodies has been technically difficult. The best demonstration of kinetochore staining was achieved in PtK_1 cells using an affinity-purified polyclonal anti-74 kDa antibody (Pfarr et al., 1990). Nonetheless, obtaining clear images of kinetochore labeling required detergent extraction prior to fixation, the staining was most obvious only during prophase and prometaphase, and most of the immunofluorescent signal was associated with the spindle and spindle poles, not with kinetochores (Pfarr et al., 1990). Immunofluorescence microscopy on chick embryo fibroblasts using mAb's to the cytoplasmic dynein heavy chain yielded similar results as well (Steuer et al., 1990). A more recent study using an affinity-purified anti-74 kDa antibody on mitotic BHK cells revealed only

very weak spindle staining and without obvious kinetochore staining (Lin and Collins, 1992). Together, these studies emphasize the difficulties in localizing putative kinetochore components in mitotic cells as compared with isolated chromosomes.

The interphase distribution of the 50 kDa polypeptide was examined in CHO, Hela, Indian muntjac, PtK_1, and 3T3 cells and found to be diffuse. A diffuse staining pattern has been observed with some antibodies to cytoplasmic dynein (Koonce et al., 1990; K. Pfister, personal communication). The distribution of cytoplasmic dynein in interphase BHK cells using an affinity-purified polyclonal antibody is punctate, showing co-alignment with lysosome-positive structures (Lin and Collins, 1992). A polyclonal antibody to the 150 kDa component of the dynactin complex also shows a punctate staining pattern (Gill et al., 1991), although it is unknown whether the immunoreactive structures co-localize with cytoplasmic dynein. Additional work using a battery of immunological probes will be required to determine whether the diffuse cytoplasmic staining with the 50-1 and 50-2 mAb's reflects the in vivo distribution.

The nuclear staining pattern obtained with the 50-2 mAb was unexpected because none of the aforementioned antibodies, nor the 50-1 mAb, stain nuclear structures. In addition, cytoplasmic dynein is not thought to have an intranuclear function. It is conceiveable that the nuclear signal is due to cross-reaction with a related epitope. Nonetheless, the apparent cell cycle-dependent appearance of the antigen in a nuclear compartment distinct from those identified with

human autoimmune sera suggests that the 50-2 mAb might be a useful reagent for laboratories interested in nuclear structure.

In summary, mAb's have been used to identify a 50 kDa component of the mammalian equivalent of the chicken dynactin complex. We have provided the first demonstration that dynactin can be isolated directly from cytosol, indicating that the complex purified from 20S dynein is unlikely to be a non-specific protein aggregate. We have localized the 50 kDa polypeptide to the kinetochore of isolated CHO chromosomes and shown that it is a component of the fibrous corona, a location which is consistent with its potential role as an activator of cytoplasmic dynein. Given that the 50 kDa polypeptide is one of the two major subunits of the dynactin particle, the reagents described in this study should prove valuable for analysis of the structure and function of the complex.

Figure Legends

Figure 13. Characterization of anti-50 kDa mAb's. (A) Immunoblot (10% gel) demonstrating that the 50-1 mAb reacts with a 50 kDa component of 20S cytoplasmic dynein (arrow) which is distinct from the 53-59 kDa subunits. Lane 1, molecular weight standards (kilodaltons); lanes 2 and 3, 20S cytoplasmic dynein. CB, Coomassie blue; HC, cytoplasmic dynein heavy chain. (B) Immunoblot (9% gel) of calf, rat, and chicken brain cytosol, PtK_1, and 3T3 cell lines using the 50-1 mAb. A single immunoreactive species with a M_r of 50 kDa was observed in each of the mammalian samples. No reactivity was detected in chicken. (C) The 50-2 mAb recognizes a component of 20S cytoplasmic dynein which is sensitive to denaturation. Approximately 5 μg of dynein was diluted into Tris-KCl buffer, 0.01% SDS, or 1x Laemmli sample buffer (followed by boiling) and applied to a nitrocellulose membrane with a slot-blotter (Schleicher and Schuell). The adsorbed protein was detected by Amido black staining (Amido) and immunoblotting with the 50-2 mAb (Blot). (D) Immunoprecipitation using the 50-1 and 50-2 mAb's and ^{35}S-methionine-labeled 3T3 cell extract prepared by lysis with 1% NP-40 (7-14% gradient gel). Both mAb's immunoprecipitated a 50 kDa polypeptide.

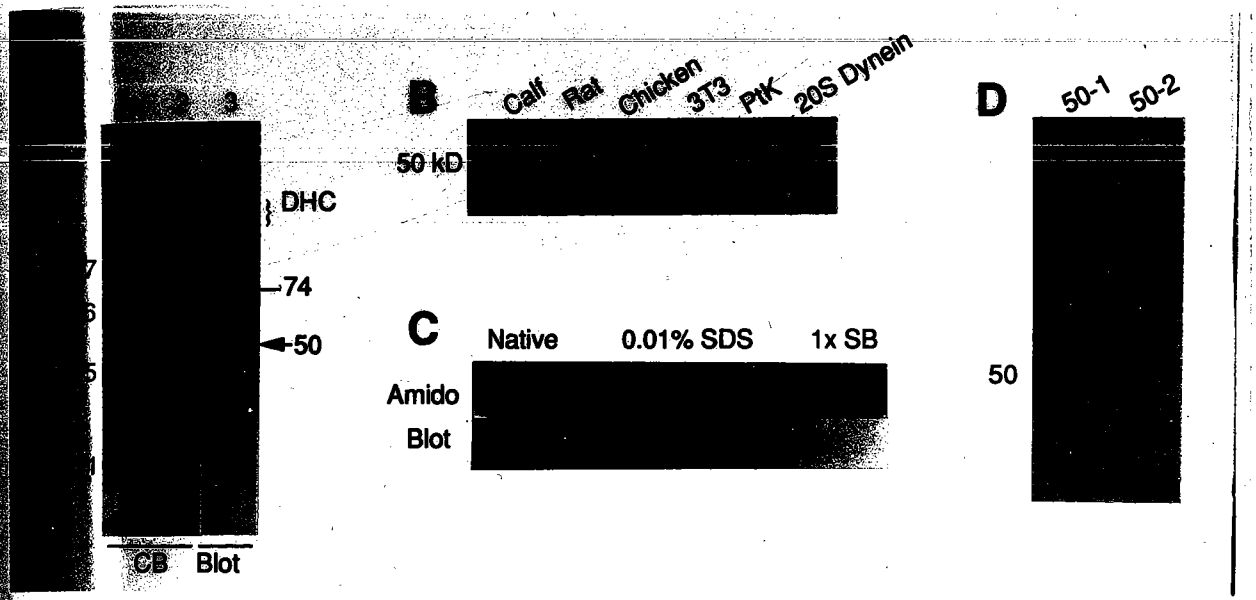
B
Calf
Rat
Chicken
3T3
PtK
20S Dynein
50 kD
C
Native
0.01% SDS
1x SB
Amido
Blot
D
50-1
50-2
50
DHC
74
50
CB
Blot

Figure 14. Preparation of cytoplasmic dynein from brain cytosol and analysis by immunoblotting. Equivalent loadings of the prep fractions were analyzed by gel electrophoresis (9% gel) and immunoblotting using anti-74 kDa and anti-50 kDa mAb's. Microtubules were assembled from calf brain white matter cytosol using taxol, washed with buffer to remove contaminating proteins, and extracted with nucleotides. Lanes 1 and 2, supernate and pellet after taxol-mediated assembly of microtubules; lanes 3 and 4, supernate and pellet after first buffer wash; lanes 5 and 6, supernate and pellet after second buffer wash; lanes 7 and 8, supernate and pellet after extraction with 3 mM GTP and 3 mM AMP-PNP; lanes 9 and 10, supernate and pellet after extraction with 5 mM ATP. Gel densitometry of the ECL reaction products (~10 second film exposure) indicated that 78% of the 74 kDa subunit and 29% of the 50 kDa polypeptide co-sedimented with microtubules (lane 2). The ATP extraction released 54% of the 74 kDa subunit and 47% of the 50 kDa polypeptide (lane 9).

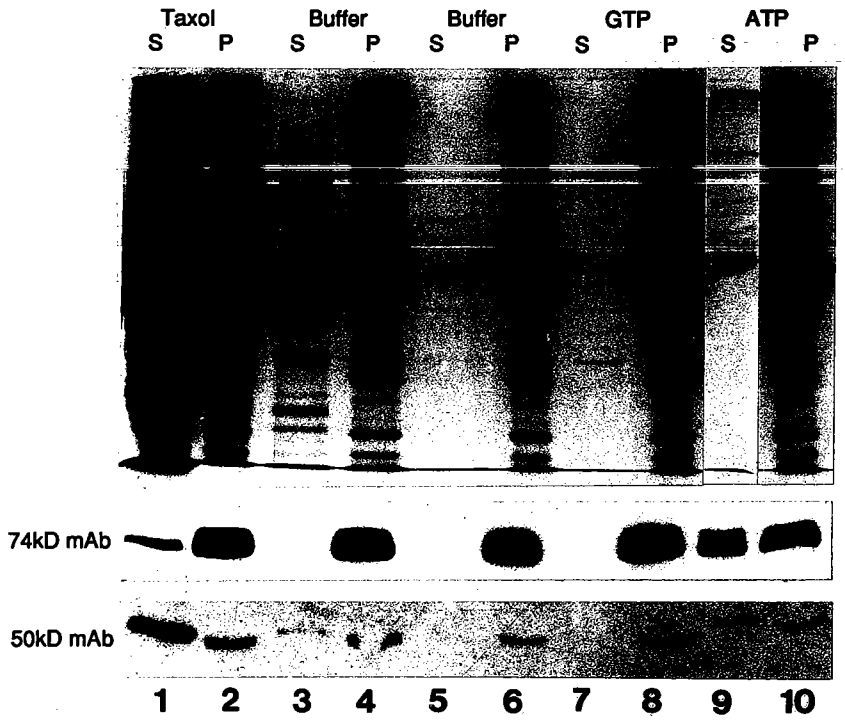
Taxol
Buffer
Buffer
GTP
ATP
S P S P S P S P S P
74kD mAb
50kD mAb
1 2 3 4 5 6 7 8 9 10

Figure 15. The 50 kDa polypeptide co-sediments with cytoplasmic dynein on a sucrose density gradient. ATP extract (similar to that in lane 9, Figure 14) was fractionated on a 5-20% sucrose gradient. (A) The gradient fractions were analyzed by gel electrophoresis (9% gel) and (B) immunoblotting with the 50-1 mAb. (C) Densitometric scans of the cytoplasmic dynein heavy chain stained by Coomassie blue (closed boxes) and the 50 kDa polypeptide detected by ECL reaction product (open boxes). HC, cytoplasmic dynein heavy chain.

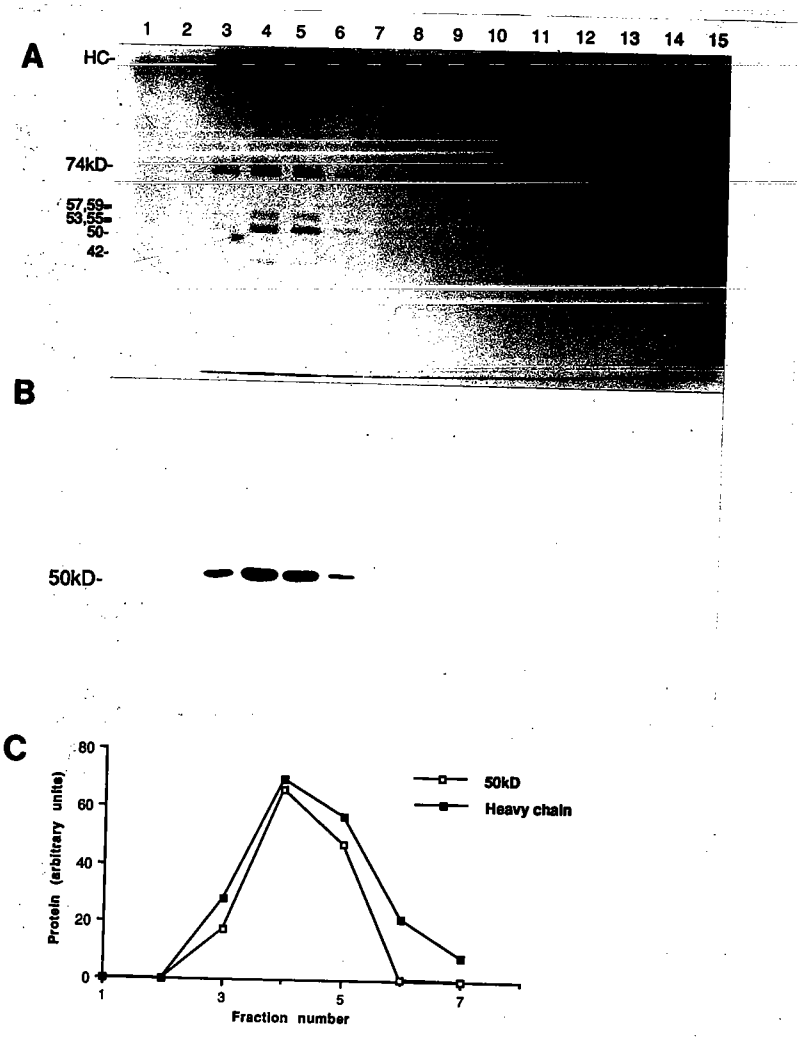
A
1 2 3 4 5 6 7 8 9 10 11 12 13 14 15
HC-
74kD-
57.59-
53.55-
50-
42-
B
50kD-
C
Protein (arbitrary units)
60
40
20
0
1
3
5
7
Fraction number
50kD
Heavy chain

Figure 16. Cytoplasmic dynein and the 50 kDa polypeptide shift from 20S to 16S in high salt buffer. ATP extract was fractionated by sucrose gradient centrifugation and analyzed by gel electrophoresis (9% gel) and immunoblotting with the 50-1 mAb. The high salt sample was prepared by dissolving 0.05 g sodium chloride in 1.5 mls ATP extract and incubating on ice for 1 hour. It was then fractionated on a 5-20% sucrose gradient made in Tris-KCl buffer supplemented with 0.58 M sodium chloride. The arrows indicate the peak fractions of the cytoplasmic dynein heavy chain as determined by Coomassie blue staining. The sedimentation standards were rabbit IgG (7S), catalase (11.3S), and thyroglobulin (19S). The sedimentation coefficient of cytoplasmic dynein in high salt (16S) was derived from a standard curve provided by Dr. Christine Collins, Northwestern University.

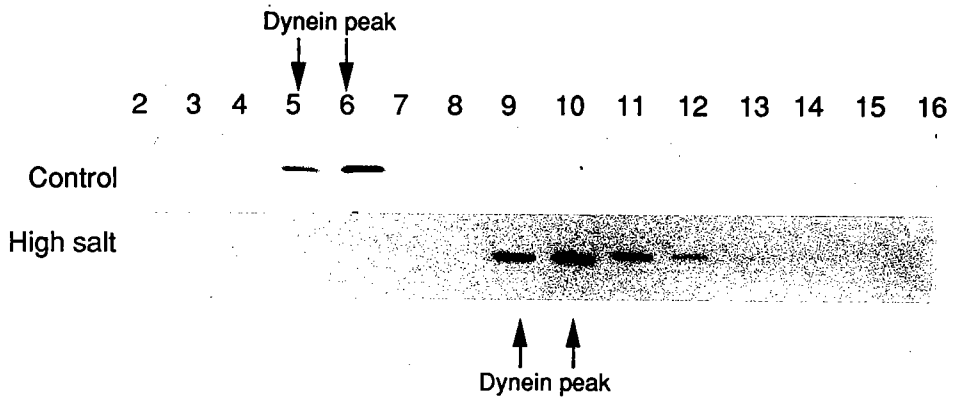
Dynein peak
2 3 4 5 6 7 8 9 10 11 12 13 14 15 16
Control
High salt
Dynein peak

Figure 17. The 50 kDa polypeptide in brain cytosol sediments quantitatively at 20S. Rat brain cytosol was subjected to sucrose gradient centrifugation (5-20% in Tris-KCl buffer), and the CTPase activity of the fractions was measured colorimetrically (Lanzetta et al., 1979). The 50 kDa polypeptide was detected with the 50-1 mAb and a peroxidase-labeled secondary antibody.

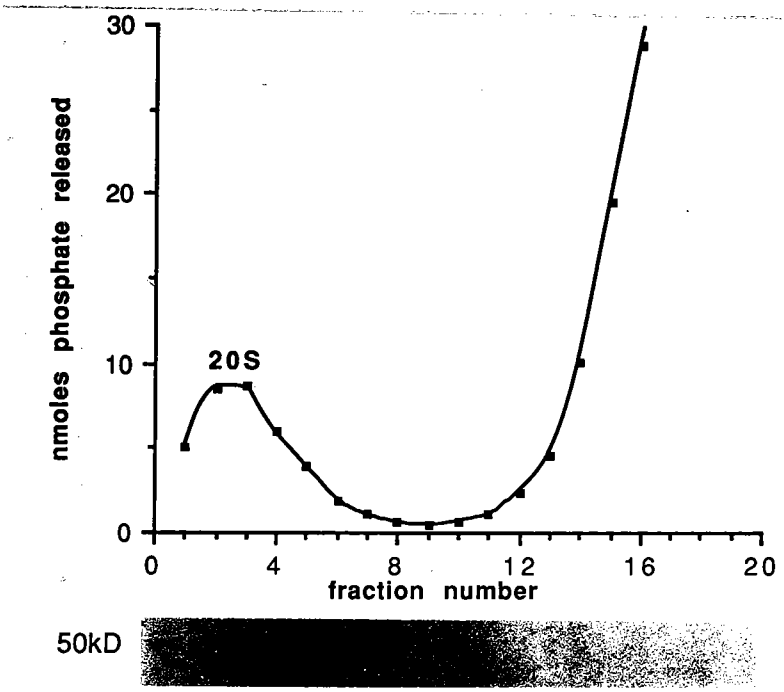
30
20
10
0
nmoles phosphate released
20S
0
4
8
12
16
20
fraction number
50kD

Figure 18. The fraction of the 50 kDa polypeptide which does not co-purify with microtubules is a 20S species. Samples of rat brain cytosol and a post-microtubule supernate (A) were fractionated on 5-20% sucrose gradients (B). The fractions were collected, spotted onto nitrocellulose, probed with the 50-1 mAb, and developed with ECL. Note that the p150^{Glued} product is labeled by the anti-74 kDa mAb on this blot (the cross-reactivity of this mAb is discussed under Results, Chapter III).

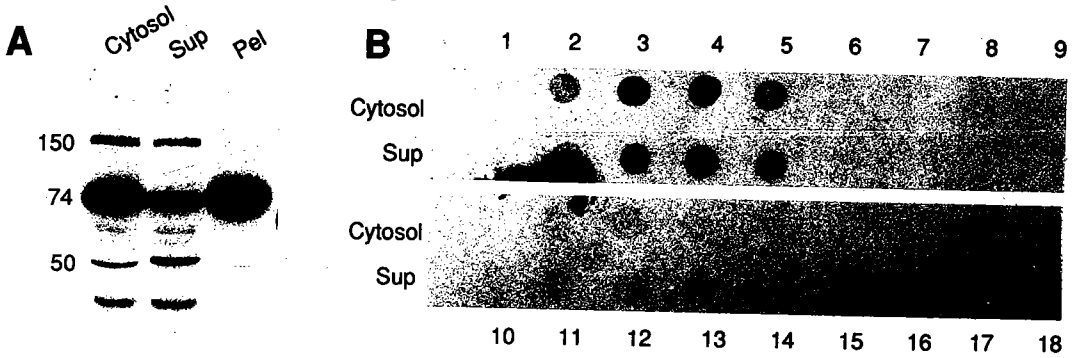
A
Cytosol
Sup
Pel
150
74
50
B
1
2
3
4
5
6
7
8
9
Cytosol
Sup
Cytosol
Sup
10
11
12
13
14
15
16
17
18

Figure 19. The anti-50 and anti-74 kDa mAb's immunoprecipitate distinct multi-subunit complexes from brain cytosol. (A) Coomassie blue staining of the immunoprecipitates, showing that electrophoretic species of M_r 150 (doublet) and 45 kDa co-immunoprecipitate with the 50 kDa polypeptide. The anti-74 kDa mAb immunoprecipitated the cytoplasmic dynein heavy chain (DHC) and 74 kDa subunits. A 60 kDa species also co-immunoprecipitated, however the identity of this polypeptide is unknown. AbHC, antibody heavy chain; AbLC, antibody light chain; CB, Coomassie blue. (B) Parallel blot of the immunoprecipitated samples probed with a mixture of the anti-50 and anti-74 kDa mAb's. (C) The same blot shown in (B) was reprobed with an affinity-purified polyclonal anti-serum to the rat $p150^{Glued}$ product. The 150 kDa protein is referred to as the 150 kDa cytoplasmic dynein-associated polypeptide in Holzbaur et al. (1991) and dynactin in Gill et al. (1991). (D) The 45, 50, and 150 kDa polypeptides are present as minor components of 20S cytoplasmic dynein. 20S cytoplasmic dynein analyzed by gel electrophoresis (9% gel) and immunoblotting. The blot was probed with a mixture of anti-50 and anti-74 kDa mAb's and subsequently reprobed with the anti-$p150^{Glued}$ antiserum (see above).

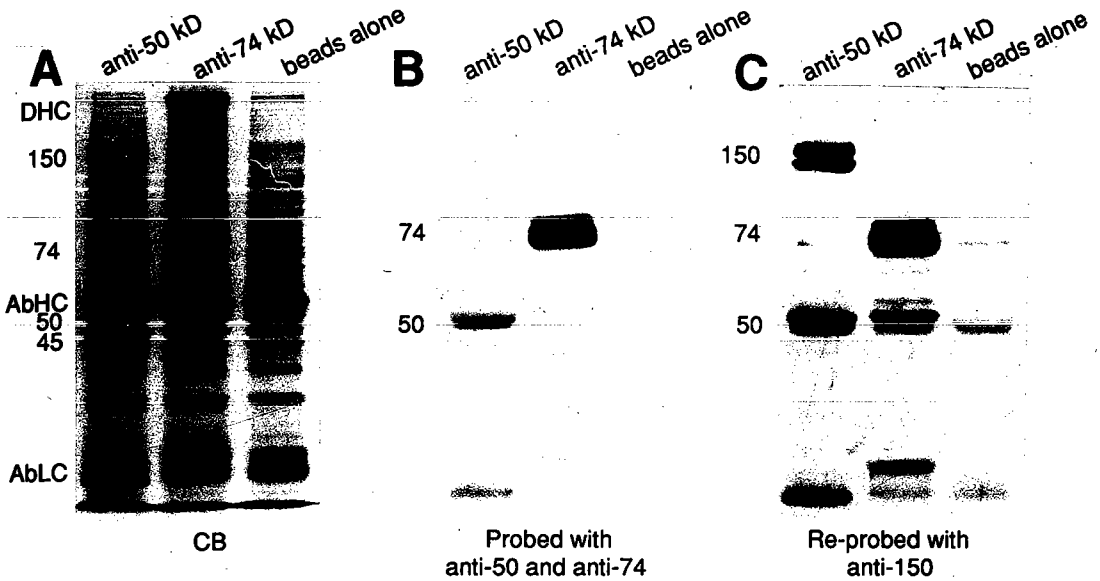
A
anti-50 kD
anti-74 kD
beads alone
DHC
150
74
AbHC
50
45
AbLC
CB
B
anti-50 kD
anti-74 kD
beads alone
74
50
Probed with
anti-50 and anti-74
C
anti-50 kD
anti-74 kD
beads alone
150
74
50
Re-probed with
anti-150

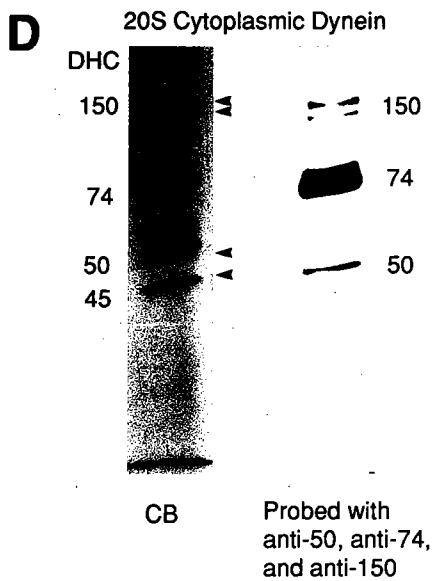
D
20S Cytoplasmic Dynein
DHC
150
74
50
45
150
74
50
CB
Probed with
anti-50, anti-74,
and anti-150

Figure 20. Immunoprecipitation and electrophoretic analysis (9% gel) of 50 kDa-associated polypeptides from ^{35}S-methionine-labeled 3T3 cell extract using the 50-1 and 50-2 mAb's. The cell extract was prepared in the absence of detergent by mechanical lysis. The co-immunoprecipitating 45 kDa species appears to be supra-stoichiometric relative to the 50 kDa polypeptide. The presence of a 150 kDa polypeptide is not obvious, perhaps due to proteolysis or dissociation from the complex. The ~60 kDa polypeptide which co-immunoprecipitated using the 50-2 mAb could be related to the 62 kDa subunit of chick brain dynactin (Gill et al., 1991).

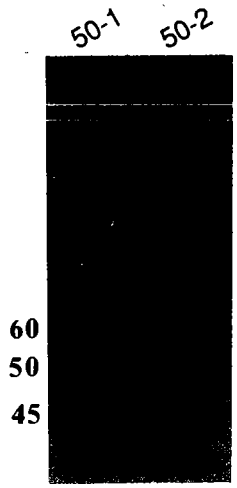
50-1
50-2
60
50
45

Figure 21. Immunofluorescence microscopy of isolated CHO chromosomes using the 50-1 mAb. The pairs of spots co-align with the primary constriction observed by phase contrast microscopy. Fixation conditions: 0.5% formaldehyde (1,8); -20°C acetone (2,5,7); 0.5% formaldehyde and -20°C methanol (3,4,6,9).

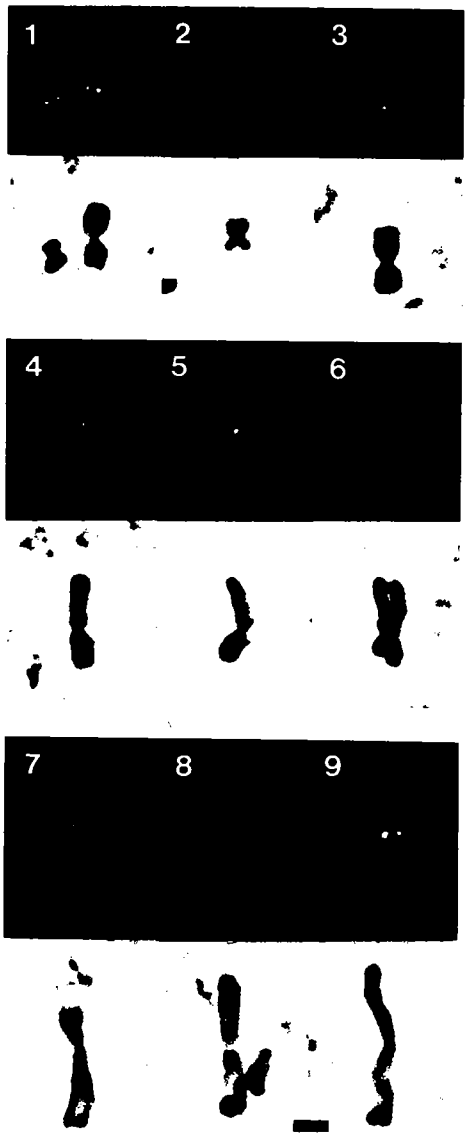
1
2
3
4
5
6
7
8
9

Figure 22. Immunoelectron microscopy of isolated CHO chromosomes. (A) Chromosome incubated with 5 nm gold-labeled secondary antibody alone. (B,C,D) Chromosomes stained with the 50-1 mAb and gold-labeld secondary antibody. The immunoelectron microscopy was performed by Dr. Linda Wordeman, UCSF. Bars, 0.2 μm.

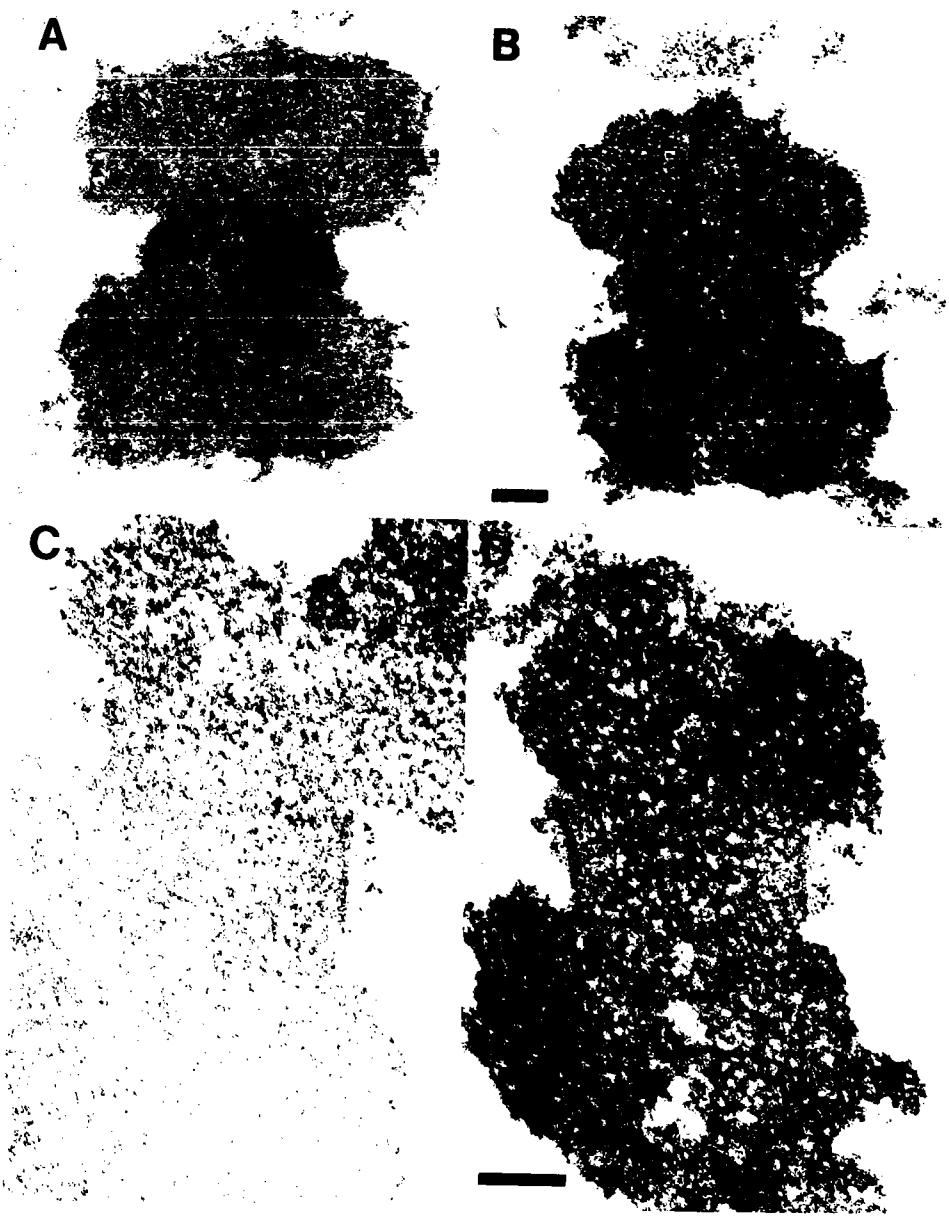
A
B
C

Figure 23. Immunoblotting of isolated CHO chromosomes. Calf brain cytosol and CHO chromosomal proteins were visualized on an Amido black-stained nitrocellulose filter (Amido). The immunoreactive species detected in the isolated CHO chromosomal fraction co-migrates with the 50 kDa polypeptide in brain cytosol (Blot).

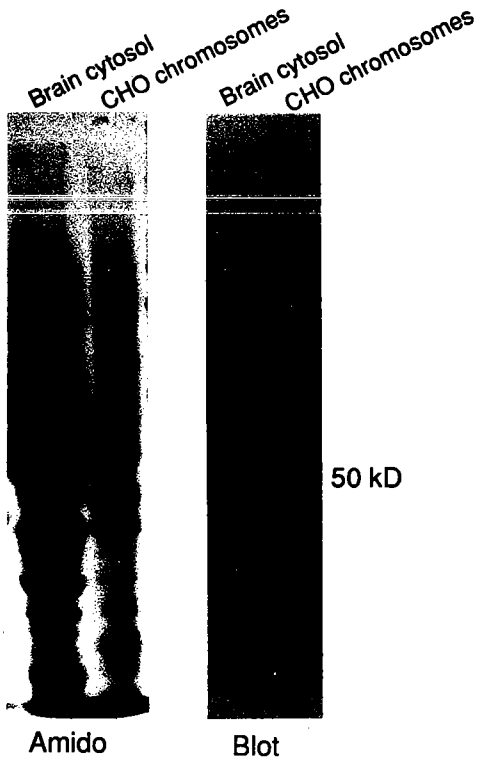
Brain cytosol
CHO chromosomes
Brain cytosol
CHO chromosomes
50 kD
Amido
Blot

Figure 24. Immunofluorescence microscopy of mitotic Indian muntjac cells. The cells were fixed in -20°C methanol and stained with the 50-1 mAb (A,C,E) or secondary antibody alone (G). The phase contrast images are shown on the right (B,D,F,H). Bar, 10 μm.

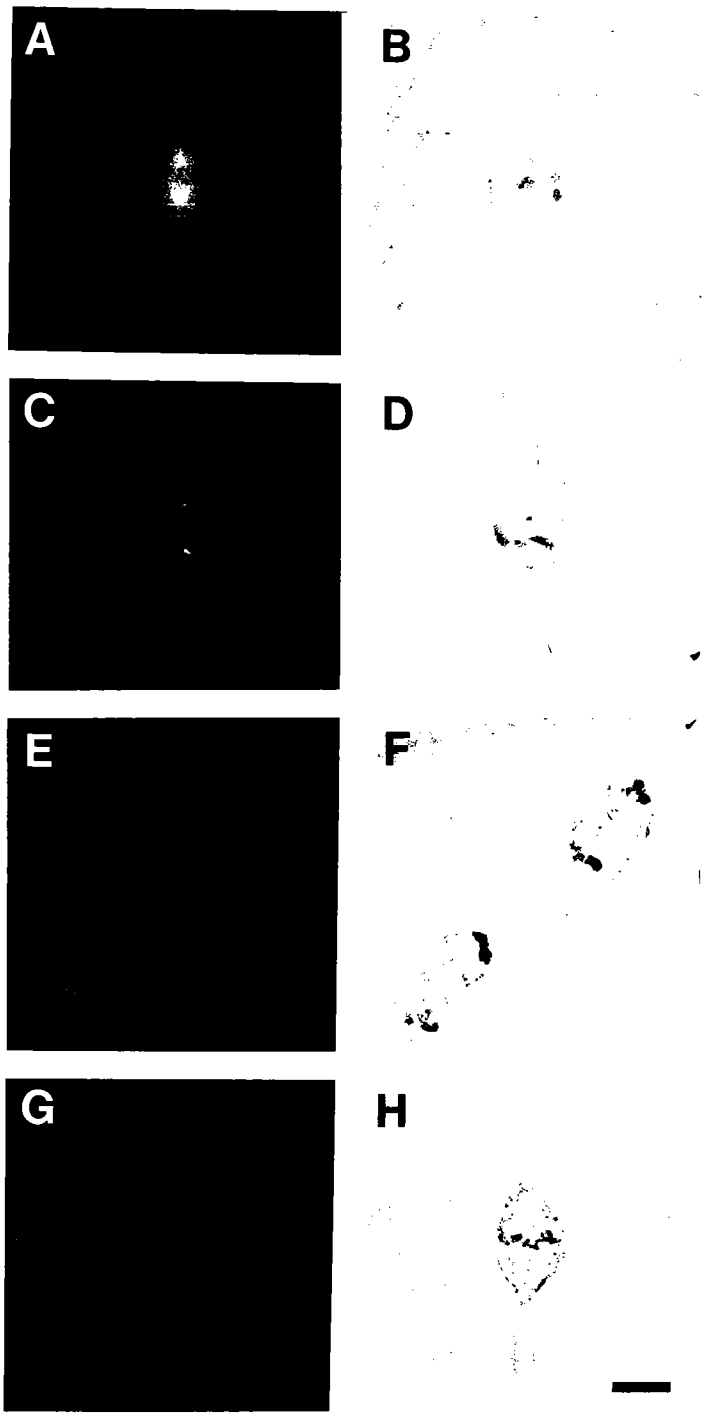
A
B
C
D
E
F
G
H

Figure 25. Immunofluorescence microscopy of a mitotic NIH 3T3 cell using the 50-2 mAb. The spindle pole staining is similar to that obtained with the 50-1 mAb using Indian muntjac cells. Bar, 10 μm.

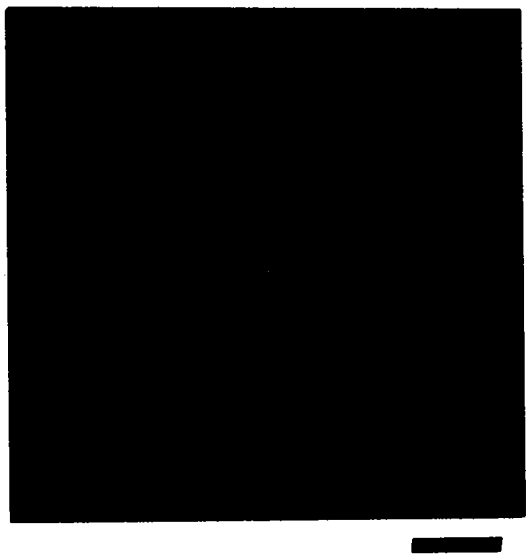

Figure 26. Double-label immunofluorescence microscopy of mitotic NIH 3T3 cells. The cells were isolated by mitotic shake-off, sedimented onto coverslips, and labeled with the 50-2 mAb (A,C,E) and CREST anti-serum (B,D,F). The centromere antigens were intensely labeled by the CREST anti-serum at metaphase (B), late anaphase (D), and telophase (F). Spindle components did not appear to be labeled by the 50-2 mAb, though there was some punctate cytoplasmic staining. Bar, 10 μm.

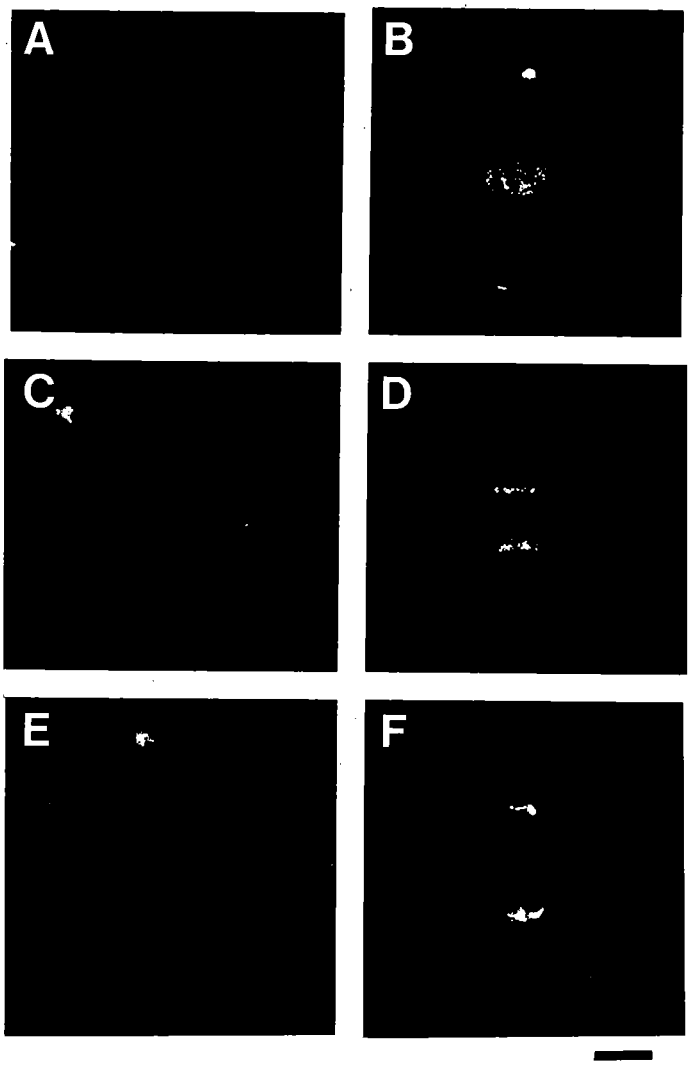
A
B
C
D
E
F

Figure 27. Immunofluorescence microscopy of interphase Indian muntjac cells using the 50-1 mAb. The staining was predominantly diffuse, though we did observe occassional labeling of a structure near the nucleus which could correspond to the microtubule-organzing center. MTOC-staining has been observed with anti-dynactin antibodies (Gill et al., 1991). The fluorescence and phase contrast images are shown in panels (A) and (B), respectively. Bar, 10 μm.

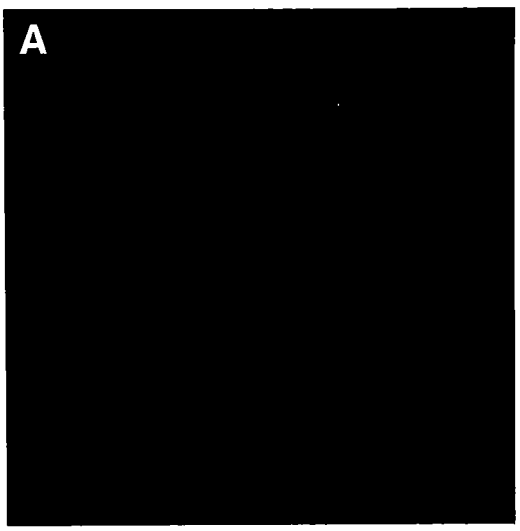
A

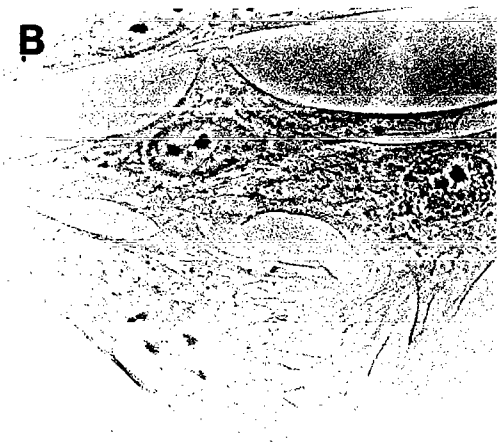
B

Figure 28. Immunofluorescence (A,C) and phase contrast microscopy (B,D) of interphase NIH 3T3 cells using the 50-2 mAb. The antibody labels foci in the nuclei of a subset of cells. Bar, 10 μm.

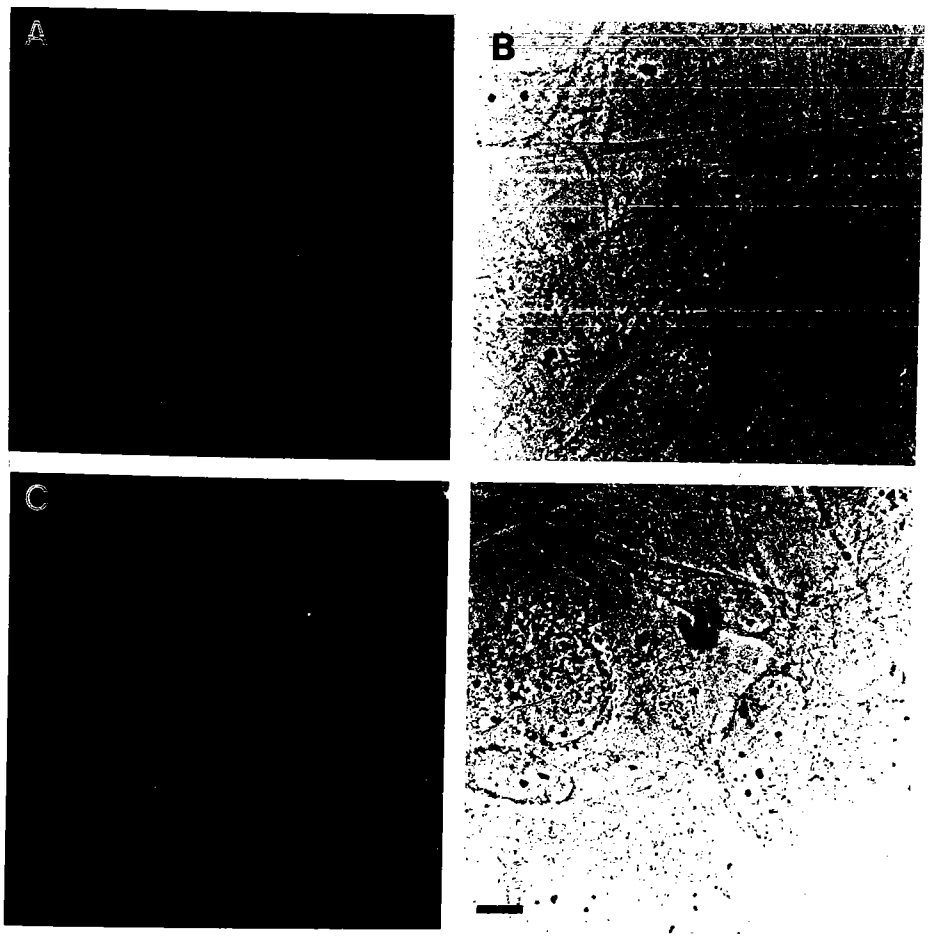
A
B
C

Figure 29. Immunofluorescence (A) and phase contrast microscopy (B) of sister interphase NIH 3T3 cells using the 50-2 mAb. The nuclear epitope appears to be resistant to aldehyde fixation. Bar, 10 μm.

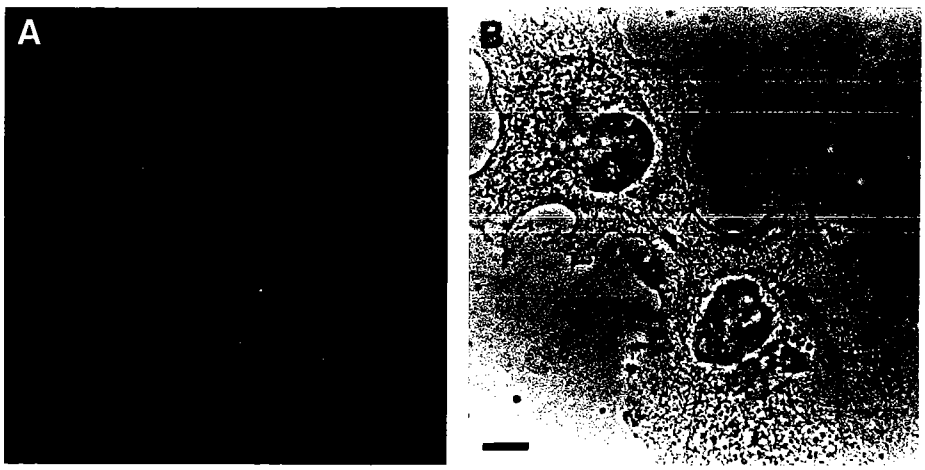
A
B

Figure 30. Double-label immunofluorescence microscopy of interphase NIH 3T3 cells. The foci labeled by the 50-2 mAb (A,D,G) are distinct from those detected by CREST autoimmune serum (B,E,H). Alignment with the phase contrast images (C,F,I) indicated the 50-2 mAb does not recognize nucleoli. Bar, 10 μm.

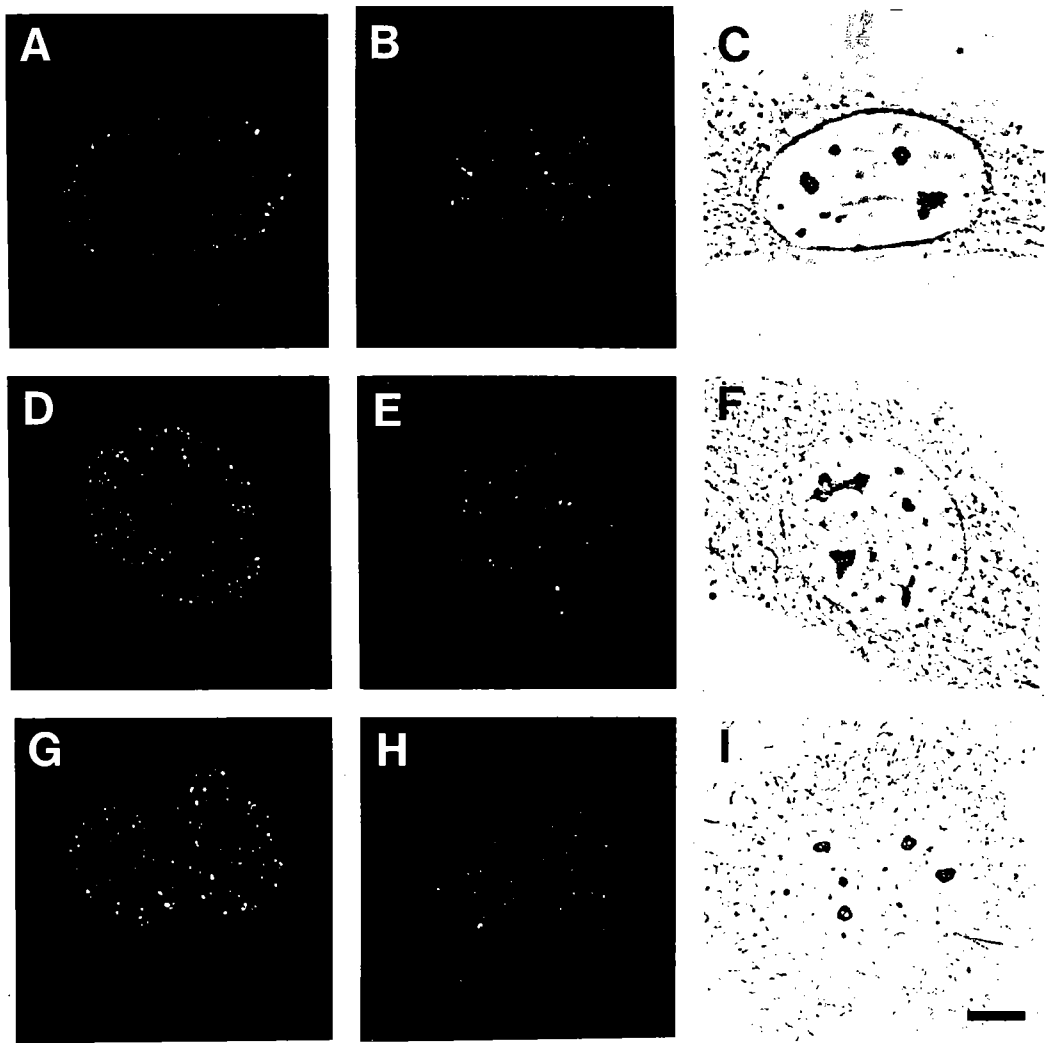
A
B
C
D
E
F
G
H
I

Table I. High S-value Multi-subunit Complexes Isolated from Eukaryotic Cytosol

Complex	S-value	Subunit mol wts	Function	Reference
DNA Replication Complex	21S	24,47,52,58,62,70, 90,125,145,183	nuclear DNA synthesis	E. Baril, personal communication
Prosomes	19S	21-35(9),56	mRNA repression	de Sa et al., 1986
Proteosomes	20S	21-32(25)	protease	Hough et al., 1987
"	26S	34,46-62(15),100,110	"	" "
Chaperonin	19S	55-62(5)	protein folding	Gao et al., 1992
U1-U6 RNP Particles	>15S	12,16,22,28,29,33,70	mRNA processing	Habets et al., 1985
Cytoplasmic Dynein	20S	53,55,57,59, 74,440	microtubule motor	Paschal et al., 1987
Dynactin	20S	32,37,45,50, 62,150,160	dynein activator	Gill et al., 1991

The mol wts are given in kDa, and the number of subunits in a particular mol wt range is shown in parenthesis.

CHAPTER V
DISCUSSION

As discussed in the previous chapters, there is a growing body of evidence indicating that cytoplasmic dynein is the motor for retrograde organelle and chromosome transport. However, the molecular details of cytoplasmic dynein-based transport are unknown. To this end, we set out to (1) define the sites of α and β-tubulin which activate the cytoplasmic dynein ATPase, (2) determine the primary structure of the 74 kDa subunit, and (3) use mAb's to study the properties of a co-purifying 50 kDa polypeptide. The results of these experiments and the implications for future work are discussed below.

Activation of the cytoplasmic dynein ATPase by tubulin.

Microtubules were found to act as specific, potent activators of the cytoplasmic dynein ATPase (Paschal et al., 1987; Shpetner et al., 1988). Based on what is known about other mechanochemical enzymes this is likely to accelerate the rate-limiting step of the cross-bridge cycle, ADP release (reviewed by Johnson, 1985). Furthermore, this provides for efficient utilization of cellular ATP since maximal nucleotide hydrolysis would occur only in association with force production along microtubules.

We have identified the acidic C-termini of α and β-tubulin as the regions responsible for activation of the cytoplasmic dynein

ATPase (Paschal et al., 1989). This conclusion, which is consistent with our finding that activation of the ATPase is sensitive to ionic conditions (Shpetner et al., 1988), is supported by two independent lines of evidence. First, MAP2, which has been shown previously to bind to the C-terminus of tubulin (Serrano et al., 1984; Littauer et al., 1986) inhibited the microtubule-activated ATPase in a dose-dependent manner. Second, removal of the C-termini of α and β-tubulin with subtilisin reduced the microtubule-activated ATPase by 97%.

Together, these data indicate that the C-terminal domains of tubulin constitute a site of interaction for both mechanochemical and structural MAPs. Recent evidence showing that MAP2 inhibits microtubule activation of the dynamin GTPase suggests that the C-terminus is probably an interactive site for other proteins as well (Shpetner and Vallee, 1992). These observations may prove useful for identifying functional domains of cytoplasmic dynein and dynamin. For example, it should be possible to chemically cross-link these proteins to the tubulin C-termini and identify the sequences which bind to α and β-tubulin (Leszyk et al., 1990). In addition, if the C-termini of α and β-tubulin are required for growth or viability in organisms such as yeast, it may be possible to clone microtubule-interacting proteins by identifying suppressors of C-terminal mutations.

Molecular cloning of a subunit of cytoplasmic dynein.

The polypeptide components of cytoplasmic dynein include two catalytic subunits and at least seven accessory subunits whose function is unknown. To gain insight into the role of these accessory subunits in dynein function, I determined the nucleotide and deduced polypeptide sequences of the 74 kDa subunit and obtained evidence for isoform diversity. This represents the first published report of a sequence for a cytoplasmic dynein subunit.

The 74 kDa subunit was found to be related to one other polypeptide, the 70 kDa subunit of Chlamydomonas flagellar outer arm dynein (Mitchell and Kang, 1991). The C-terminal ~300 amino acids of the two subunits are 26.4% identical, suggesting that this domain mediates a function conserved between the cytoplasmic and axonemal polypeptides such as binding to the catalytic heavy chain. In contrast, the N-termini of the two subunits appear to be unrelated. We speculate that this region of the 74 kDa polypeptide may specify a cytoplasmic-specific function such as targeting the holoenzyme to membranous organelles or kinetochores.

It should be possible to test this hypothesis by analyzing the subcellular distribution of 74 kDa transfected into cultured cells. If the 74 kDa subunit is sufficient for targeting, then transfected polypeptide (epitope-tagged) should localize to retrogradely-transported organelles such as endosomes, lysosomes, and mitotic chromosomes. Expression of N-terminal nested deletion mutants might then, in principle, allow the identification of domains

necessary for targeting to these organelles. In addition, bacterially-expressed 74 kDa could be used as a ligand to purify interacting proteins such as the putative cytoplasmic dynein "receptor".

Identification of a major 50 kDa subunit of a 20S cytosolic complex.

We have used mAb's to investigate the properties of a 50 kDa polypeptide which co-purifies with cytoplasmic dynein by sucrose gradient centrifugation. Immunoprecipitation experiments indicated that the 50 kDa polypeptide is a major subunit of a distinct 20S particle which contains additional polypeptides of 45 and 150 kDa. The 50 kDa polypeptide, like the 74 kDa and catalytic subunits of cytoplasmic dynein, was localized to the kinetochores of isolated chromosomes by light and electron microscopy. This result, together with data reporting that the 50 kDa-associated complex (dynactin) stimulates cytoplasmic dynein motility in vitro (Gill et al., 1991), raises the possibility that the complex plays a role in regulating the activity of dynein at the kinetochore.

In the course of mitosis, chromosomes are translocated towards the spindle midzone during prometaphase and subsequently directed poleward during anaphase. It seems reasonable to expect that the activity of one or several proteins controls the timing and direction of these movements. In this regard, Hyman and Mitchison (1991) used an in vitro assay to demonstrate a cytoplasmic dynein-like microtubule-motor activity present in the kinetochores of isolated chromosomes. Interestingly, the direction of transport could be

switched by thiophosphorylation, suggesting a possible mechanism for regulating motor activity. It is of obvious interest, therefore, to further characterize the 50 kDa polypeptide and its associated subunits and examine their potential role in mitosis.

BIBLIOGRAPHY

Abersold, R. 1989. Internal amino acid sequence analysis of proteins after "in situ" protease digestion on nitrocellulose. *In* A practical guide to protein and peptide purification for microsequencing. P.T. Matsudaira, editor. Academic Press, Inc., San Diego. 71-88.

Allen, R.D., N.S. Allen, and J.L. Travis. 1981. Video-enhanced contrast, differential interference contrast (AVEC-DIC) microscopy: a new method capable of analyzing microtubule related motility in the recticulopodial network of Allogromia laticollaris. Cell. Motil. 1:291-302.

Allen, R.D., D.T. Brown, S.P. Gilbert, and H. Fujiwake. 1983. Transport of vesicles along filaments dissociated from squid axoplasm. Biol. Bull. 165:523.

Banerjee, A., M.C. Roach, K.A. Wall, M.A. Lopata, D.W. Cleveland, and R.F. Luduena. 1988. A monoclonal antibody against the type II isotype of β-tubulin. J. Biol. Chem. 263:3029-3034.

Bhattacharyya, B., D.L. Sackett, and J. Wolff. 1985. Tubulin, hybrid dimers, and tubulin S. J. Biol. Chem. 260:10208-10216.

Bomsel, M., R. Parton, S.A. Kuznetsov, T.A. Schroer, and J. Gruenberg. 1990. Microtubule- and motor-dependent fusion in vitro between apical and basolateral endocytic vesicles from MDCK cells. Cell. 62:719-731.

Breitling, F. and M. Little. 1986. Carboxy-terminal regions on the surface of tubulin and microtubules. J. Molec. Biol. 189:367-370.

Brendel. V. and S. Karlin. 1989. Association of charge clusters with functional domains of cellular transcription factors. Proc. Natl. Acad. Sci. USA. 86:5698-5702.

Brown, H.R. and H.P. Erickson. 1983. Assembly of proteolytically cleaved tubulin. Arch. Biochem. Biophys. 220:46-51.

Burns, R.G., K. Islam, and R. Chapman. 1984. The multiple phosphorylation of microtubule-associated protein MAP2 controls the MAP2:tubulin interaction. Eur. J. Biochem. 141:609-615.

Calvin, H.I. 1976. Isolation and subfractionation of mammalian sperm heads and tails. *In*: Methods in Cell Biology, vol. 13. D.M. Prescott, ed. Academic Press, New York. 85-104.

Cantor C.R. and P.R. Schimmel. 1980. Techniques for the study of biological structure and function. W.H. Freeman and Company, San Franciso. 607-614.

Clark, T.G. and J.L. Rosenbaum. 1982. Pigment particle translocation in detergent-permeabilized melanophores of Fundulus heteroclitus. Proc. Natl. Acad. Sci. USA. 79:4655-4659.

Cleveland, D.W. and K.F. Sullivan. 1985. Molecular biology and genetics of tubulin. Ann. Rev. Biochem. 54:331-365.

Collins, C.A. and R.B. Vallee. 1986. A microtubule-activated ATPase from sea urchin eggs, distinct from cytoplasmic dynein and kinesin. Proc. Natl. Acad. Sci. USA. 83:4799-4803.

Collins, C.A. and R.B. Vallee. 1989. Preparation of microtubules from rat liver and testes: cytoplasmic dynein is a major microtubule-associated protein. Cell Motil. Cytoskel. 14:491-500.

Dabora, S.L. and Sheetz, M.P. 1988. Cultured cell extracts support organelle movement on microtubules in vitro. Cell Motil. Cytoskeleton 10:482-495.

De Camilli, P., P.E. Miller, F. Navone, W.E. Theurkauf, and R.B. Vallee. 1984. Distribution of microtubule-associated protein 2 in the nervous system of the rat studied by immunofluorescence. Neuroscience 11:819-846.

de Sa, C.M., M.-F. de Sa, O. Akhayat, F. Broders, K. Scherrer, A. Horsch, and H.P. Schmid. 1986. Prosomes. J. Mol. Biol. 187:479-493.

Eisenberg, E. and C. Moos. 1968. The adenosine triphosphatase activity of acto-heavy meromyosin. A kinetic analysis of actin activation. Biochemistry. 7:1486-1489.

Emini, E.A., J.V. Hughes, D.S. Perlow, and J. Boger. 1985. Induction of hepatitis A virus-neutralizing antibody by a virus-specific synthetic peptide. J. Virol. 55:836-839.

Forman, D.S., K.J. Brown, and D.R. Livengood. 1983a. Fast axonal transport in permeabilized lobster giant axons is inhibited by vanadate. J. Neurosci. 3:1279-1288.

Forman, D.S., K.J. Brown, and M.E. Promersberger. 1983b. Selective inhibition of retrograde axonal transport by erythro-9-[3-(3-hydroxynonyl)]adenine. Brain Res. 272:194-197.

Gao, Y., J.O. Thomas, R.L. Chow, G.-H, Lee, and N.J. Cowan. 1992. A cytoplasmic chaperonin that catalyzes β-actin folding. Cell 69:1043-1050.

Gibbons, I.R., M.P. Cosson, J.A. Evans, B.H. Gibbons, B. Houck, K.H. Martinson, W.S. Sale, and W.J. Tang. 1978. Potent inhibition of dynein adenosinetriphosphatase and of the motility of cilia and sperm flagella by vanadate. Proc. Natl. Acad. Sci. USA. 75:2220-2224.

Gill, S.R., T.A. Schroer, I. Szilak, E.R. Steuer, M.P. Sheetz, and D.W. Cleveland. 1991. Dynactin, a conserved, ubiquitously expressed component of an activator of vesicle motility mediated by cytoplasmic dynein. J. Cell Biol. 115:1639-1650.

Goodenough, U. and J. Heuser. 1984. Structural comparison of purified dynein proteins with in situ dynein arms. J. Mol. Biol. 180:1083-1118.

Gooderham, K. 1984. In situ peptide mapping of proteins following polyacrylamide gel electrophoresis. *In* Methods in Molecular Biology. J.M. Walker, editor. Humana, Clifton. 193-202.

Gunderson, G.G., M.H. Kalnoski, and J.C. Bulinski. 1984. Distinct populations of microtubules: tyrosinated and nontyrosinated alpha tubulin are distributed differently in vivo. Cell 38:779-789.

Gunderson, G.G., S. Khawaja, and J.C. Bulinski. 1987. Postpolymerization detyrosination of α-tubulin: a mechanism for subcellular differentiation of microtubules. J. Cell. Biol. 105:251-264.

Habets, W., M. Hoet, P. Bringmann, R. Luhrmann, and W. van Venrooij. 1985. Autoantibodies to ribonucleoprotein particles containing U2 small nuclear RNA. EMBO J. 4:1545-1550.

Hastie, A.T. 1991. Purification and characterization of dynein from pig tracheal cilia. Methods Enzymol. 196:223-234.

Herman, B. and D.F. Albertini. 1984. A time-lapse video image intensification analysis of cytoplasmic organelle movements during endosome translocation. J. Cell Biol. 98:565-576.

Hirokawa, N., G.S. Bloom, and R.B. Vallee. 1985. Cytoskeletal architecture and immunocytochemical localization of microtubule-associated proteins in regions of axons associated with rapid axonal transport: the β,β'-iminodipropionitrile-intoxicated axon as a model system. J. Cell Biol. 101:227-239.

Hirokawa, N., R. Sato-Yoshitake, N. Kobayashi, K.K. Pfister, G.S. Bloom, and S.T. Brady. 1991. Kinesin associates with anterogradely transported membranous in vivo. J. Cell Biol. 114: 295-302.

Hirokawa, N., R. Sato-Yoshitake, T. Yoshida, and T. Kawashima. 1990. Brain dynein (MAP1C) localizes on both anterogradely and retrogradely transported membranous organelles in vivo. J. Cell Biol. 111:1027-1037.

Hirokawa, N., Y. Shiomura, and S. Okabe. 1988. Tau proteins: the molecular structure and mode of binding to microtubules. J. Cell Biol. 107:1449-1459.

Hirokawa, N., R. Sato-Yoshitake, T. Yoshida, and T. Kawashima. 1991. Brain dynein (MAP1C) localizes on both anterogradely and

retrogradely transported membranous organelles in vivo. J. Cell Biol. 111:1027-1037.

Holzbaur, E.L.F., J.A. Hammarback, B.M. Paschal, N.G. Kravit, K.K. Pfister, and R.B. Vallee. 1991. Homology of a 150K cytoplasmic dynein-associated polypeptide with the Drosophila gene Glued. Nature (Lond.). 351:579-583.

Ho, W.C., V.J. Allan, G. van Meer, E.G. Berger, and T.E. Kreis. 1989. Reclustering of scattered Golgi elements occurs along microtubules. Eur. J. Cell Biol. 48:250-263.

Hough, R., G. Pratt., and M. Rechsteiner. 1987. Purification of two high molecular weight proteases from rabbit reticulocyte lysate. J. Biol. Chem. 262:8303-8313.

Hyman, A.A. and T.J. Mitchison. 1991. Two different microtubule-based motor activities with opposite polarities in kinetochores. Nature (Lond.). 351:206-211.

Innis, M.A. and D.H. Gelfand. 1990. Optimization of PCRs. *In* PCR Protocols. M.A. Innis, D.H. Gelfand, J.J. Sninsky, and T.J. White, eds. Academic Press, San Diego. 3-20.

Johnson, K.A. 1985. Pathway of the microtubule-dynein ATPase and the structure of dynein: a comparison with actomyosin. Ann. Rev Biophys. Biophys. Chem. 14:161-188.

Johnson, K.A. and J.S. Wall. 1983. Structure and molecular weight of the dynein ATPase. J. Cell Biol. 96:669-678.

Kamiya, R. 1988. Mutations at twelve independent loci result in absence of outer dynein arms in Chlamydomonas reinhardtii. J. Cell Biol. 107: 2253-2258.

King, S.M. and G.B. Witman. 1990. Localization of an intermediate chain of outer arm dynein by immunoelectron microscopy. J. Biol. Chem. 265:19807-19811.

King, S.M., J.L. Gatti, A.G. Moss, and G.B. Witman. 1990. Outer arm dynein from trout spermatozoa: substructural organization. Cell Motil. Cytoskeleton 16:266-278.

King, S.M., C.G. Wilkerson, and G.B. Witman. 1991. The M_r 78,000 intermediate chain of Chlamydomonas outer arm dynein interacts with α-tubulin in situ.. J. Biol. Chem. 266:8401-8407.

Koonce. M.P. and J.R. McIntosh. 1990. Identification and immunolocalization of cytoplasmic dynein in Dictyostelium. Cell Motil. Cytoskel. 15:51-62.

Kozak, M. 1991. An analysis of vertebrate mRNA sequences: intimations of translational control. J. Cell Biol. 115:887-903.

Kraus, E., M. Little, T. Kempf, R. Hofer-Warbinek, W. Ade, and H. Ponstingl. 1981. Complete amino acid sequence of β-tubulin from porcine brain. Proc. Natl. Acad. Sci. USA. 78:4156-4160.

Kumar, N. and M. Flavin. 1981. Preferential action of a brain detyrosinating carboxypeptidase on polymerized tubulin. J. Biol. Chem. 256:7678-7686.

Kusnetsov, S.A. and V.I. Gelfand. 1986. Bovine brain kinesin is a microtubule-activated ATPase. Proc. Natl. Acad. Sci. USA. 83:8530-8534.

Lacy, M.L. and L.T. Haimo. 1992. Cytoplasmic dynein is a vesicle protein. J. Biol. Chem. 267:4793-4798.

Laemmli, U.K. 1970. Cleavage of structural proteins during the assembly of the head of the bacteriophage T4. Nature (Lond.). 227:680-685.

Lathe, R. 1985. Synthetic oligonucleotide probes deduced from amino acid sequence data. J. Mol. Biol. 183:1-12.

Lee, G., N.J. Cowan, and M. Kirschner. 1988. The primary structure and heterogeneity of tau protein from mouse brain. Science 239:285-288.

Lewis, S.A., D. Wang, and N.J. Cowan. 1988. Microtubule associated protein MAP2 shares a microtubule-binding motif with tau protein. Science 242:936-939.

Leszyk, J. Z. Grabarek, J. Gergely, and J.H. Collins. 1990. Characterization of zero-lenth cross-links betweeb rabbit skeletal muscle troponin C and troponin I: evidence for direct interaction between the inhibitory region of troponin I and the NH_2-terminal, regulatory domain of troponin C. Biochemistry 29:299-304.

Lin, S.X. and C.A. Collins. 1992. Immunolocalization of cytoplasmic dynein to lysosomes in cultures cells. J. Cell Sci. 101:125-137.

Lipman, D.J. and W.R. Pearson. 1985. Rapid and sensitive protein similarity searches. Science 227:1435-1441.

Littauer, U.Z., D. Giveon, M. Thierauf, I. Ginzburg, and H. Ponstingl. 1986. Common and distinct tubulin binding sites for microtubule-associated proteins. Proc. Nat. Acad. Sci. USA. 83:7162-7166.

Little, M. and T. Seehaus. 1988. Comparative analysis of tubulin sequences. Comp. Biochem. Physiol. 90B:655-670.

Lupas, A., M. Van Dyke, and J. Stock. 1991. Predicting coiled coils from protein sequences. Science 252:1162-1164.

Maccioni, R., C.I. Rivas, and J.C. Vera. 1988. Differential interaction of synthetic peptides from the carboxyl-terminal regulatory domain of tubulin with microtubule-associate proteins. EMBO J. 7:1957-1963.

Maccioni, R.B., L. Serrano, J. Avila, and J.R. Cann. 1986. Characterization and structural aspects of the enhanced assembly of tubulin after removal of its carboxyl-terminal domain. Eur. J. Biochem. 156:375-381.

Margulis, L. 1981. Symbiosis in cell evolution. W.H. Freeman and Company, San Francisco. 419 pp.

Matsudaira, P. 1987. Sequence from picomole quantities of proteins electroblotted onto polyvinylidene difluoride membranes. J. Biol. Chem. 262:10035-10038.

Matteoni, R. and T.E. Kreis. 1987. Translocation and clustering of endosomes and lysosomes depends on microtubules. J. Cell Biol. 105:1253-1265.

Miller, R.H., R.J. Lasek, and M.J. Katz. 1987. Preferred microtubules for vesicle transport in lobster axon. Science 235:220-222.

Mitchell, D.R. and Y. Kang. 1991. Identification of oda6 as a Chlamydomonas dynein mutant by rescue with the wild-type gene. J. Cell Biol. 113:835-842.

Mitchell, D.R. and J.L. Rosenbaum. 1986. Protein-protein interactions in the 18S ATPase of Chlamydomonas outer dynein arms. Cell Motil. Cytoskeleton 6:510-520.

Neely, M.D. and K. Boekelheide. 1988. Sertoli cell processes have axoplasmic features: an ordered microtubule distribution and an abundant high molecular weight microtubule-associated protein (cytoplasmic dynein). J. Cell Biol. 107:1767-1776.

Nudel, U., R. Zakut, M. Shani, S. Neuman, and D. Yaffee. 1983. The nucleotide sequence of the rat cytoplasmic β-actin gene. Nucleic Acids Res. 11:1759-1771.

Oakley, B.R., D.R. Kirsch, and N.R. Morris. 1980. A simplified ultrasensitive silver stain for detecting proteins in polyacrylamide gels. Anal. Biochem. 105:361-363.

Paschal, B.M., A. Mikami, K.K. Pfister, and R.B. Vallee. Molecular cloning of a cytoplasmic dynein subunit: homology with a flagellar dynein polypeptide. J. Cell Biol. In press.

Paschal, B.M., R.A. Obar, and R.B. Vallee. 1989. Interaction of brain cytoplasmic dynein and MAP2 with a common sequence at the C terminus of tubulin. Nature 341:569-572.

Paschal, B.M., H.S. Shpetner, and R.B. Vallee. 1987. MAP1C is a microtubule-associated ATPase which translocates microtubules in vitro and has dynein-like properties. J. Cell Biol. 105:1273-1282.

Paschal, B.M., H.S. Shpetner, and R.B. Vallee. 1991. Purification of brain cytoplasmic dynein and characterization of its in vitro properties. Methods Enzmol. 196:181-191

Paschal, B.M. and R.B. Vallee. 1987. Retrograde transport by the microtubule-associated protein MAP1C. Nature (Lond.). 330:181-183.

Penningroth, S.M. 1986. Erythro-9-[3-(2-hydroxynonyl)]adenine and vanadate as probes deo microtubule-based cytoskeletal mechanochemistry. Methods Enzymol. 134:477-487.

Piperno, G. and D.J. Luck. 1979. Axonemal adenosine triphosphatases from flagella of Chlamydomonas reinhardtii. J. Biol. Chem. 254:3084-3090.

Pfarr, C.M., M. Coue, P.M. Grissom, T.S. Hays, M.E. Porter, and J.R. McIntosh. 1990. Cytoplasmic dynein is localized to kinetochores during mitosis. Nature(Lond.). 345:263-265.

Pfister, K.K., R.B. Fay, and G.B. Witman. 1982. Purification and polypeptide composition of dynein ATPases from Chlamydomonas flagella. Cell Motil. 2:525-547.

Ponstingl, H., E. Krauhs, M. Little, and T. Kempf. 1981. Complete amino acid sequence of α-tubulin from porcine brain. Proc. Natl. Acad. Sci. USA. 78:2757-2761.

Rieder, C.L. and S.P. Alexander. 1990. Kinetochores are transported poleward along a single astral microtubule during chromosome attachment to the spindle in newt lung cells. J. Cell Biol. 110:81-95.

Robbins, J., S.M. Dilworth, R.A. Laskey, and C. Dingwall. 1991. Two interdependent basic domains in nucleoplasmin nuclear targeting sequence: identification of a class of bipartite nuclear targeting sequence. Cell 64:615-623.

Rodionov, V.I., F.K. Gyoeva, A.S. Kashina, S.A. Kuznetsov, and V.I. Gelfand. 1990. Microtubule-associated proteins and microtubule-based translocators have different binding sites on tubulin molecule. J. Biol. Chem. 265:5702-5707.

Rogalski, A.A. and S.J. Singer. 1984. Associations of elements of the Golgi apparatus with microtubules. J. Cell Biol. 99:1092-1100.

Sackett, D.L., B. Bhattacharyya, and J. Wolff. 1985. Tubulin subunit carboxyl termini determine polymerization efficiency. J. Biol. Chem. 260:43-45.

Sambrooke, J., E.F. Fritsch, and T. Maniatis. 1989. Molecular cloning: a laboratory manual, Vol. I and II. Cold Spring Harbor Laboratory Press, Cold Spring Harbor.

Schnapp, B.J. and T.S. Reese. 1989. Dynein is the motor for retrograde transport of organelles. Proc. Natl. Acad. Sci. USA. 86:1548-1552.

Schroer, T.A. and M.P. Sheetz. 1989. Cytoplasmic dynein is a minus-end-directed motor for membranous organelles. 1989. Cell. 56:937-946.

Schroer, T.A. and M.P. Sheetz. 1991. Two activators of microtubule-based vesicle transport. J. Cell Biol. 115:1309-1318.

Serrano, L., J. Avila, and R.B. Macioni. 1984. Controled proteolysis of tubulin by subtilisin: localization of the site for MAP2 interaction. Biochemistry 23:4675-4681.

Serrano, L. F. Wandosell, J. Torre, and J. Avila. 1986. Proteolytic modification of tubulin. Meth. Enzymol. 134:179-190.

Shpetner, H.S., B.M. Paschal, and R.B. Vallee. 1988. Characterization of the microtubule-activated ATPase of brain cytoplasmic dynein (MAP1C). J. Cell Biol. 107:1001-1009.

Shpetner, H.S. and Vallee. 1989. Identification of dynamin, a novel mechanochemical enzyme that mediates interactions between microtubules. Cell. 59:421-432.

Shpetner, H.S. and R.B. Vallee. 1992. Dynamin is a GTPase stimulated to high levels by microtubules. Nature 355:733-735.

Smith, P.K., R.I. Krohn, G.T. Hermanson, A.K. Mallia, F.H. Gartner, M.D. Provenzano, E.K. Fujimoto, N.M. Goeke, B.J. Olsen, and D.C. Klenk. 1985. Measurement of protein using bicinchonic acid. Anal. Biochem. 150:76-85.

Steuer, E.R., L. Wordeman, T.A. Schroer, and M.P. Sheetz. 1990. Localization of cytoplasmic dynein to mitotic spindles and kinetochores. Nature(Lond.). 345:266-268.

Tang, W.-J., C.W. Bell, W.S. Sale, and I.R. Gibbons. 1982. Structure of the dynein-1 outer arm in sea urchin sperm flagella. J. Biol. Chem. 257:508-515.

Towbin, J., T. Staehelin, and J. Gordon. 1979. Electrophoretic transfer of proteins from polyacrylamide gels to nitrocellulose sheets: procedure and some applications. Proc. Natl. Acad. Sci. USA. 76:4350-4354.

Vale, R.D., T.S. Reese, and M.P. Sheetz. 1985a. Identification of a novel force-generating protein, kinesin, involved in microtubule-based motility. Cell. 42:39-50.

Vale, R.D., B.J. Schnapp, T. Mitchison, E. Steuer, T.S. Reese, and M.P. Sheetz. 1985b. Different axoplasmic proteins generate movement in opposite directions along microtubules in vitro. Cell. 43:623-632.

Vale, R.D., B.J. Schnapp, T.S. Reese, and M.P. Sheetz. 1985c. Organelle, bead, and microtubule translocations promoted by soluble factors from the squid giant axon. Cell. 40:559-569.

Vallee, R.B. 1980. Structure and phosphorylation of microtubule-associated protein 2 (MAP2). Proc. Natl. Acad. Sci. USA. 77:3206-3210.

Vallee, R.B. 1982. A taxol-dependent procedure for the isolation of microtubules and microtubule-associated proteins (MAPs). J. Cell Biol. 92:435-442.

Vallee, R.B. 1986. Reversible assembly purification of microtubules without assembly-promoting agents and further purification of tubulin, microtubule-associated proteins, and MAP fragments. Methods Enzymol. 134:89-104.

Vallee, R.B. 1991. Movement on two fronts. Nature 351:187-188.

Vallee, R.B. and H.S. Shpetner. Motor proteins of cytoplasmic microtubules. Ann. Rev. Biochem. 59:909-932.

Vallee, R.B., J.S. Wall, B.M. Paschal., and H.S. Shpetner. 1988. Microtubule-associated protein 1C from brain is a two-headed cytosolic dynein. Nature 332:561-563.

Voter, W.A., and H.P. Erickson. 1982. Electron microscopy of MAP2 (microtubule-associated protein 2). J. Ultrastruct. Res. 80:374-382.
Witman, G.B., K.A. Johnson, K.K. Pfister, and J.S. Wall. 1983. Fine structure and molecular weight of the outer arms of dyneins of Chlamydomonas. J. Submicrosc. Cytol. 15:193-197.

Wehland, J., M. Henkart, R. Klausner, and I.V. Sandoval. 1983a. Role of microtubules in the distribution of the Golgi apparatus: effect of taxol and microinjected anti-alpha-tubulin antibodies. Proc. Natl. Acad. Sci. USA. 80:4286-4290.

Wehland, J., M.C. Willingham, and I.V. Sandoval. 1983b. A rat monoclonal antibody reacting specifically with the tyrosinated from of α-tubulin. I Biochemical characterization, effects on microtubule polyperization in vitro, and microtubule polymerization and organization in vivo. J. Cell Biol. 97:1467-1475.

Wordeman, L., E.R. Steuer, M.P. Sheetz, and T. Mitchison. 1991. Chemical subdomains within the kinetochore domain of isolated CHO mitotic chromosomes. J. Cell Biol. 114:285-294.